CHARACTERIZING THE PLUMBING SYSTEMS OF ACTIVE VOLCANOES THROUGH POTENTIAL FIELD STUDIES

by

Jeffrey Zurek
BSc., University of Victoria 2007

THESIS SUBMITTED IN PARTIAL FULFILLMENT OF
THE REQUIREMENTS FOR THE DEGREE OF

MASTER OF SCIENCE

Department of Earth Sciences

SIMON FRASER UNIVERSITY

Fall 2010

APPROVAL

Name: **Jeffrey Zurek**

Degree: **Master of Science**

Title of Thesis: **Characterizing the Plumbing Systems of Active Volcanoes through Potential Field Studies**

Examining Committee:

Chair: **Dr. Gwenn Flowers**
Associate Professor, Department of Earth Sciences

Dr. Glyn Williams-Jones
Senior Supervisor
Associate Professor, Department of Earth Sciences

Dr. Doug Stead
Supervisor
Professor, Department of Earth Sciences

Dr. Albert Eggers
Supervisor, University of Puget Sound

By video teleconference from Washington
Dr. Dan Dzurisin
Supervisor, Cascades Volcano Observatory, USGS

By telephone teleconference from Hawaii
Dr. Mike Poland
Supervisor, Hawaiian Volcano Observatory, USGS

By video teleconference from England
Dr. Hazel Rymer
Supervisor, Open University, UK

By video teleconference from New Zealand
Dr. Nicolas Fournier
External Examiner
Wairakei Research Centre, GNS Science, NZ

Date Defended/Approved: November 15, 2010

Declaration of
Partial Copyright Licence

ABSTRACT

The processes involved with mass transport through a volcanic plumbing system are poorly understood. Through the use of potential field studies, this thesis aims to identify volcanic structures, processes and Earth properties that control volcanic activity. Gravity and total magnetic surveys at Kīlauea (Hawaii, USA), Masaya (Nicaragua) and South Sister (Oregon, USA) volcanoes, allowed for development of models to investigate magma transport at different spatial and temporal resolutions.

At Kīlauea rapid, short term mass flux perturbations were characterized within the shallow plumbing system and long term mass increases were inferred in the creation of a large intrusive complex. Constraints on crustal viscosity were obtained at South Sister through gravity and deformation models. At Masaya, constraints were obtained for void space in the active crater and shallow geologic properties. Potential field studies at active volcanoes can clearly bring insight into the fundamental processes of magma transport and emplacement.

Keywords: Volcano; Kīlauea; Masaya; Three Sisters; Continuous gravity; Microgravity; Bouguer gravity; total magnetic surveys; Magmatic plumbing systems; Mass flux

ACKNOWLEDGEMENTS

There are many people who have made my journey through academia possible and enjoyable; unfortunately it isn't possible for simple words to convey all my gratitude. First my supervisory committee, as they have been my friends, my colleagues and my mentors through my M.Sc. Glyn has helped to make this a wonderful experience allowing complete academic freedom, while also challenging me and my ideas. Without his easygoing nature and support, this document that is now in your hands would probably only scratch the surface and not provide the new scientific information that it does. Albert Eggers (Al) made this journey possible as he was my biggest champion and badgered Glyn into giving me a shot. Al opened doors of understanding by taking the time to casually talk about scientific projects and their significance to a keen would-be student at Kīlauea. Mike Poland took me as a volunteer at HVO and encouraged my participation with anything and everything volcanic in Hawaii. I was given the space to take some initiative and gather GPS survey data where I thought it would be useful to provide a more robust kinematic dataset. Mike provided the tools that allowed me to get to Hawaii and complete the caldera wide Bouguer map. He helped with the proposal, facilitated much of the logistical problems and provided insight on the project; without Mike, the Kīlauea portion of this thesis would not have occurred. On the suggestion of Glyn (and assumedly Al and Mike), Dan Dzurisin (Dz) took me with him to Three Sisters to continue a dataset

originally started by Dr. Dan Johnson. That snowy landscape became our 20 mile long battlefield. Although the attrition rate was high, we completed the survey and discussed volcanism at Three Sisters and Kīlauea and sports along the way. It was suggested that I take up the microgravity dataset afterwards and see it through to completion. We went back to the field again together later, however, this time at Kīlauea. Dz, a USGS scientist, took the time out of his schedule to be my field hand in a strange reversal of roles. Without his help the logistics may have been too much and definitely it would have been less enjoyable. Hazel Rymer has been a part of my field campaigns in Nicaragua and like Glyn, encourages her students to find their own way allowing academic freedom and ownership of the project. It is hard to imagine what my time in Nicaragua would be like without Hazel, surly drab and boring I think. Doug Stead is the only other person from SFU on my supervisory committee and has provided the access to different ideas and technologies in the form of rock mechanic software and slope stability modelling. Through Doug and his students, I have received a lot of support with learning how to use difficult software and apply it to a task which it is not traditionally used for.

Much of the project support and ideas that I have used throughout each study have come from someone I have never met and, unfortunately, will never get the opportunity to. Dr. Dan Johnson was the man behind both microgravity surveys at Kīlauea and the Three Sisters but died in 2005 in a tragic accident. I have referred to the Kīlauea study many times throughout this thesis and also had the opportunity, thanks to Al, to work on the project briefly. The surveys

completed at the Three Sisters are part of my Chapter 4 and without Dan Johnson there would be no Chapter 4.

I would be remiss if I did not thank friends and family members who have supported me through the long process that got me here. Your patience to allow me to prattle on and think my thoughts out loud has helped a lot. I do not know how to thank all of you without either a list or writing a very long acknowledgments sections. Seeing the length of this document already I'd like to thank, Jolane, Nathalie, Guillaume, Mathieu, Gabriel, Rafael, and Peter for their help and patience listening to my ideas. Anna, thank you for your love and support, you kept me sane through the thesis process. To my Mom, Dad, grandparents and my sister, I wouldn't be here without your support and push to follow my childhood dream. Don't worry one day I'll stop asking for money, I promise.

TABLE OF CONTENTS

LIST OF FIGURES

LIST OF TABLES

1: GENERAL INTRODUCTION AND LITERATURE REVIEW

1.1 Introduction

There are potentially active volcanoes across the globe in a variety of different geologic settings. Regardless of the geologic setting, the fundamental processes which control their activity are the same. However, many basic processes such as transportation of material from the mantle to the surface via a volcano's plumbing system are still poorly understood. Mass movements within a volcano are generally responsible for volcanic unrest detected at the surface. There are a number of different signs that can be used to indicate that magma is moving beneath the ground, but not limited to, ground deformation, seismic events, increased fumarole activity, and mass changes. The first step towards understanding any dynamic volcanic system requires the use of methods to record the evolution of these phenomena. However, to move forward, different approaches are needed to provide a more complete picture.

While direct observation of volcanic processes with personnel and/or equipment is ideal, it is often not practical due to safety concerns or site inaccessibility. Therefore, remote monitoring techniques are often required to record and monitor volcanic activity; the most common remote geophysical techniques utilized are deformation and seismicity. Gravity field measurements are an example of a technique, often overlooked as a monitoring tool that provide

information about density and mass flux within an active volcano. Gravity field surveys can be done in several ways including microgravity, Bouguer gravity and continuous gravity measurements. The usefulness of these survey methods for measuring mass change and studying volcanic processes have been shown in a number of different cases (e.g., Rymer and Brown 1986; Rymer, 1996; Gudmundsson and Milson, 1997; Williams-Jones et al., 2003). Magnetic survey techniques are another tool, also rarely utilized in volcanic geophysical studies, that can be used to obtain the depth to the Curie point in regions of high heat flow as well as imaging geologic structures (e.g., Bhattacharyya and Leu, 1975; Hildenbrand et al., 1993; Gudmundsson and Milson, 1997).

The goal of this thesis is to build upon the current understanding of processes and structures involved with magma transport. The use of gravity and magnetic field surveys tailored to individual locations provide an unsurpassed resolution for imaging material property contrasts beneath the Earth's surface. When potential field data is combined with other datasets such as deformation, seismic or heat flux, we can begin to build robust models to explain the processes of a volcanic system.

1.1.1 Location and Geologic Setting

Kīlauea volcano is located in the Pacific Ocean on the Big Island of Hawaii, which is the surface expression of a hotspot theorized to exist beneath the Island. It is possible to trace this hot spot backwards in time by following it from the Big Island of Hawaii nearly 6000 km northwest to the Bering Sea (Fig 1-1). The Hawaiian Islands make up the first 3450 km after which the hotspot track

bends, and Emperor Seamount chain begins, stretching another 2300 km north. Extrapolating from seamount ages and paleo plate reconstructions, the Hawaiian hotspot probably formed 90 to 100 million years ago beneath an ancient spreading ridge (Clague and Darlrymple, 1987). The total eruptive volumes for the Hawaiian and Emperor Sea Mounts have been estimated to be approximately 1 million cubic kilometres from 107 different volcanic centers (Bargar and Jackson, 1974).

The Big Island of Hawaii consists of five different volcanic edifices of which Kĩlauea, Mauna Loa and Hualalai have had historical activity; the most recent eruption from Mauna Loa was in 1984 and Hualalai in 1801 (Peterson and Moore, 1987). The two inactive edifices are Kohala, which last erupted approximately 120,000 years ago, and Mauna Kea, which is the highest peak on the island at 4205 m above sea level and last erupted between 4000 to 6000 years ago. The newest volcano in the Hawaiian Chain of volcanic islands and seamounts is Lo`ihi, located approximately 30 km south of Kĩlauea and 969 m beneath the ocean surface. Its most recent known eruption was in 1996 (Garcia et al., 1998).

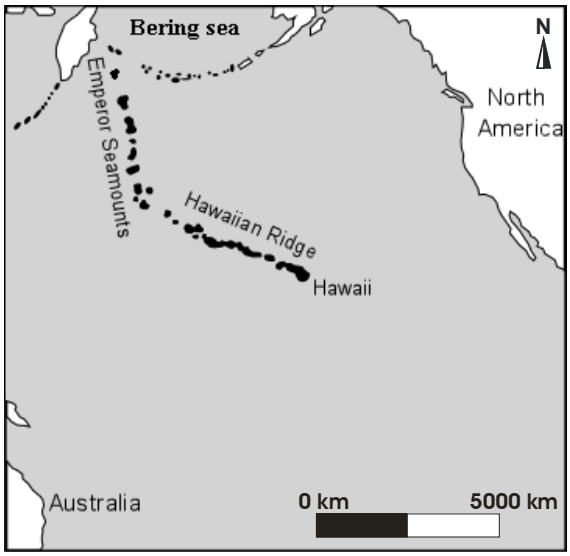

Figure 1-1 Hawaiian and Emperor Sea mount hot spot track.

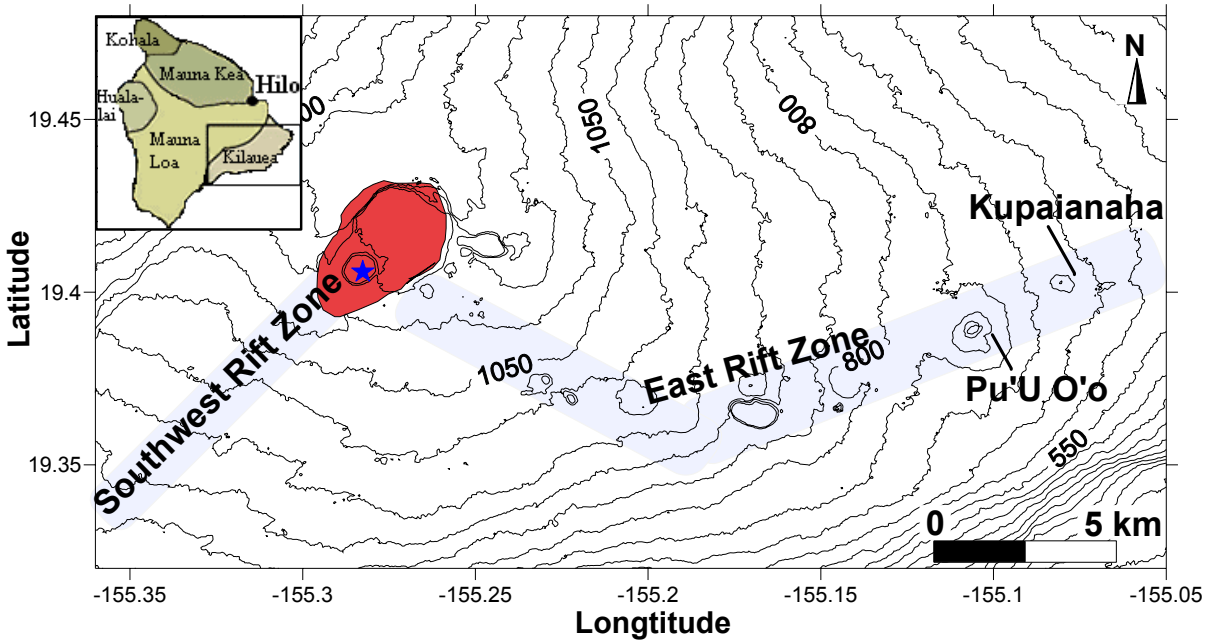

Figure 1-2 Topographic map of Kīlauea with the summit caldera highlighted in red, both rift zones in gray and a blue star representing the current summit vent in the summit pit crater of Halema'uma'u. Inset: Big Island of Hawaii with the 5 volcanic centres of the island.

All of these volcanoes are basaltic in composition and form large broad shield complexes. Mauna Loa, Kīlauea, Hualalai, and Lo'ihi have erupted from well defined rift zones that connect through their summits. Kīlauea's two rift zones, the Southwest Rift Zone and the East Rift Zone connect to Kīlauea's summit caldera (Fig. 1-2). Kīlauea's East Rift Zone has been historically more active than the Southwest Rift Zone and is center of the current ongoing eruption of Pu`u `Ō`ō – Kupaianaha.

1.1.2 The Formation and Evolution of the Hawaiian Islands

The first precursor to the accepted theory of hot spots and formation of the Emperor-Hawaiian island chain was described by Wilson (1963). He suggested that the Hawaiian Islands were created due to a stationary source of magma while the Pacific plate moved over it. Later Christofferson (1968) coined the term hotspot and included the Emperor Sea mounts as part of the Hawaiian island trend. He also suggested that the characteristic bend at the intersection of the two chains, is caused by a change in plate movement. The modern theory of mantle plumes in a reference frame that is fixed relative to the Earth's axis of spin was put forward by Morgan (1972). Magnetic data collected from the rocks of the Hawaiian Islands agrees with this theory by suggesting that the rocks throughout the island chain had been formed at nearly the same magnetic latitude. The mantle plume theory cannot explain all observations, as convection cells within fluids with similar properties to that of the mantle become unstable with time (Turcotte and Oxburgh, 1978). Partial melting of material from the theorized heat source at the core mantle boundary also cannot reproduce

Hawaiian lavas (Turcotte and Oxburgh, 1978). Many authors have suggested variations on the mantle plume model (e.g., Green, 1971; Richter, 1973; Anderson, 1975; Richter and Parson, 1975) to explain the source of increased heat flow, but none have gained the same support as Morgan's (1972) original theory. One theory that does not require a change in the thermal properties of the mantle is the fracture propagation theory. Dana (1849) was the first to suggest a propagating fracture system as the cause of the Hawaiian volcanic chain. This theory has gone through many revisions and adaptations by numerous authors (e.g., Stearns, 1946; Eaton and Murta, 1960; Jackson and Wright, 1970; Jackson and Shaw, 1975) and while it lacks hard evidence, it does have a few advantages. In its current form, the propagating-fracture theory relies on the stresses created by plate tectonics and not an abnormal, unknown source of heat in the asthenosphere to drive volcanism.

Hot spot theories can explain why there is volcanism in the middle of the Pacific Ocean; however, they do not explain the relative positions of each volcano. It has been suggested from their age and position that Hawaiian volcanoes lie in two different curving lines (e.g., Moore et al., 1982). One line includes Hualalai, Mauna Loa, and Lo'ihi and other Kohala, Mauna Kea and Kīlauea. In other words, Kīlauea is related to Mauna Kea, as Lo'ihi is related to Mauna Loa. This pattern can be traced back towards the island of Maui, however, it becomes much harder to trace with the older volcanoes. None of the current hotspot models can explain all the kinematic, chemical, and physical observations.

Previous studies on the eruptive history of Hawaiian volcanoes show that there were at least four stages to their eruptive behaviour (Stearns, 1946; Macdonald and Abbott, 1970; Clague and Dalrymple 1987). Clague and Dalrymple (1987) revised the original classification scheme to reflect new petrological data from the youngest volcano in the island chain, Loihi. Their four stages are: 1) pre-shield stage with alkalic lavas, 2) shield stage with theoleiitic lavas, 3) post-shield alkalic stage with alkalic lavas and 4) rejuvenation stage with alkalic and highly differentiated lavas. The pre-shield stage represents the birth of the volcano and its initial infrequent submarine eruptive phase, lasting approximately 250 ka (Macdonald and Abbott, 1970). Geochemical studies of mantle xenoliths in pre-shield lavas suggest that no intermediate or shallow magma chambers had time to develop (Clague, 1987). The shield building stage has voluminous and frequent eruptions that provide about 95% of the total volume of the volcano. It lasts approximately 500 ka with significant time spent erupting underwater. Xenolith and geochemistry data suggest that the increase in volume also results in a more complex magma storage system, with probably two separate magma chambers (Clague, 1987). The post-shield alkalic stage represents a decline in both the frequency and volume of eruptions and a return to the eruption of alkalic lava. This stage is not represented in some Hawaiian volcanoes such as Ko'olau and Lana'i. The final rejuvenation phase is also not shown by every volcano and usually takes place after a significant quiescent period of 400 ka to 2 ma. At this point, the volcanic edifice is generally highly

eroded and infrequent and low volume eruptions are usually confined to existing stream channels.

1.1.3 Kīlauea's Eruptive History and Activity

Kīlauea volcano is currently in its shield phase erupting theolitic lava, with its first eruption estimated to be 300,000 to 600,000 years ago. The largest challenge building a detailed geologic history for Kīlauea is that approximately 70 % of the volcano's surface is younger than 500 years and about 90% is younger than 1100 years (Holcomb, 1987). This means that past events such as caldera formation must be pieced together with poor constraints on age. Kīlauea has probably had many different summit calderas, caused by cycles of infill and collapse, with the oldest inferred caldera forming 1500 to 2100 years ago (Powers, 1948). The timing of the modern caldera has been pieced together through the reinterpretation of oral Hawaiian traditions and geologic evidence to be between 540 to 570 years ago (Swanson, 2008). The first written record detailing an eruption at Kīlauea was 33 years after it occurred as native Hawaiians told the story to Ellis (1823). At this time, the summit was the centre of sustained activity with an active lava lake at the lowest part of the caldera. Sustained summit activity continued to fill in the caldera with minor collapses, often in conjunction with infrequent rift zone eruptions (Holcomb, 1987). Continuous sustained summit activity ended in 1924 after the lava column at the summit dropped and an earthquake swarm propagated down the East Rift Zone (Jagger and Finch, 1924; Stearns 1926). No subaerial eruption occurred, but the lowered lava column led to 17 days of phreatic explosions and caused the

collapse of the caldera around Halema'uma'u. The next 44 years consisted of intermittent eruptions at both the summit and rift zones with an increasing concentration at the East Rift Zone after 1955.

The eruption of Mauna Ulu began in May 1969 and lasted until June 1974 (Swanson et al, 1979; Duffield et al, 1982). Besides being the longest eruption since 1924, it was also the first time that a sustained volcanic eruption had been observed outside the summit region. Following brief eruptions at the summit and Southwest Rift Zone, the second largest Hawaiian earthquake, recorded at a 7.2 magnitude, took place on November 29, 1975. In the following 8 years, intrusions into East Rift Zone dominated the volcanic activity of Kīlauea instead of the more common eruptive behaviour before the earthquake (Holcomb, 1987). In January 1983, the eruption of Pu`u `Ō`ō - Kupaianaha started and continues at the time of this writing.

Figure 1-3 Pu'U O'o cone in 2004 looking up at West Gap from approximately 1.5 km

Figure 1-4 View from the summit of Pu'U O'o looking east towards the current erupting vents 2.25 km down rift from Pu'U O'o, 2008.

The Pu`u `Ō`ō – Kupaianaha eruption is the most significant and largest eruption outside of the summit in at least 600 years (Heliker and Mattox, 2003). It covers an area larger than 121 km^2, its eruptive products total about 3.3 km^3 and has led to the destruction of 202 structures over the last 25 years (Heliker and Mattox, 2003).The eruption has now progressed through four different epochs. The first epoch began with the start of the eruption on January 3, 1983 and lasted 3.5 years with episodic fire fountaining that mostly erupted from a vent that was later called Pu`u `Ō`ō (Heliker and Mattox, 2003). The eruptive products from this epoch consist of a large cinder cone (Pu`u `Ō`ō) and many `a`a flows. The second epoch, which lasted 5.5 years, started when the eruption moved down rift 3.25 km to Kupaianaha in July 1986 (Heliker and Mattox, 2003). With a

change in location, the style of the eruption also changed to continuous effusive activity. Kupaianaha flows built a large shield and pahoehoe tubes that flowed to the ocean. The third epoch saw a return of activity to Pu`u `Ō`ō in March 1992 and lasted for the next 15.5 years (Heliker and Mattox, 2003). The nearly continuous activity filled the crater of Pu`u `Ō`ō and built a large shield complex while passively feeding pahoehoe through tubes towards the ocean. The fourth epoch began on June 17, 2007 when the summit of Kīlauea rapidly deflated and an intrusion and small eruption took place up rift of Pu`u `Ō`ō (Poland et al., 2008). In response, the floor of Pu`u `Ō`ō collapsed and caused a pause in the eruption. The summit began to re-inflate shortly after the intrusion and small eruption finished. Effusive activity returned to Pu`u `Ō`ō on July 1, quickly filling the majority of the crater as the summit continued to inflate. Kīlauea's summit began to deflate rapidly after a new fissure opened up on the east side of Pu`u `Ō`ō (Poland et al., 2009). This changed the focus of the eruption to 2.25 km down rift from Pu`u `Ō`ō or 1 km up rift of Kupaianaha. Eruptive activity continues at present and is dominated by continuous effusive behaviour of pahoehoe tubes feeding an ocean entry. From the start of the second epoch, the eruption has been nearly continuous and completely centered on Pu`u `Ō`ō and Kupaianaha. The notable exceptions are the short-lived Napau fissure eruption (1997), short-lived Father's day dike intrusion/eruption (2007), and ongoing Summit eruption (March 2008 – ongoing).

Starting in March 2008, the summit of Kīlauea became an active site of an ongoing eruption with a series of explosions taking place from a vent on the east

side of Halemau'ma'u. The Hawaiian Volcano Observatory (HVO) GPS network recorded continual summit contraction from the initiation of the new eruptive fissure (July 2008) on the flank of Pu`u `Ō`ō until late 2009 to early 2010 (per. Comm; Poland, 2010). Meanwhile, seismic tremor levels at the summit started to increase beyond previous background levels in November 2007 and by early 2008, levels were 5 times larger than the previous background (Wilson et al., 2008, Poland et al., 2009). Starting in late December 2007, SO_2 gas levels at summit increased beyond background levels of 400 metric tonnes per day and by time of the first explosion on March 19, 2008, SO_2 levels had almost reached 1600 t d^{-1}. This was the highest SO_2 level recorded at the summit since measurements were started in 1979 (Wilson et al., 2008). The first explosion sent dense rock fragments over an area of 50 hectares but no juvenile material was erupted (Wooten et al., 2009). Night time video observations recorded the first juvenile material ejected on Mach 22-23, 2008. Eight explosions took place from the vent during 2008 with the sixth explosion on September 2nd, being the largest. Throughout 2008, incandesce was often observed from the summit vent indicating magma was close to the surface (Wooten et al., 2009). By June 2009, the vent had reached a diameter of over 120 m and there had been visual observations of the rise and fall of magma levels. Very long period (VLP) and long period (LP) seismic events, continued high levels of SO_2, vent wall collapse, and rise and fall of the magma levels in the vent represent the typical activity from the summit vent since the last large explosion on October 12, 2008.

Figure 1-5 Ash cloud from Kīlauea's summit vent in Halemau'ma'u after a very long period seismic event on May 8, 2009.

1.1.4 Pertinent Previous Studies

Kīlauea is possibly the best studied volcano in the world and thus there is too much material to synthesize here. However, there are few geophysical studies which look at Kīlauea with either gravity or magnetic data. Hildenbrand et al. (1993) used aeromagnetic data from 1978 and 1986 to study the subsurface structure and properties of the entire Big Island of Hawaii. The study used a number of processing techniques to filter shallow anomalies from the data set to investigate broad subsurface features. In the resulting magnetic map (Fig. 1-6),

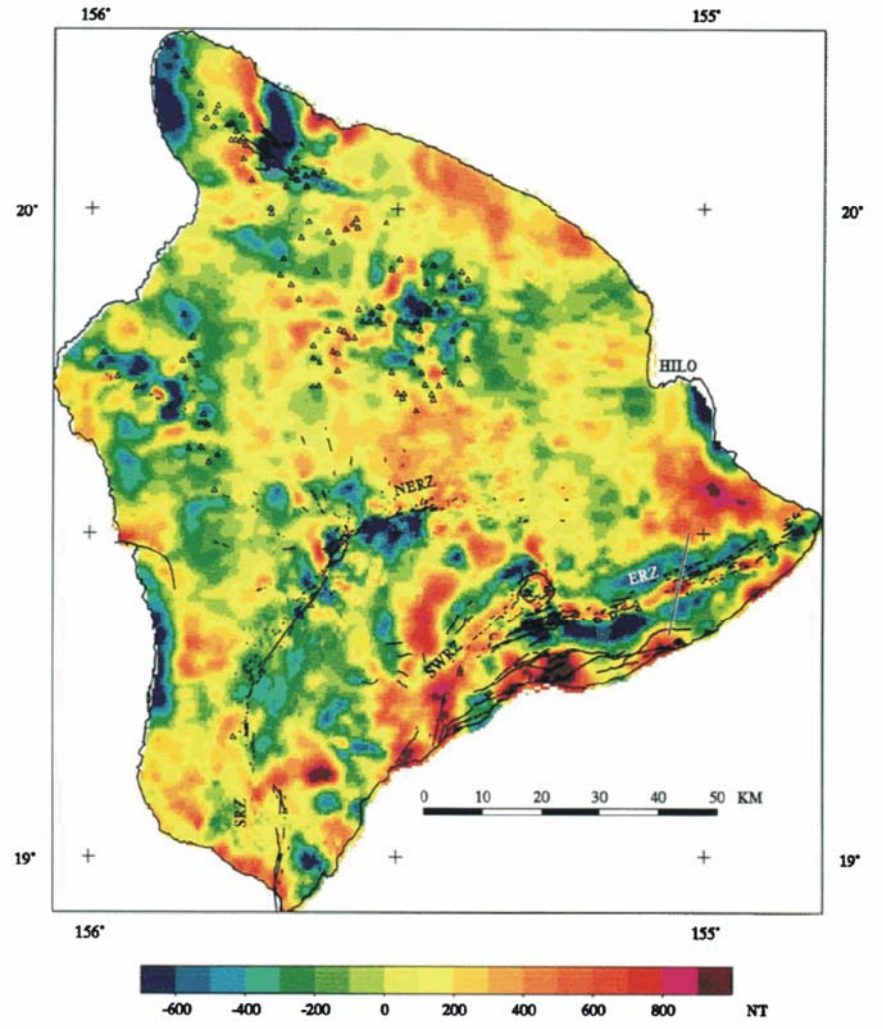

Figure 1-6 Residual aeromagnetic map of the Big Island of Hawaii. From Hildenbrand et al. (1993) where ERZ is Kīlauea East Rift Zone, SWRZ is Kīlauea's Southwest Rift Zone, NERZ is Mauna Loa's Northeast Rift Zone and SRZ is Mauna Loa's South Rift Zone.

Kīlauea's East Rift Zone is shown as areas of high field strength flanked by magnetic lows and are interpreted as an intrusive complex surrounded by hydrothermally altered rock (Hildenbrand et al., 1993). The resolution of the data is insufficient to resolve changes over small areas (it was flown at 300 m above

topography) and thus may miss important shallow features associated with structure within the caldera.

There have been several gravity surveys on the Big Island of Hawaii utilizing both Bouguer and microgravity survey techniques (Chapter 3). Kauahikaua et al. (2000) interpret the results of 3300 gravity measurements distributed across the Big Island of Hawaii. The coarse Bouguer gravity anomaly map shows the rift zones of Kĩlauea and Mauna Loa as dense linear features that connect to dense bodies at their summits. They interpret the dense bodies as intrusive complexes; the dense intrusion beneath Kĩlauea's summit is calculated to be 5-6 km below sea level. Microgravity data sets go back to 1975 where the first two surveys were made before and after the large volcano tectonic (7.2 magnitude) earthquake in 1975 (Jachens and Eaton, 1980). These datasets showed that gravity decreased in the summit region of Kĩlauea following the earthquake and were interpreted to represent the creation of void space. Since then, microgravity surveys have been periodically made in Kilauea's summit region (e.g., Kauahikaua and Miklius, 2003; Johnson et al., 2010). The results show that the gravitational field on the southern edge of Halema`uma`u in Kĩlauea's summit caldera has been increasing since the 1975 earthquake until June 2008 (Bagnardi et al., 2008; Johnson et al., 2010). This is remarkable as it is uncorrelated to volcanic activity. The decreases detected between the gravity surveys in 2008 are likely a short term decrease related to the summit activity. Two hypotheses put forward to explain the mass increase are the formation of an olivine cumulate fractionating from the magma supply to the volcano and the

filling of void space (Bagnardi et al, 2008; Johnson et al., 2010). Johnson et al. (2010) reject an olivine cumulate as the cause of the gravity signal as this would require a continual influx of fresh magma and associated deformation. Regardless, it is unknown how a dense body at depth or large amounts of void space may affect volcanic activity, Kīlauea's shallow plumbing system or the current summit eruption.

Kīlauea periodically has transient deformation events (DI events and DID events where D: Deflation, and I: Inflation) that start at the summit and propagate down the East Rift Zone to Pu`u `Ō`ō. Typically the DI or DID events start with rapid decaying deflation corresponding to a decrease in eruptive output at the eruption site. Cervelli and Miklius (2003) used tilt data from DID transient deformation events to infer that the source is centred just east of Halema`uma`u at a depth of 450 m below the surface and interpret these events as being due to blockages in the magma supply from a shallow summit reservoir.

1.1.5 Outline of Present Work

One of the objectives for this project is to test further hypothesis put forward by Dan Johnson's study (Johnson et al., 2010) suggesting that the filling of void space is responsible for an increasing gravitational field. To accomplish this, a Bouguer gravity survey and a total magnetic survey were completed to build a static picture of material property variations beneath the floor of Kīlauea's summit caldera (Chapter 3). The recent summit activity has also lead to an increase in interest regarding the shallow summit plumbing system. The static picture obtained through magnetic and gravity techniques should provide

information on the geological structures at depth which control how material is transported near the surface. In order to investigate temporal changes in mass flux associated with the activity of the summit vent, a gravimeter was deployed to continuously measure the gravitational field. This is then used to identify processes that occur within the shallow magmatic system to better understand the dynamic nature of the recent summit activity (Chapter 2).

1.2 Las Sierras-Masaya Volcanic complex, Nicaragua

1.2.1 Location

The Las Sierras-Masaya volcanic complex (often referred to as just Masaya volcano) (11.984°N, 86.161°W) is part of the Central America Volcanic Arc that includes volcanoes from Mexico to Panama, and is formed by the subduction of the Cocos plate beneath the Caribbean Plate on the margin of the Pacific Ocean (Fig. 1-7). Nicaragua is one of many Central American countries that host a large number of volcanic centres along the Cocos subduction zone, with 18 potentially active volcanic centres. The most persistently active volcano in Nicaragua is Masaya volcano, which has been well studied because of this activity as well as ease of access. However, as with the extreme resources at Kīlauea, many questions still remain regarding the structure and eruptive activity at Masaya.

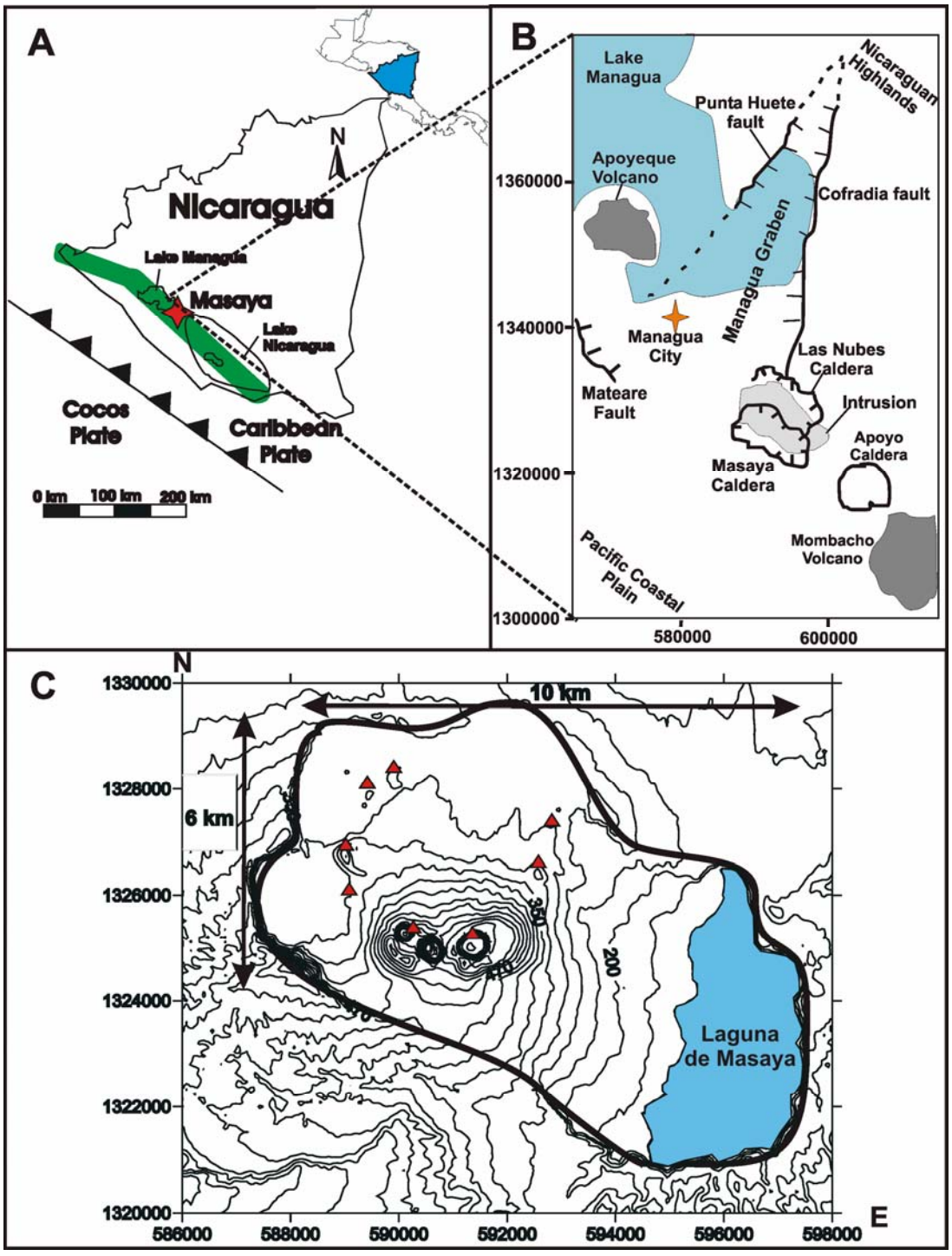

Figure 1-7 A) Inset of Central America with a map of Nicaragua and the location of Masaya represented by a red star and the Central American volcanic arc highlighted in salmon. B) Location of the Managua Graben with respect to Las Sierras-Masaya volcanic complex (modified from Girard et al., 2005). C) Topographic map centered on Masaya Caldera with each cone represented by an orange triangle. Names and labels of the major cones and pit craters are in Fig 1-8.

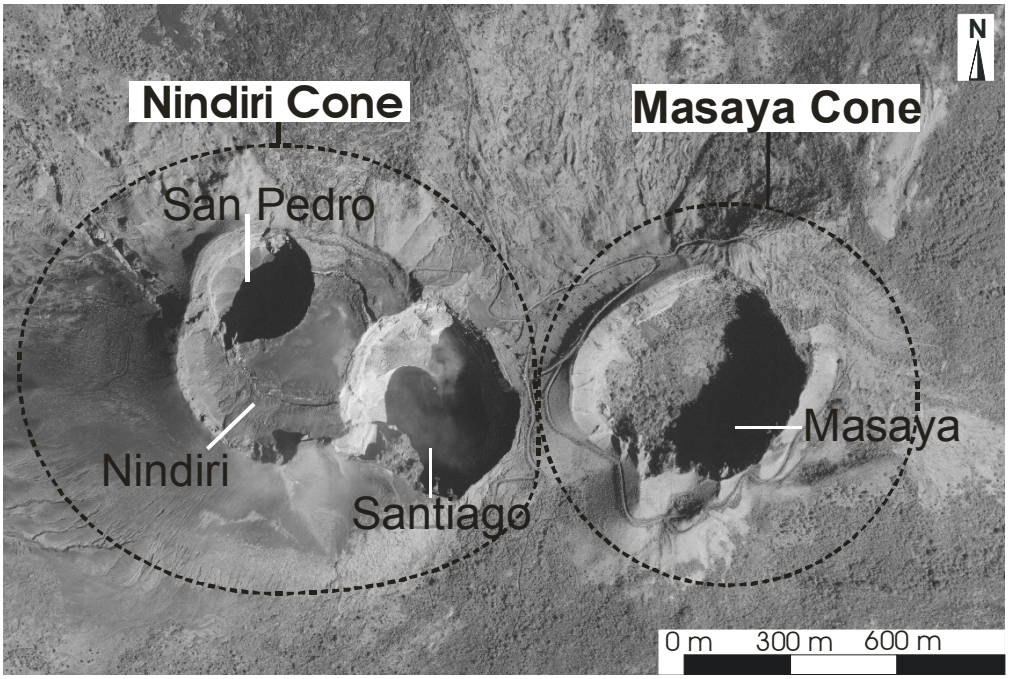

Figure 1-8 Aerial photo of Masaya and Nindir cones outlined with dashed lines and each pit crater labelled (San Pedro, Nindiri, Santiago, and Masaya).

1.2.2 Geological Setting

Las Sierras-Masaya is a basaltic caldera complex which sits within the Nicaraguan Depression on the southern end of the Managua Graben. The Managua Graben is the most active tectonic feature in Nicaragua and has been interpreted as a pull-apart basin (Sebesta, 1997) (Fig 1-7b). There is significant scientific debate about the effect of tectonic stresses from both the Caribbean and the Pacific plate on the Managua Graben and associated volcanism (e.g., Burkart and Self, 1985; van Wyk de Vries, 1993; van Wyk de Vries and Merle, 1998). Volcanism at Masaya is likely related to the Managua Graben, however, the link is still not clear. Girard and van Wyk de Vries (2005) suggest that the

Managua Graben is the result of a large intrusive complex associated with volcanism centred at Las Sierras-Masaya instead of being due to tectonic stresses. This idea is based on analogue models that show that a large ductile intrusion beneath Masaya volcano can cause pull-apart features in response to transtensive regional stresses.

The Las Sierras-Masaya volcanic complex consists of a set of nested calderas (Perez et al., 2009); the largest and oldest caldera is Las Sierras (15 km by 15 km) and the youngest is Masaya caldera (6 km by 11 km) (Van Wyk de Vries, 1993). From evidence of basaltic fallout deposits, each caldera probably formed through numerous basaltic Plinian eruptions (Williams, 1983). Based on dated fallout deposits, Masaya caldera formed 6000 years ago with the eruption of the San Antonio Tephra (Pérez and Freundt, 2006). Kutterrolf et al. (2007) estimate the total fallout tephra volume of the San Antonio Tephra to be 13.5 km^3. In addition to the initial caldera forming eruptions, two other Plinian eruptions took place 2100 and 1800 years ago with tephra volumes of 3.4 and 6.6 km^3, respectively. Masaya caldera has therefore been in its present shape since the last large Plinian eruption 1800 years ago.

The volcanic edifices within the Masaya caldera primarily consist of two cinder cone complexes called Nindiri and Masaya, which together form a broad shield (Fig. 1-8). Masaya cone hosts one large pit crater that shares the same name (Masaya crater). Masaya cone has not been the centre of activity since 1772, when a fissure opened on the northeast side and erupted basaltic a'a lava. Nindiri cone contains a nested set of pit craters; the largest is Nindiri crater, with

San Pedro and Santiago crater nested within it (Fig 1-7). Historical activity is best characterized by repeat formation/collapse of lava lakes and strong persistent degassing at one of the central pit craters (Rymer et al., 1998; Willams-Jones et al., 2003). At least five degassing episodes have occurred since 1852, which have led to significant environmental damage in the local area. The most recent degassing episode started in 1993 and continues at present. Since 1852, an estimated 10 km^3 of basaltic magma has degassed while only a very small amount has erupted (Stoiber et al. 1986). Currently, all visible activity is concentrated in Santiago crater and has been since it formed in 1858-1859, with one exception in 1909 where gas issued from fissures on the north side of Masaya cone (McBriney and Williams 1965; Rymer et al., 1998).

During the ongoing degassing crisis, small short term changes to the observed activity have occurred. Wall collapses from the edges of Santiago crater periodically block the actively degassing vents at the crater bottom. In some cases, this can cause the pressure build until a minor explosion takes place clearing the blockage. These explosions typically send small ash plumes several hundred meters in the air and eject juvienile and crater wall material around the crater rim. Small Strombolian explosions have also been observed and must occur with some frequency as indicated by deposits of Pele's hair within Nindiri crater (Moune et al., 2007).

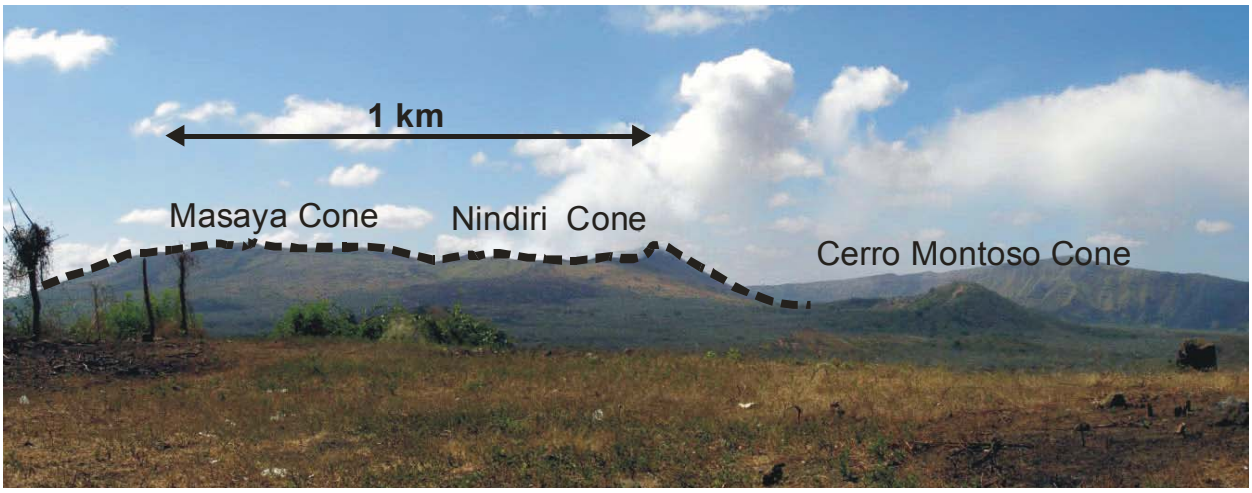

Figure 1-9 View from the edge of Masaya caldera looking south towards the basaltic shield of Masaya and Nindiri cones (dashed line).

1.2.3 Pertinent Previous Studies

Processes that control degassing at Masaya have been investigated by a number of different researchers (e.g., Rymer et al., 1998; Williams-Jones, 2003; Stix, 2007). Rymer et al (1998) used gravity measurements and visual observations to study the structure and evolution of Santiago crater. They observed that Nindiri, San Pedro and Santiago pit craters are actively changing through wall collapse and subsidence. They suggest that the area beneath the craters must then be a chaotic region with pockets of magma and gas. Rymer et al. (1998) also concluded that the current degassing crisis did not occur due to an injection of new material in 1993 but instead that a convective overturn in the plumbing system brought gas rich material closer to the surface. Williams-Jones et al., (2003) made gas and microgravity measurements at Masaya volcano and observed a correlation between gas flux and gravity. An increase in gas flux

corresponded to a decrease in gravity measured around the active craters of Santiago and Nindiri. To explain this correlation, Williams-Jones et al. (2003) suggest that an increase in gas increases the size of a low density foam layer of magma and gas beneath Santiago crater.

Coarse resolution Bouguer gravity surveys of Masaya volcano have been carried out in the past by Metaxian (1994) and Conner et al. (1989). Both surveys show a large positive anomaly offset northward from the caldera. This is interpreted to be a deep basaltic intrusion which likely predates the current volcanism as it is not centred beneath the current caldera. The Metaxian (1994) study's resolution was significantly better than Conner et al. (1989) and found gravity lows associated with both Masaya and Nindiri cones. No new Bouguer surveys have been done at Masaya volcano, however, work has been done to reprocess the existing data with better constraints on elevation (Pascal, 2008). While the error in the dataset was reduced, there was no improvement in the resolution.

1.2.4 Outline of Present Work

Masaya's shallow magmatic plumbing system is dynamic and changes frequently. Observational evidence for this includes changing glow intensities, new vent formation, and inferred dynamic cavern structure beneath Santiago crater. Bouger gravity and total magnetic surveys were completed in order to acquire a high spatial resolution map inside Nindiri cone on the lava plain between San Pedro and Santiago craters (Chapter 3). Gravity and magnetic results obtained through this study are compared with previous survey results

and modelled. These models will enable a more detailed interpretation of the shallow magmatic plumbing system.

1.3 Three Sisters Volcanic complex

1.3.1 Location

The Cascade volcanic arc stretches from northern California to south-western British Columbia and is caused by the subduction of the Juan de Fuca plate beneath North America (Fig 1-9). Volcanism in the Washington to British Columbia part of the arc is localized at discrete volcanic centers separated by significant distances. In central Oregon, arc volcanism forms a volcanic plateau with hundreds of volcanic vents rather than a few localized centers (Bacon, 1985; Guffanti and Weaver, 1988; Sherrod and Smith, 1990). The Three Sisters Complex is one of many volcanic centers in this area with a complex history and a wide range of eruptive products ranging from basaltic to rhyolitic compositions. The peaks of Three Sisters have local historical names (beginning from the north) "Mount Faith", "Mount Hope", and "Mount Charity". These names are not commonly used therefore the three peaks will be referred to throughout the thesis as North, Middle and South Sister (Fig 1-11).

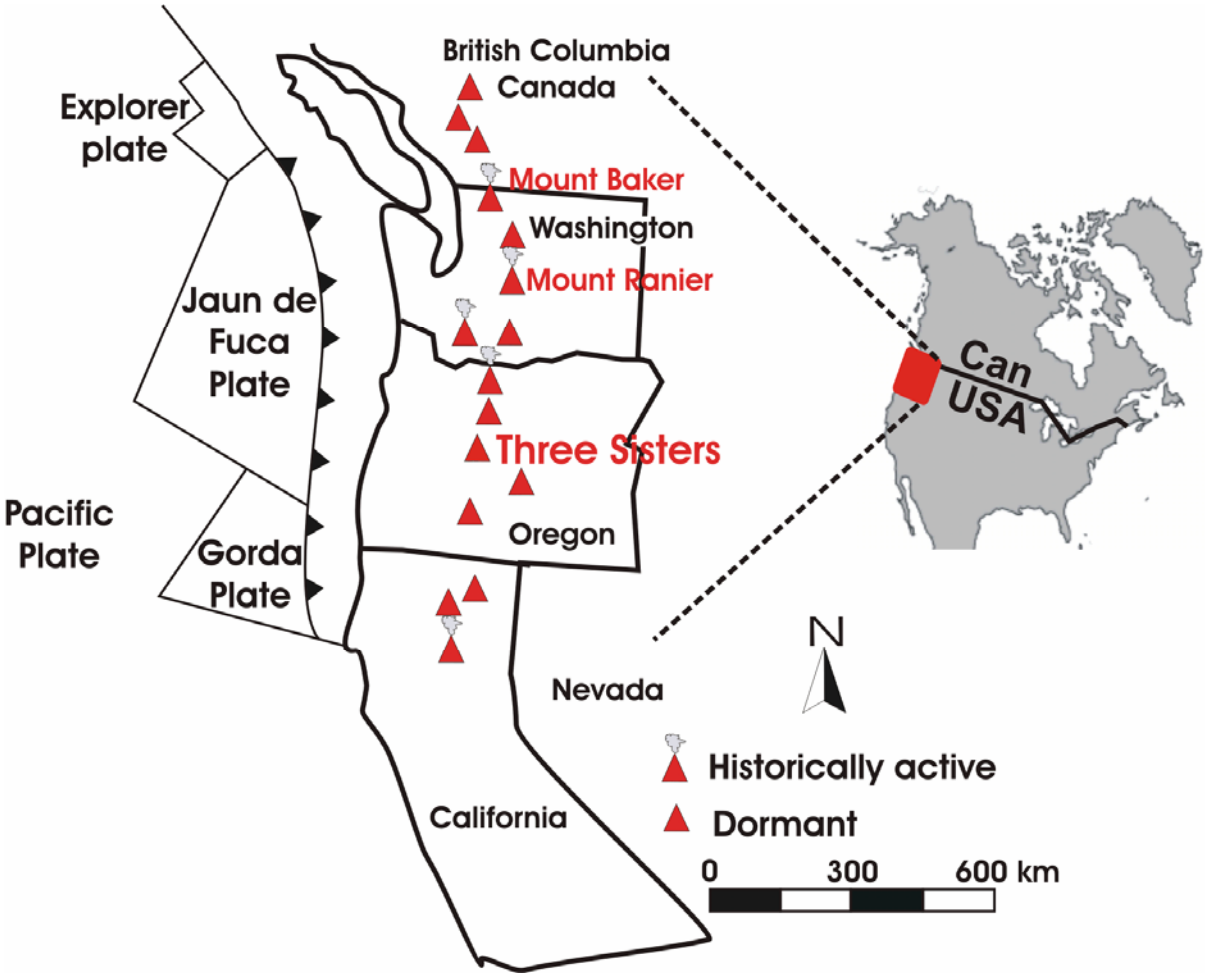

Figure 1-10 The Cascade Volcanic Arc with major volcanic centres denoted by red triangles and select volcanic centers labelled in red. Inset: North America with the Cascade Volcanic Arc highlighted in red.

1.3.2 Geologic Setting

The central Oregon section of the Cascade volcanic arc has produced more Cenozoic vents and lava than any other part of the arc. There is a wide range of estimates for the rate and amount of volcanic products erupted during the Cenozoic. Priest (1990) and Sherrod and Smith (1990) estimated volcanic volumes from detailed geologic maps and average them to a volume per kilometer of arc, per million years. They obtained estimates

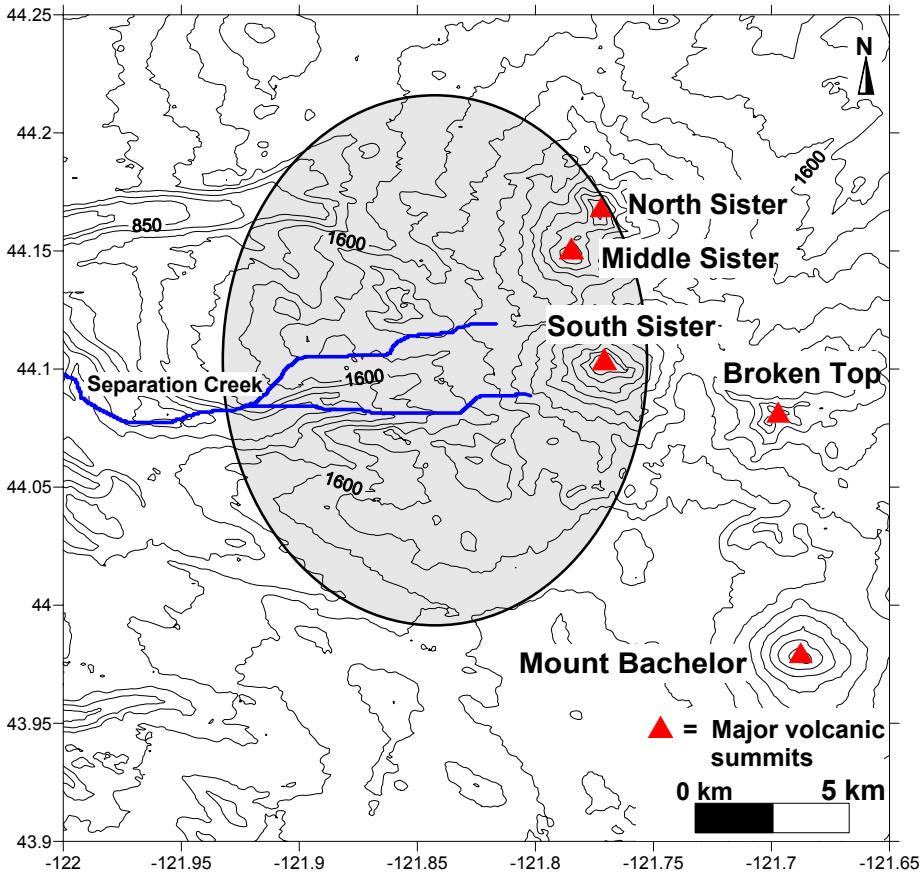

Figure 1-11 Topographic map of the Three Sisters Volcanic Complex with the grey circle representing the approximate area affected by the current deformation event. Five large Quaternary cones are indicated with red triangles.

ranging from 3 to 12.3 km^3 km^{-1} Ma^{-1} for the volcanic intrusive rate over the last 0.73 Ma. The large range in supply rates is due to different assumptions on the rate of subsidence in grabens in Central Oregon. Regardless of which rate is used, it is significantly higher than the eruptive rate from Mount Jefferson northward to British Columbia with 1.6 km^3 km^{-1} Ma^{-1} along the arc.

Tectonic stresses in the Oregon Cascades also differ from the rest of the arc to the north as they are in an extensional stress regime (Priest 1990). Geological evidence includes normal faults near Newberry volcano and the

orientations of vents and dykes showing a vertical principal stress over the last 7 Ma. This seems to be coincident with plate reconstructions that suggest subduction off the coast of Oregon has become more oblique by a factor of 7 over the last 40 Ma (Verplank and Duncan, 1987). The obliqueness of subduction has also been used to explain how the coasts of southwestern Washington and Oregon have been rotated clockwise as interpreted from paleomagnetic measurements. The total clockwise rotation has been estimated from 18˚ to 36˚ at a steady rate of 1.3˚ my^{-1} near the coast (e.g., Beck and Burr, 1979; Bates et al., 1981; Magill et al., 1981; Beck et al., 1986; Dzurisin et al., 2009). The rate of rotation decreases inland and to the north and the pivot zone is thought to be in south central Washington near Mount Rainer (Wells, 1990). The continued rotation due to oblique convergence between the Juan de Fuca plate and North America is the probable cause for both the change in tectonic stresses and the increased eruptive output of the Oregon section of the arc (e.g., Priest 1990).

The Central Oregon Cascades also has a significantly increased regional heat flow that corresponds to a large wavelength gravity anomaly (Blackwell et al., 1982, 1990); it averages over 100 mW m^{-2} in comparison to 60 mW m^{-2} in the Washington section of the arc. The high heat flow raises both the brittle ductile transition zone and the Curie point for rocks in the area. This effect has been observed through aeromagnetic surveys where ground-based heat flow measurements agree well with areas of a shallow Curie point isotherm (Blackwell et al., 1990). The raising of the brittle ductile transition zone is proposed to explain the lack of historical seismic events in the area (eg., Weaver and

Michaelson, 1985). The Three Sisters volcanic complex is within the 100 mW m^{-2} heat flow contour and may reflect an elevated brittle ductile transition zone (Blackwell et al., 1982, 1990).

There are five large Quaternary aged cones that dominate the area including: North Sister, Middle Sister, South Sister, Broken Top, and Mount Bachelor (Fig 1-10, 1-11). The ages of most of the volcanic edifices in the Three Sisters region are not known precisely. North Sister is a basaltic andesite cone older than 300,000 years B.P. and is the oldest of the Three Sisters (Taylor, 1987). Middle Sister is intermediate in age between South and North Sister, with compositionally diverse eruptive products from basalt to rhyolite (Scott et al., 1987). The heavily eroded, deeply dissected Broken Top is older than South Sister, however, its age relative to Middle or North Sister is unknown (Hill and Taylor, 1989). Mount Bachelor is a large basaltic shield volcano and is the northern most cone in the Mount Bachelor volcanic chain. Based on dated glacier deposits, the cone is between 11,000 and 15,000 years old.

South Sister is the youngest cone and like Middle Sister, is compositionally diverse with erupted products ranging from ryholite to basalt. During the last period of volcanic activity, approximately 2000 years ago, South Sister erupted rhyolite tephra and lava flows (e.g., Taylor, 1978; Wozniak, 1982; Scott, 1987; Taylor, 1987). There has also been considerable eruptive activity away from the main cone with 10s of monogenetic vents erupting over the last 4000 years (Taylor, 1981; Hill, 1985; Scott et al., 2001). The most recent eruptive

event away from the main cones occurred approximately 1500 years ago, north of South Sister, with an eruption of basaltic and andesitic lavas.

While most eruptions from the Three Sisters area have been small, there have been exceptions recorded in the rock record. Large Plinian eruptions have occurred at least four times in the last 700,000 years (Scott et al., 2001). Based on fall deposits, volumes for some of the eruptions are estimated between 10 km^3 and 20 km^3 (Hill, 1985). Eruptions of this magnitude are rare, and have not occurred since the formation of the Three Sisters. There is also no evidence of hydrothermal heat or activity to support the presence of a large silicic magma chamber.

Starting in 1998, the ground in the Separation creek drainage area on the northwest side of South Sister began to deform and uplift (Wicks et al., 2002) (Fig. 1-10). The only notable seismic activity recorded with deformation was a seismic swarm in March 2004, following six years of aseismic deformation (Dzurisin et al., 2006). This is the only known activity in region for the last 1500 years and has been the focus of several studies.

Figure 1-12 Three Sisters Volcanic Complex looking approximately North at four of the major volcanic edifices in the area.

1.3.3 Pertinent Previous Studies

The Three Sisters Complex has not been historically active and hence, until recently, there has been little interest in this dormant system. Wicks et al. (2002), using interferometry synthetic aperture radar (InSAR) images, discovered that the ground southwest of South Sister was deforming aseismically. Starting at the beginning of 1998, the ground deformed at a steady rate of 3 to 5 cm yr^{-1} near Separation creek northwest of South Sister. Deformation point source

models based on the InSAR data indicate a source depth of 6.5 km which was interpreted as an intrusion with a volume of 2.3 x 10^7 m^3 (Wicks et al., 2002). Since then, campaign GPS, levelling, ground water geochemical, and gravity surveys were performed to quantify the deep-seated process.

The first spring water geochemistry study in the Three Sisters area was completed in 1994 prior to the start of the deformation event (Ingebritsen et al., 1994). The study shows that there was a mantle derived component of CO_2 and chlorine in the drainage of Separation creek suggesting a wide but low energy hydrothermal system. A second study in 2001 in the Separation creek drainage area, at the centre of the deforming area, attempted to detect change within the hydrothermal system (Evans et al., 2004). This study confirmed the presence of mantle-derived components but did not find any increase in hydrothermal activity. The steady state of the hydrothermal system suggests that the intrusion may be too deep to affect the surface water and that previous intrusive episodes are controlling the hydrothermal system in the Separation creek drainage.

The slow continuation of the deformation event (1998 - 2010) has created a laboratory in which to study and monitor the deep intrusive process. Continuous GPS, campaign GPS and levelling have been the principal datasets used to describe and update deformation models. The most recent models (Dzurisin et al., 2009) describe the intrusion as a prolate spheroid at a depth of about 5 km. The associated volume change is calculated to be between 37 and 46 x 10^6 m^3 for the deformation through August 2006 (Dzurisin et al., 2009). The mechanism that is most favoured for the cause of the deformation is the intrusion

of basaltic material at the brittle ductile transition zone (Wicks et al., 2001; Dzurisin et al., 2006, 2009). In total, three possible models were purposed as possible causes of the ongoing deformation event. The first conceptual model has the crust responding hydraulically to the continual injection of material at depth. The second is a viscoelastic response as the crust relaxes after an intrusion at depth. The final and least likely, conceptual model is uplift due to the pressurization of hydrothermal systems.

1.3.4 Outline of Current Work

In 2002, Dr. Dan Johnson (formally of the University of Puget Sound) set up a small network of 5 microgravity stations that stretch from the edge of the deforming area to its centre. Dr. Johnson collected microgravity data in 2002, 2004, and 2005. Before he could complete the study, he died tragically in 2005. The main objective of the work at the Three Sisters was to complete this study. In October 2008 and September 2009, two more gravity surveys were completed and by providing constraints on the mass flux from 2002 to 2009, it should be possible to test which of the three conceptual models put forward by Dzurisin et al. (2006, 2009) is the most likely.

1.4 Thesis Structure

The main chapters, excluding the introduction and conclusion, are written in manuscript form with the aim of eventual publication in appropriate peer-reviewed journals. This will lead to some repetition, however, this allows for each chapter to be read separately without needing references to the other chapters.

As with most publications, there are many authors that have contributed to each individual study, however, the majority of the work presented here is my own. It is important to note Chapter 4 in this regard, as the survey design and much of the field work (2002-2005) was done by Dr. Dan Johnson, however, data processing, modelling, and interpretation are my own. Detailed methodologies for Chapters 2, 3 and 4 can be found in Appendix 1 for gravity surveys and Appendix 2 for total magnetic surveys.

Gravity and magnetic survey methods were applied in three different volcanic areas to investigate volcanic plumbing structures and processes at a range of spatial and temporal resolutions. In Hawaii, on Kīlauea volcano, different gravity surveys were used to study the magmatic processes at two different depth and time scales. In Chapter 2, continuous gravity measurements were employed to investigate short period and shallow (less than 500 m deep) processes associated with transient deformation events at the summit of Kīlauea. In Chapter 3, static Bouguer gravity and total magnetic surveys were used to identify structures to depths greater than 1 km on Masaya and Kīlauea volcanoes. The surveys are then compared in order to investigate the differences between these basaltic systems and how their magmatic plumbing systems function. In the last chapter (Chapter 4), microgravity surveys were completed from 2002 to 2009, to investigate the continuing deformation event at Three Sisters Volcanic Complex. The surveys show long period changes associated with the deformation event and provide information to determine the cause of the event at depth.

Regardless of location or survey type, the aim of these studies is to increase the understanding of the volcanic processes involved in transport of material from depth to the surface.

1.5 Reference List

Anderson, D.L., 1975, Chemical plumes in the mantle: Geological Society of American Bulletin, v. 86, p. 1593-1600.

Bacon, C.R., 1985, Implications of silicic vent patterns for the presence of large crustal magma chambers: Journal of Geophysical Research, v. 90, p. 11,243-11,252

Bagnardi, M., Eggers, A.A., Battaglia, M., Poland, M.P., and Johnson, D.J., 2008, Mass intrusion beneath Kilauea Volcano, Hawaii, constraints from gravity and geodetic measurements: American Geophysical Union, Fall Meeting 2008.

Bargar, K.E., and Jackson, E.D., 1974, Calculated volumes of individual shield volcanoes along Hawaiian-Emporer Chain: Geological Survey Journal of Research, v. 2, p. 545-550.

Bates, R.G., Beck, M.E., and Burmester, R.F., 1981, Tectonic rotations in the Cascade Range of southern Washington: Geology, v. 9, no. 4, p. 184-189.

Beck, M., Burmester, R., Craig, D., Gromme, C., and Wells, R., 1986, Paleomagnetism of middle Tertiary volcanic rocks from the Western

Cascade series, northern California: Journal of Geophysical Research, v. 91, p. 8219-8230.

Beck, M.E., and Burr, C.D., 1979, Paleomagnetism and tectonic significance of the Goble Volcanic Series, southwestern Washington: Geology, v. 7, no. 4, p. 175-179.

Bhattacharyya, B.K., and Leu, L., 1975, Analysis of magnetic anomalies over Yellowstone National Park: mapping of Curie point isothermal surface for geothermal reconnaissance: Journal of Geophysical Research, v. 80, no. 32, p. 4461-4465.

Blackwell, D., Bowen, R., Hull, D., Riccio, J., and Steele, J., 1982, Heat flow, arc volcanism, and subduction in northern Oregon: Journal of Geophysical Research, v. 87, no. B10, p. 8735-8754.

Blackwell, D., Steele, J., Frohme, C., Murphey, G., Priest, G.R., and Black, G., 1990, Heat flow in the Oregon Cascade Range and its correlation with regional gravity, Curie point depths, and geology: Journal of Geophysical Research, v. 95, no. B12, p. 19475-19493.

Burkart, B., and Self, F., 1985, Extension and rotation of crustal blocks in northern Central America and effect on the volcanic arc: Geology, v. 13, p. 22-26.

Carbone, D., Buetta, G., Greco, F., and Zuccarello, L., 2007, A data sequence acquired at Mt. Etna during the 2002-2003 eruption highlights the potential of continuous gravity observations a tool to monitor and study active volcanoes: Journal of Geodynamics, v. 43, p. 320-329.

Cervelli, P.F., and Miklius, A., 2003, The Shallow Magmatic System of Kilauea Volcano: U.S. Geological Survey Professional Paper 1676, p. 149-163.

Christofferson, E., 1968, The relationship of sea-floor spreading in the Pacific to the origin of the Emperor Seamounts and the Hawaiian Island chain: EOS American Geophysical Union Transactions, v. 49, p. 214.

Clague, D.A., 1987, Hawaiian xenolith populations, Magma supply rates, and development of magma chambers: Bulletin of Volcanology, v. 49, no. 4, p. 577-587

Clague, D., A., and Dalrymple, B.G., 1987, The Hawaiian Emperor Volcanic chain Part 1 Geologic evolution: U.S. Geological Survey Professional Paper, 1350, p. 5-54.

Connor, C.B., Williams, S.N., Lawe, D.K., and Draper, G., 1989, Interpretation of Gravity Anomalies, Masaya Caldera Complex, Nicaragua: Transactions of the 12th Caribbean Conference, St. Croix, v. 12, p. 495-502.

Dana, J.D., 1849, Geology, United States Exploring Expedition, durring the years 1838, 1839, 1840, 1841, 184, under the command of Charles Wilkes: U.S.N: Philidephia, v. 10, p. 756.

Duffield, W.A., Christiansen, R.L., Koyanagi, R.Y., and Peterson, D.W., 1982, Storage migration, and eruption of magma at Kilauea Volcano, Hawaii 1971-1972: Journal of Volcanology and Geothermal Research, v. 13, p. 273-307.

Dzurisin, D., Lisowski, M., and Wicks, C.W., 2009, Continuing Inflation at Three Sisters volcanic center, central Oregon Cascade Rand, USA, from GPS, leveling, and InSAR observations: Bulletin of Volcanology, v. 71, no. 10, p. 1091-1110.

Dzurisin, D., Lisowski, M., Wicks, C.W., Poland, M.P., and Endo, E.T., 2006, Geodetic observations and modeling of magmatic inflation at the Three Sisters volcanic center, central Oregon Cascade Range, USA: Journal of Volcanology and Geothermal Research, v. 150, no. 1-3, p. 35-54.

Eaton, J.P., and Murata, K.J., 1960, How volcanoes grow: Science, v. 132, p. 925-938.

Ellis, W., 1823 (Reprinted Honolulu 1917), A narrative of tour through Hawaii: London, p. 367.

Evans, C.W., Soest, C.M., Mariner, H.R., Hurwitz, S., Ingebritsen, S., Wicks, C.W., and Schmidt, M., E., 2004, Magmatic intrusion west of Three Sisters,

central Oregon, USA; the perspective from spring geochemistry: Geology, v. 32, no. 1, p. 69-72.

Garcia, M.O., Rubin, K.H., Norman, M.D., Rhodes, J.M., Graham, D.W., Muenow, D.W., and Spencer, K., 1998, Petrology and geochronology of basalt breccia from the 1996 earthquake swarm of Loihi seamount, Hawaii: magmatic history of its 1996 eruption, Springer Berlin / Heidelberg, 577 p.

Girard, G., and van Wyk de Vries, B., 2005, The Managua Graben and Las Sierras-Masaya volcanic complex (Nicaragua); pull-apart localization by an intrusive complex: results from analogue modeling: Journal of Volcanology and Geothermal Research, v. 144, p. 37-57.

Green, D.H., 1971, Composition of basaltic magma as indicators of origin: Application to oceanic volcanism: Philosophical Transactions of the Royal Society of London, Series A, v. 268, p. 707-725.

Gudmundsson, M.T., and Milsom, J., 1997, Gravity and magnetic studies of the subglacial Grímsvötn volcano, Iceland: Implications for crustal and thermal structure: Journal of Geophysical Research, v. 102, no. B4, p. 7691-7704.

Guffanti, M., and Weaver, C.S., 1988, Distribution of late Cenozoic volcanic vents in the Cascade Range: Volcanic arc segmentation and regional tectonic considerations: Journal of Geophysical Research, v. 93, p. 6513-6529.

Heliker, C., and Mattox, T.N., 2003, The first two decades of the Pu'u 'Ō'ō-Kūpaianaha eruption: chronology and selected bibliography: U.S. Geological Survey Professional Paper 1676, p. 1-27.

Hildenbrand, T.G., Rosenbaum, J.G., and Kauahikaua, J.P., 1993, Aeromagnetic study of the Island of Hawaii: Journal of Geophysical Research, v. 98, no. B3, p. 4099-4119.

Hill, B.E., 1985, Petrology of the Bend Pumice and Tumalo Tuff, a Pleistocene Cascade eruption involving magma mixing: Corvallis, Oregon State University, M.S. Thesis (unpublished).

Holcomb, R.T., 1987, Eruptive History and long-term behavior of Kilauea volcano: U.S. Geological Survey Professional Paper 1350, p. 261-350.

Ingebritsen, S., Mariner, H.R., and Sherrod, D.R., 1994, Hydrothermal Systems of the Cascade Range, north-central Oregon U.S. Geological Survey Profesional Paper, v. 1044-L, p. 86.

Jachens, R.C., and Eaton, G.P., 1980, Geophysical observations of Kilauea volcano, Hawaii, 1. Temporal gravity variations related to the 29 November, 1975, M = 7.2 earthquake and associated summit collapse: Journal of Volcanology and Geothermal Research, v. 7, no. 3-4, p. 225-240

Jackson, E.D., and Shaw, H.R., 1975, Stress fields in central positions of the Pacific plate: deliniated in time by linear volcanic chains: Journal of Geophysical Research, v. 80, p. 1861-1874.

Jackson, E.D., and Wright, T.L., 1970, Xenoliths in the Honolulu Volcanic series, Hawaii: Journal of Petrology, v. 11, p. 405-430.

Jagger, T.A., and Finch, R.H., 1924, The explosive eruption of Kilaueain Hawaii: American Journal of Science, v. 8, no. 5, p. 353-374.

Johnson, D.J., Eggers, A.A., Bagnardi, M., Battaglia, M., Poland, M.P., and Miklius, A., 2010, Shallow magma accumulation at Kīlauea Volcano, Hawai‘i, revealed by microgravity surveys: Geology, v.38 p. 1139-1142.

Kauahikaua, J., Hildenbrand, T., and Webring, M., 2000, Deep magmatic structures of Hawaiian volcanoes, imaged by three-dimensional gravity models: Geology, v. 28, no. 10, p. 883-886.

Kauahikaua, J., and Miklius, A., 2003, Long-term trends in microgravity at Kīlauea's summit durring the Pu`u `Ō`ō - Kupaianaha eruption: U.S. Geological Survey Professional Paper 1676, p. 165-171.

Kutterolf, S., Freundt, A., and Peréz, W., 2008, Pacific offshore record of plinian arc volcanism in Central America: 2. Tephra volumes and erupted masses: Geochemistry, Geophysics, Geosystems, v. 9, no. 2, p. Q02S02.

Macdonald, G.A., and Abbott, A.T., 1970, Volcanoes in the sea: University of Hawaii Press, p. 441.

Magill, J., Cox, A., and Duncan, R., 1981, Tillamook Volcanic Series: Further evidence for tectonic rotation of the Oregon Coast Range: Journal of Geophysical Research, v. 86, no. B4, p. 2953-2970.

McBriney, A.R., and Williams, H., 1965, Volcanic history of Nicaragua: University of California Publications in Geological Sciences, v. 55, no. 65.

Metaxain, J.P., 1994, Etude sismologique et gravimetrique d'un volcan actif. Dynamisme interne et structure de la Caldeira Masaya Nicaragua, Unpublished PhD Thesis. University of Savoie, Chambery, France,

Moore, J.G., Clague, D.A., and Normark, W.R., 1982, Diverse basalt types from Loihi seamount, Hawaii: Geology, v. 10, no. 2, p. 88-92.

Morgan, W.J., 1972, Deep mantle convection plumes and plate motions: American Association of Petroleum Geologists Bulletin, v. 56, p. 201-213.

Moune, S., Faure, F., Gauthier, P-J., and Sims, K.W.W., 2007, Pele's hairs and tears: Natural probe of volcanic plume: Journal of Volcanology and Geothermal Research, v. 164, no. 4, p. 244-253

Okubo, Y., and Shibuya, A., 1993, Thermal and crustal structure of the Aso volcano and surrounding regions constrained by gravity and magnetic data,

Japan: Journal of Volcanology and Geothermal Research, v. 55, no. 3-4, p. 337-350.

Pascal, K., 2008, 3D Modelling of multi-parameter geophysical data from Masaya volcano, Nicaragua: BSc Honors Thesis, University of Leeds, Leeds, West Yorkshire, England.

Pérez, W., Freundt, A., Kutterolf, S., and Schmincke, H., 2009, The Masaya Triple Layer: A 2100 year old basaltic multi-episodic Plinian eruption from the Masaya Caldera Complex (Nicaragua): Journal of Volcanology and Geothermal Research, v. 179, p. 191-205.

Pérez, W., and Freundt, A., 2006, The youngest highly explosive basaltic eruptions from Masaya Caldera (Nicaragua): Stratigraphy and hazard assessment: Geological Society of America Special Papers, v. 412, p. 189-207.

Peterson, D.W., and Moore, R.B., 1987, Geologic history and evolution of geologic concepts, Island of Hawaii: U.S. Geological Survey Professional Paper 1350, p. 149-189.

Poland, M.P., Miklius, A., Orr, T., Sutton, J., Thornber, C., and Wilson, D., 2008, New episodes of volcanism at Kilauea Volcano: EOS American Geophysical Union Transactions, v. 89, no. 5, p. 37-40.

Poland, M.P., Sutton, J.A., and Gerlach, T.M., 2009, Magma degassing triggered by static decompression at Kilauea Volcano, Hawaii: Geophysical Research Letters, v. 36. p. L16306.

Powers, H.A., 1948, A chronology of explosive eruptions of Kilauea: Pacific Science, v. 2, p. 278-292.

Priest, G.R., 1990, Volcanic and Tectonic Evolution of the Cascade Volcanic Arc, Central Oregon: Journal of Geophysical Research, v. 95, no. B12, p. 19583-19599.

Richter, D.H., 1973, Convection and the large-scale circulation of the mantle: Journal of Geophysical Research, v. 78, no. 35, p. 8735-8745.

Richter, D.H., Eaton, J.P., Murata, K.J., Ault, W.U., and Krivoy, H.L., 1970, Chronological Narrative of the 1959-60 Eruption of Kilauea Volcano, Hawaii: U.S. Geological Survey Professional Paper 537.

Richter, D.H., and Parsons, B., 1975, On the interaction of two scales of convection in the mantle: Journal of Geophysical Research, v. 80, p. 2529-2541.

Rymer, H., 1996, Microgravity monitoring. Monitoring and Mitigation of Volcano Hazards: Springer-Verslag, Berlin, p. 169-168.

Rymer, H., and Brown, G.C., 1986, Gravity fields and the interpretation of volcanic structures: Geological discrimination and temporal evolution:

Journal of Volcanology and Geothermal Research, v. 27, no. 3-4, p. 229-254.

Rymer, H., 1994, Microgravity change as a precursor to volcanic activity: Journal of Volcanology and Geothermal Research, v. 61, no. 3-4, p. 311-328.

Rymer, H., van Wyk de Vries, Benjamin, Stix, J., and Williams-Jones, G., 1998, Pit crater structure and processes governing persistent activity at Masaya Volcano, Nicaragua: Bulletin of Volcanology, v. 59, no. 5, p. 345-355

Scott, W.E., 1987, Holocene rhyodacite eruptions on the flanks of South Sister volcano, Oregon in Fink, J.H., ed., The emplacement of silicic domes and lava flows: Geological Society of America Special Paper, v. 212, p. 35-53.

Scott, W.E., Iverson, R.M., Schilling, S.P., and Fisher, B.J., 2001, Volcano hazards in the Three Sisters Region, Oregon: U.S. Geological Survey Open-File Report 99-437.

Sebesta, J., 1997, Dynamic development of the relief in the Managua area, Nicaragua. Acta Universitatis Carolinae: Geographica, Universita Karlova. Thesis unpublished.

Sherrod, D.R., and Smith, J.G., 1990, Quaternary extrusion rates of the Cascade Range, northwestern United States and southern British Columbia: Journal of Geophysical Research., v. 95, no. B12, p. 19465-19474

Stearns, H.T., 1926, The Keaiwa or 1823 lava flow from Kilauea volcano, Hawaii: Journal of Geology, v. 34, p. 336-351.

Stearns, H.T., 1946, Geology of the Hawaiian Islands: Hawaii Divison of Hydrography Bulletin, v. 8, p. 105.

Stix, J., 2007, Stability and instability of quiescently active volcanoes: The case of Masaya, Nicaragua: Geology, v. 35, no. 6, p. 535-538.

Stoiber, R.E., Williams, S.N., and Huebert, B.J., 1986, Sulfur and halogen gases at Masaya Caldera Complex, Nicaragua: total flux and variations with time: Journal of Geophysical Research., v. 91, p. 12215-12231

Swanson, D.A., 2008, Hawaiian oral tradition describes 400 years of volcanic activity at Kīlauea: Journal of Volcanology and Geothermal Research, v. 176, no. 3, p. 427-431

Swanson, D., 2003, Kilauea's caldera and the Keanakako'i ash: Abstract volume, Cities on Volcanoes 3, Hilo, Hawaii p. 125.

Swanson, D.A., Duffield, W.A., Jackson, D.B., and Peterson, D.W., 1979, Chronological narrative of the 1969-71 Mauna Ulu eruption of Kilauea Volcano, Hawaii: Geological Survey Professional Paper 1056.

Taylor, E.M., 1978, Field geology of the SW quarter of the Broken Top quadrangle, Oregon: Special paper Oregon department of Geology and Mining Industry, v. 2, p. 1-50.

Taylor, E.M., 1981, Central High Cascades roadside geology, Bend, Sisters, McKenzie Pass, and Santiam Pass, Oregon in Johnston, D.A., and Donnelly-Nolan, Julie, eds., Guides to some volcanic terrains in Washington, Idaho, Oregon, and Northern California: U.S. Geological Survey Circular 838, p. 55-58.

Taylor, E.M., 1987, Field Geology of the northwestern quarter of the Broken Top 15 minute quadrangle, Oregon: Special paper Oregon department of Geology and Mining Industry, p. 1-20.

Turcotte, D.L., and Oxburgh, E.R., 1978, Intra-plate volcanism: Philosophical Transactions for the Royal Society of London. Series A, Mathematical and Physical Sciences, v. 288, no. 1355, p. 561-578.

van Wyk de Vries, B., 1993, Tectonics and magma evolution of Nicaraguan volcanic systems: Open University, Milton Keynes, UK, : PhD thesis (unpublished).

van Wyk de Vries, Benjamin, and Merle, O., 1998, Extension induced by volcanic loading in regional strike-slip zones: Geology, v. 26, p. 983-986.

Verplanck, E., and Duncan, R., 1987, Temporal variations in plate convergence and eruption rates in the western Cascades, Oregon: Tectonics, v. 6, no. 2, p. 197-209.

Weaver, C.S., and Michaelson, C., 1985, Seismicity and volcanism in the Pacific Northwest: Evidence for the segmentation of the Juan De Fuca Plate: Geophysical Research Letters, v. 12, no. 4, p. 215-218.

Wells, R.E., 1990, Paleomagnetic rotations and the Cenozoic tectonics of the Cascade Arc, Washington, Oregon, and California: Journal Geophysical Research., v. 95, p. 19409-19417.

Wicks, C.W., Dzurisin, D., Ingebritsen, S., Thatcher, W., Lu, Z., and Iverson, J., 2002, Magmatic activity beneath the quiescent Three Stisters volcanic center, central Oregon Cascade Range, USA: Geophysical Research Letters, v. 29, no. 7, p. 1122.

Williams, S.N., 1983, Plinian airfall deposits of basaltic composition: Geology, v. 11, no. 4, p. 211-214

Williams-Jones, G., Rymer, H., and Rothery, D.A., 2003, Gravity changes and passive SO_2 degassing at the Masaya caldera complex, Nicaragua: Journal of Volcanology and Geothermal Research, v. 123, no. 1-2, p. 137-160

Wilson, D., Elias, T., Orr, T., Patrick, M., Sutton, J., and Swanson, D., 2008, Small explosion from new vent at Kilauea's summit: EOS American Geophysical Union Transactions, v. 89, no. 22, p. 203.

Wilson, T.J., 1963, A possible origin of the Hawaiian Islands: Canadian Journal of Physics, v. 41, p. 863-870.

Wooten, K.M., Thornber, C.R., Orr, T.R., Ellis, J.F., and Trusdell, F.A., 2009, Catalog of tephra Samples from Kilauea's summit eruption, March-December 2008: U.S. Geological Survey Open-File Report 2009-1134.

Wozniak, K.C., 1982, Geology of the northern part of the southeast Three Sisters quadrangle, Oregon: Corvallis, Oregon State University, M.S. Thesis (unpublished).

2: RAPID VOLCANIC CHANGES AT KĨLAUEA VOLCANO, HAWAII, DETECTED BY CONTINUOUS GRAVITY MEASUREMENTS

Jeffrey Zurek, Glyn William-Jones, Mike Poland, Daniel Dzurisin , Tamar Elis, Todd Ericksen, Ben Brooks, David Wilson, Tim Orr

2.1 Abstract

Changes in volcanic activity are commonly associated with the transport of mass through the movement of magma, hydrothermal fluids and gas. By using continuous gravity measurements, mass flux associated with volcanic activity can be constrained and used in monitoring. In this study, continuous gravity data from a vent on the floor of Kĩlauea volcano's summit pit crater, Halema'uma'u, is presented and analyzed. A gravity anomaly (85 μGal in amplitude lasting 90 minutes) was recorded on May 9, 2009, during a transient deformation event. To further describe the observed anomaly and volcanic activity, RSAM, borehole tilt, SO_2 flux, LIDAR and infrasound data were recorded. Simple forward modeling based on continuous gravity measurements suggests that the gravity anomaly is best explained by a magma level rise of 75 to 90 m into the summit vent followed by rapid drain back. The conceptual model that best explains the signal and fits with the observed volcanic activity is a deep-seated volatile pulse, unconnected

to the deformation event, causing magma rise in the vent. This study clearly shows the importance of continuous gravity monitoring as component of a comprehensive volcano monitoring program.

2.2 Introduction

Kīlauea volcano is a broad shield volcano on the Big Island of Hawaii located directly over the Hawaiian hot spot. Kīlauea is one of the best monitored volcanoes in the world and has been in nearly continuous activity since the beginning of the Pu`u `Ō`ō – Kupaianaha eruption in January 1983, which continues at present. Starting in early 2007, SO_2 gas levels at the summit increased by approximately an order of magnitude above background levels. This was followed by a series of small explosions that took place on the floor of the Halema'uma'u pit crater located within the summit caldera of Kīlauea (Wooten et al., 2009). Juvenile spatter, ash and lithic blocks were ejected from Halema'uma'u during a second explosion on April 9, 2008; this was the first time in over 25 years that Kīlauea erupted juvenile material from the summit (Wooten et al., 2009). Incandescence and views of the lava surface have been observed periodically throughout this recent activity.

The new summit activity at Kīlauea provides the possibility to further investigate vent dynamics and the shallow magmatic system. One notable change in the shallow magmatic system is an increase in deflation-inflation (DI) events since the appearance of the summit vent. Prior to development of the summit vent, approximately 10 DI events were recorded per year, however, 47 DI

events were recorded in 2008. Deformation models, seismic studies and microgravity surveys point to shallow sources inferred to be a reservoir approximately 1 km below the surface near the Halema'uma'u pit crater (e.g., Ohminato et al., 1998; Dawson et al., 1999; Battaglia et al., 2003; Cervelli and Miklius, 2003; Johnson et al., 2010). Although DI events start at the summit, the deformation propagates down the East Rift Zone to the eruption site at Pu`u `Ō`ō. The deflation phase results in a decrease in eruptive flux, while the inflation phase leads to increased effusion (Cervelli and Miklius, 2003). Simultaneous observations of deformation and eruptive flux suggest that these events may be caused by interruptions in the magma supply to the shallow reservoir beneath Halema'uma'u (Cervelli and Miklius, 2003). If the deflationary phase of DI events is due strictly to the draining of the shallow summit reservoir, the mass flux should be measurable with continuous gravity studies. Furthermore, the level of lava in the open vent in the floor of Halema'uma'u should reflect the deeper process within the shallow magma chamber and show a decrease during the deflation portion of the DI event. However, to date, the 2002 eruption of Etna volcano, Italy, was the only example where continuous gravity monitoring successfully detected mass movement preceding an eruption, in this case due to magma rising passively through a dry fissure (Branca et al., 2003).

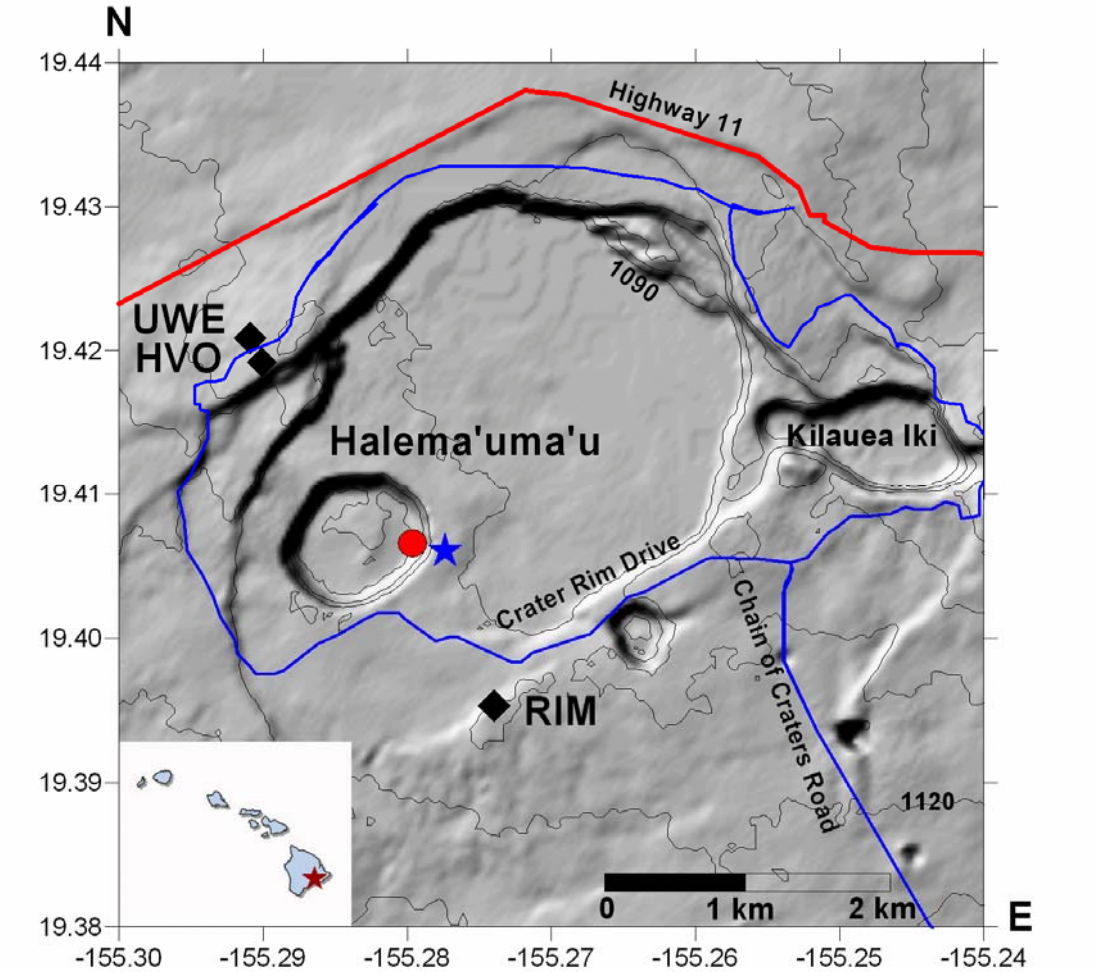

Figure.2-1 A shaded relief map of Kĩlauea's summit caldera with an inset of the Hawaiian Islands. The summit vent is outlined in red and the continuous gravity station is represented by the blue star on the rim of Halema'uma'u pit crater. The black diamonds represent the Hawaiian Volcano Observatory (HVO), the UWE tilt station and RIM broad band seismic station.

The current dynamic activity of Kĩlauea's summit vent is characterized by oscillations of the magma column, seismic events, and vent widening via collapse (Wooten et al., 2009). One method to increase our understanding of the processes that occur in the vent and shallow magmatic system is to constrain mass flux via gravity change (e.g., Eggers, 1983; Rymer, 1996). Although not previously observed in continuous gravity studies, large changes of the magma

levels within Kīlauea's summit vent should be relatively simple to detect. Significant changes in magma column heights within vents and lava lakes have been observed in past Hawaiian eruptions (e.g., Richter et al., 1970; Swanson et al., 1979). During the Mauna Ulu eruption (1969-1974), gas pistoning was described as a lava column rising up to 50 meters over the course of ten minutes to hours with a rapid and violent drain back (Swanson et al., 1979). Similar rise and fall in the current summit vent has also been observed with and without the violent drain back associated with gas pistoning. Eruption and magmatic flow models have been used to describe the mechanisms by which magmatic rise can occur (e.g., Jaupart and Vergniolle, 1988; Vergniolle and Jaupart 1990). However, in order to apply these models to real systems, a multi-parameter approach is required.

2.3 Experiment and Results

In order to investigate the DI events and the new summit vent activity at Kīlauea, a continuous recording gravimeter was installed on the rim of Halema'uma'u, directly above the vent (Fig. 2-1). Gravity measurements were collected during two periods from May 3 to 5 and May 7 to 11, 2009. The instrument, a LaCoste and Romberg spring gravimeter (G-127) was equipped with an Alliod feedback system, allowing for continuous data collection. The gravimeter was installed directly on a small outcrop of pahoehoe lava, covered to isolate it from wind and precipitation, and powered by two deep cycle marine batteries. The raw gravity data consists of 1 minute averages of measurements collected at 2 Hz. Seismic, deformation, and gas flux data used in this study were

recorded by the Hawaiian Volcano Observatory (HVO). The seismic data is in the form of real time seismic amplitude measurements (RSAM) averaged every minute (Fig. 2-2). The short period station (RIM) is approximately 1.2 km from the summit vent, while the tiltmeter data was recorded at 30 s intervals in the Uwekahuna vault (UWE), 2.1 km from the vent. SO_2 gas flux measurements were collected using a FLYSPEC ultraviolet spectrometer (Horton et al., 2006) along Crater Rim Drive with wind speed and direction recorded at HVO (Fig. 2-1). In addition, LIDAR (light detection and ranging) (e.g., Pesci et al., 2007) and infrasound data from a network maintained by M. Garces (University Of Hawaii) was used to constrain vent geometries and detectable audio sources, respectively (Fee et al., 2010). To characterize any environmental influence on the gravity data, ambient temperature, pressure and relative humidity measurements were obtained from the National Park Service at the Hawaiian Volcanoes National Park; these meteorological measurements were made every 15 minutes and resampled to match the gravity sampling rate (1 minute intervals).

Before the gravity data can be used to investigate any volcanic signals, it must be corrected for the effects of earth tide, ocean loading, atmospheric pressure and deformation (residual gravity). These corrections are discussed extensively in the literature (e.g., Rymer, 1989; Rymer, 1996; Battaglia et al., 2008) and hence will only be briefly described here. Deformation was not constrained at the gravity station; however based on summit tilt measurements, the amount of ground movement was small thus not corrected for. The

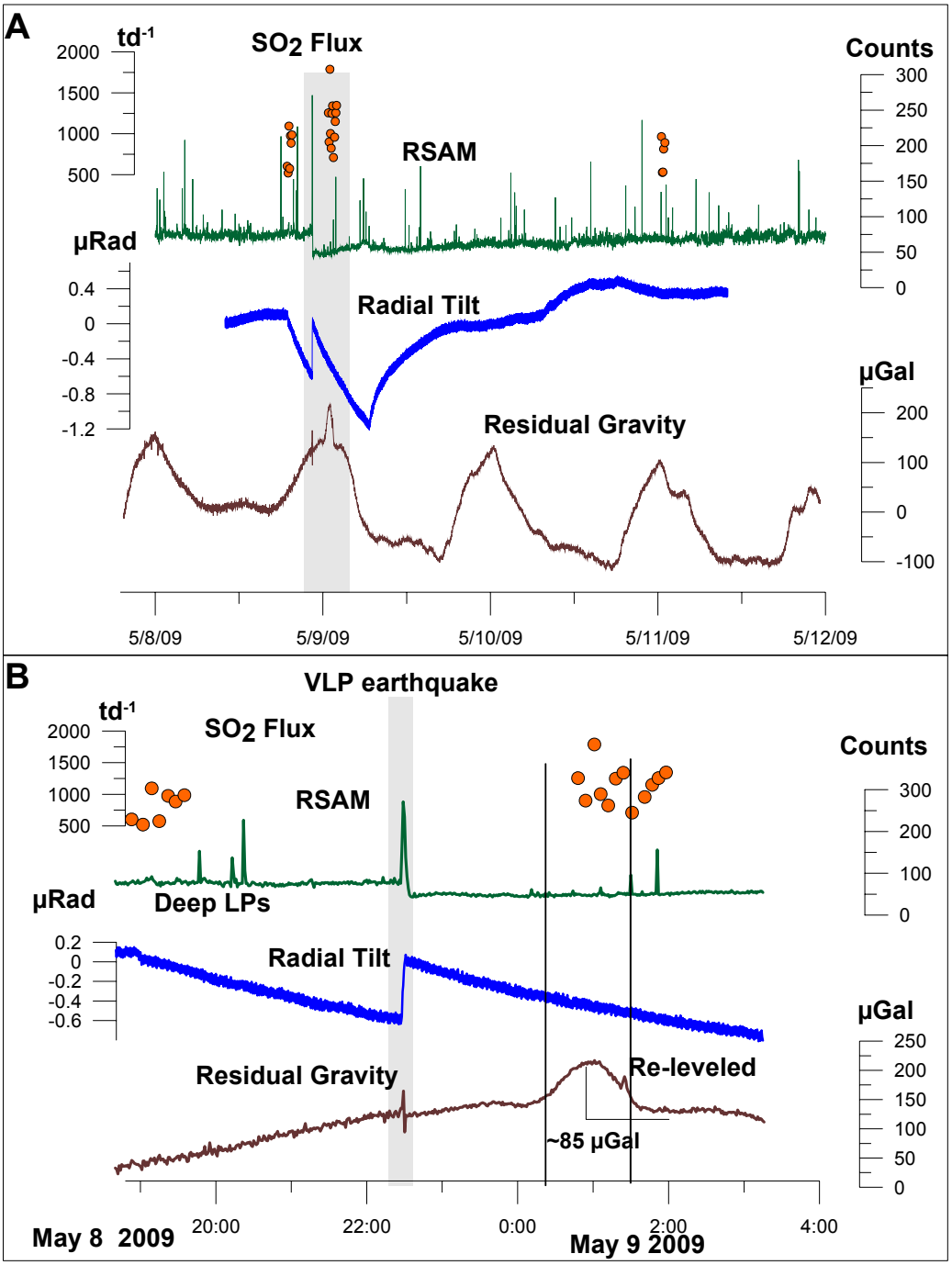

Figure 2-2 SO_2 flux (t d^{-1}, orange circles), real-time seismic amplitude measurements (RSAM, counts, green), radial tilt (µRad, blue) and residual gravity (µGal, brown) for May 7 to May 11 2009. A) The complete May 7 to 11 occupation with the observed gravity anomaly highlighted. B) A set of three deep LP events are shown. The recorded VLP is highlighted in grey across all datasets and two shallow LP events are represented by lines bracketing the gravity anomaly.

theoretical Earth tide and ocean loading corrections were calculated using QuickTide Pro software (Micro-g Lacoste). Atmospheric pressure was corrected using recorded weather data and a theoretical factor of 3.06 μGals per mbar (Boy et al., 1998). Although the summit of Kīlauea is an actively deforming region, the amount of measured vertical deformation was insignificant over the survey period (Fig. 2-2). The effects of temperature and humidity on gravity measurements are not constrained and remain part of the residual gravity signal, which has a regular daily oscillation throughout the deployment, with one exception, late on May 8 to early May 9 2009 (UTC) (Fig. 2-2).

During the deployment from May 7 to 11, a DI event was recorded by the HVO tilt network. The deflationary part of the DI event started at approximately 18:30 on May 8, 2009 (UTC). 48 minutes following the start of the DI, the first of 3 long period (LP) seismic events occurred, between 1.6 to 2.3 km below Halema'uma'u crater. 120 minutes following the start of the DI event, at 22:27, a very long period (VLP) seismic event was recorded by the tilt, seismic and infrasound networks, as well as the deployed gravimeter. The gravimeter, which can act as a long period seismometer, recorded the event as a 60 μGal spike (Fig. 2-2b). Immediately following the VLP, tremor levels at the summit dropped by a factor of 2 and 1.5 minutes after the start of the VLP, the gas plume rising out of the summit vent became ash rich. Two small LP seismic events occurred at 00:10 and 01:38 in the summit vent area at approximately 200 m depth. These two events bracket a short period spike in the gravity data (Fig. 2-2).

The first shallow LP seismic event is virtually coincident with the start of the gravity anomaly. The increase lasts 50 min. with an amplitude of 85 μGals at a rate of 1.7 μGals $min.^{-1}$. Following the peak in the anomaly, it decreases at a rate of 2.1 μGals $min.^{-1}$ for 45 min. as it returns to its original level (Fig. 2-2, 2-3). 5 minutes before the gravity signal levels out, the second shallow LP event occurs. In the time between the two shallow LP events, the tilt network recorded no change above its background level of 0.1 μrad and there were no locatable seismic events recorded in the summit region. Although continuous gas measurements are not available, FLYSPEC measurements were made before and after the VLP (Fig. 2-2). The second set of SO_2 gas measurements span the gravity signal and show an apparent increase from 800 +/- 230 metric tonnes per day ($t\ d^{-1}$) before the VLP to 1150 +/- 300 $t\ d^{-1}$. Direct observations made from the rim of Halema'uma'u include auditory changes in the character of the noise coming from the summit vent. Following the VLP event, there was an increase in rock fall activity and gas jetting noises from the vent. Subsequently, during the gravity anomaly, the sound from the summit vent became more characteristic of spatter and the rate of rock fall decreased.

LIDAR measurements were made in June 2009, approximately one month after the gravity occupation. The vertical distance from the rim of Halema'uma'u to the floor near the gravity occupation is 85 m and distance to lava surface was 292 m (Fig. 2-4). Although the shape of the vent may have changed over this time, there was no major collapse or widening of the vent between early May and

the LIDAR measurements; this data is thus used as the vent geometry for the purposes of modeling.

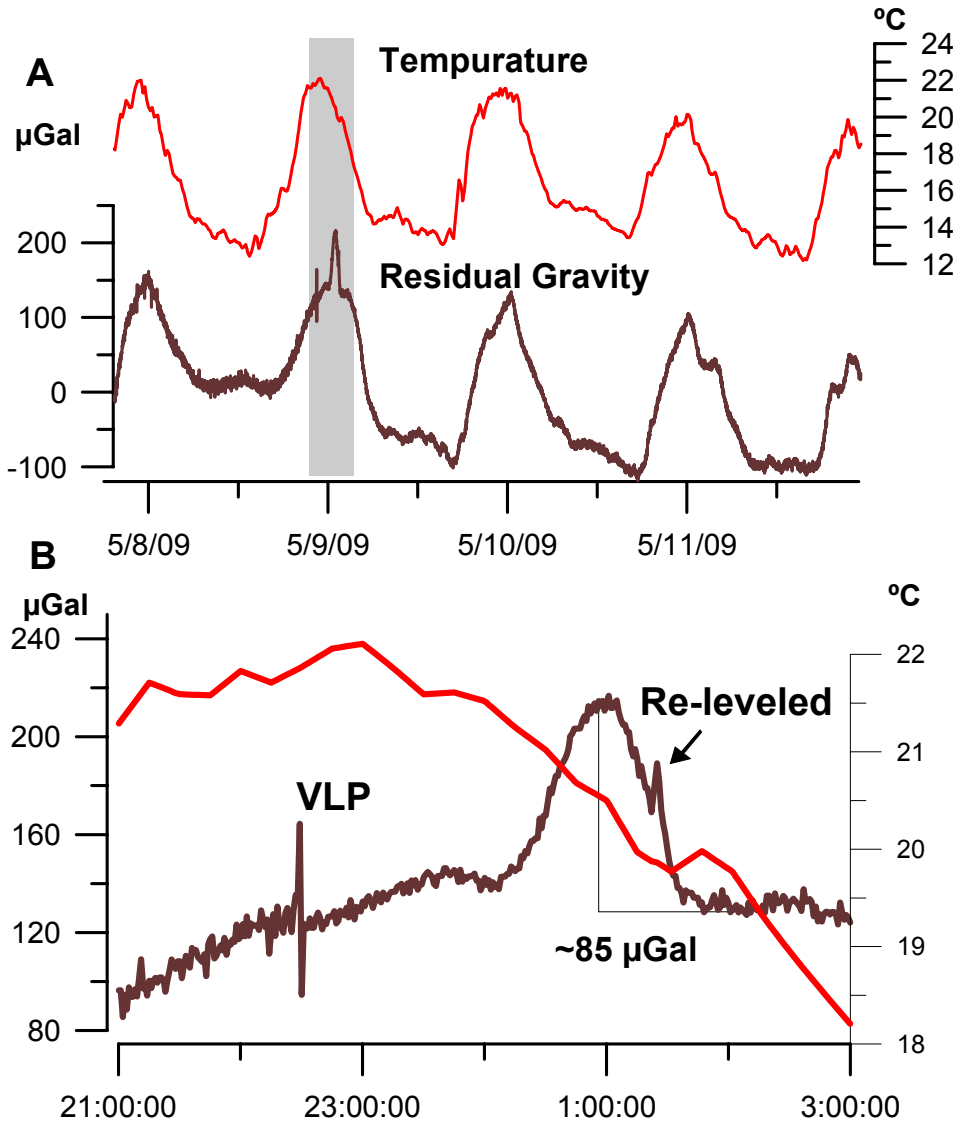

Figure 2-3 Residual gravity (brown) and ambient temperature (red) from A) May 7 to May 11, 2009; the highlighted region is displayed in B). A VLP event (22:37 May 8) and re-leveling of the instrument (01:22 May 9) are shown.

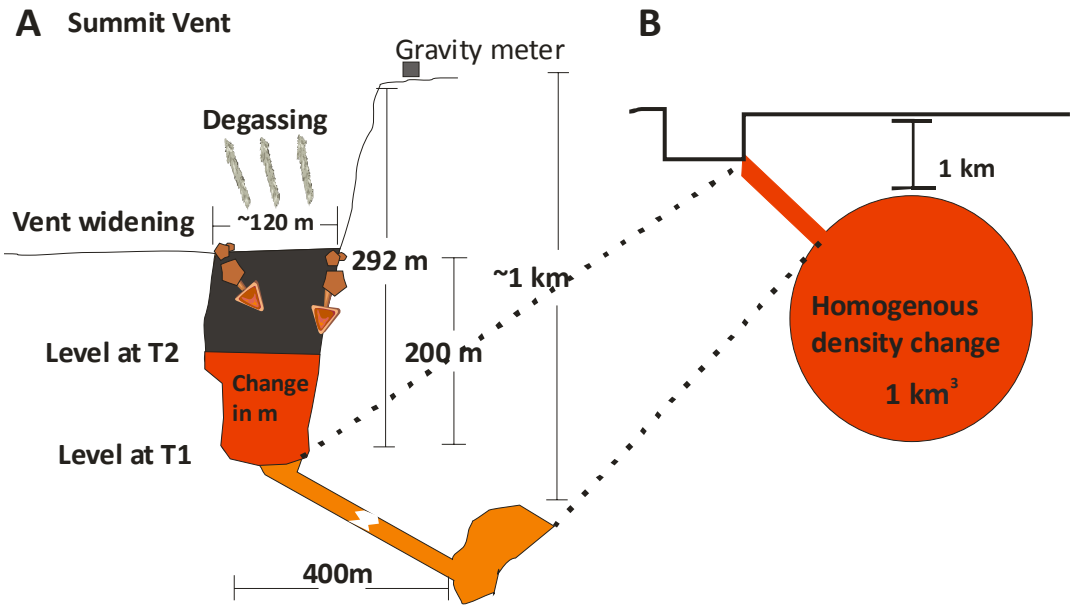

Figure 2-4 Schematics of the models used to test possible causes of the recorded gravity anomaly. A) Magma rise and fall from time T1 to time T2 within the summit vent. B) Tests of density variations in the shallow magmatic system including Kīlauea's summit reservoir.

2.4 Error Discussion

To date, continuous gravity has only been infrequently used as a continuous monitoring technique due to logistical difficulties and the need to control many different parameters (e.g., Carbone et al., 2007). Measurements with continuous spring gravimeters require a strict control of environmental parameters, or at the very least the ability to record and characterize them (Ando and Carbone, 2001; Battaglia et al., 2008). Although the internal instrument temperature is controlled by a thermostat, ambient temperature and pressure changes can result in large deviations in the measured gravity signal, due to temperature gradients within each instrument (El Wahabi et al., 1997). Ando and

Carbone (2004) used mathematical algorithms to remove the effect of temperature; however, the process requires a long standing data set at the measurement site to evaluate temperature correlations. Although there have been other attempts to quantify the effect of temperature on gravity signals (El Wahabi et al., 1997; Ando and Carbone, 2001, 2004, 2006), at this time, no direct correction exists which can be used for a short term survey.

The residual gravity data for both survey periods has a cosine shape that correlates strongly with temperature (Fig. 2-3). The correlation coefficient between the residual gravity signal and ambient temperature is 0.84, affecting any long period signals in the data set. However, short period events, unrelated to changes in temperature can be identified and analyzed. The short period event recorded early on May 9 (Fig. 2-2, 2-3) is the only event which can be definitively identified from the data set. There are no anomalous changes in ambient temperature, atmospheric pressure or humidity over the course of the short period event, ruling out atmospheric forcing. The recorded instrumental temperature and voltage levels also show no fluctuations. The instrument's tilt does change slightly over the deployment but this cannot account for the signal as there were no significant short period deviations recorded. The instrument was also re-leveled near the end of the gravity anomaly at 01:22 (May 9, 2009) causing the only data collection interruption and lasting for 45 seconds (Fig. 2-3). Re-leveling resulted in a small offset in the data but did not change the slope of the remaining signal. Furthermore, a VLP event, recorded by the seismic,

deformation and infrasound networks, was also detected by the gravimeter 95 minutes before the short period event.

While temperature is the largest noise source, the noise level of the instrument and error embedded in gravity corrections also require special attention. The largest source of noise, aside from temperature, is seismic energy (e.g., Carbone et al.,2007; Battaglia et al., 2008). The summit area of Kīlauea often has significant tremor levels that will cause the gravimeter spring to vibrate. The seismic induced noise levels can be seen directly in the dataset by correlating the gravity data with RSAM tremor levels. One example is seen immediately following the VLP event on May 8, 2009; as tremor levels decreased, the amount of noise in the gravity data also decreased (Fig. 2-2b). Although noise due to human influence around the meter during the occupation is possible, the area was off limits to the public at this time. The error associated with Earth tide is small as the models are accurate to less than 1 μGal. The error due to the effect of ocean loading is larger than Earth tide as tidal models are not sufficiently accurate (e.g., Hautmann et al., 2010). However, the effect here is small, as the maximum peak to peak amplitude of the ocean loading models is smaller than 20 μGals in Kīlauea's summit region (Quick Tide Pro; Micro-g Lacoste).

2.5 Modeling

The recorded gravity anomaly suggests that there was a short transient change in the amount of mass near the gravimeter on May 9, 2009. To investigate the possible causes and the amount of material involved, a potential

field forward modeling software (Grav3D, 2007) was used. Although modeling this problem does not produce a unique solution, it can help determine the most probable cause of the recorded gravity anomaly. In order to produce simple realistic models, constraints on the volume and density of the material involved and its distance to the gravimeter are required. From these parameters, two different general scenarios are investigated: density variations of the shallow magmatic system and the rise and fall of magma levels in the summit vent.

To model the gravity anomaly using density variations, the entire shallow magmatic system, including the inferred 1 km^3 shallow summit reservoir was used (Fig. 2-4). This shallow reservoir was modeled as a uniform sphere at a depth of 1 km below the surface, immediately east of Halema'uma'u (Cervelli and Miklius, 2003). The density was increased incrementally to reproduce the signal and the best fit shows that a density change of between 25 and 50 kg m^{-3} or the addition of 2.5 to 5 x 10^{10} kg, can reproduce the 85 μGal signal measured at the gravity station location.

The second scenario models the increase in the observed gravity as a rise of the magma surface in the summit vent. The density in each model was varied from 2500 to 2800 kg m^{-3} to investigate the sensitivity of the model to density. To provide a basis for comparison with a more complicated vent geometry, two very simple geometries were investigated (Fig. 2-4). The first was a simple cylinder with a radius of 60 m extending to 200 m from the floor of Halema'uma'u. For this geometry, a rise of approximately 55 m in the magma surface or an increase in volume of 6 x 10^5 m^3 would recreate the observed signal. The second more

complex geometry used a symmetrical step wise cone with a 60 m surface opening, narrowing to 20 m at 200 m depth. This narrower geometry would require a volume of 4.6 x 10^5 m^3 of magma and a rise of 75 to 90 m to reproduce the observed signal. The latter vent geometry was created from LIDAR measurements made in April 2009. Although the LIDAR measurements do not completely image the vent in three dimensions, they nevertheless provide constraints on depth to the free surface and the east-west walls of the vent. At the time of the measurements, the west side of the vent was overhanging by approximately 80 m while the east consisted of a steep unstable talus slope with an irregular transition between the two. The irregular transition between east and west was not constrained by the LIDAR measurements so an approximation was made and applied symmetrically for both the north and south sides of the vent. A rise of 85 to 105 m with a corresponding volume of 5.1 x 10^5 m^3 would be required to reproduce the recorded signal using this geometry.

2.6 Discussion

The gravity signal recorded on May 9, 2009 in Kīlauea's summit caldera can best be explained by either a transient change in the density of the shallow magmatic system, or a rise and fall in the magma surface in the summit vent. The simple modeling done to test the first hypothesis assumes that the whole shallow system would change uniformly. However, a gravitational increase without significant deformation requires an increase in material and not just densification of material already present. While the uniform density change is probably not realistic, the amount of additional mass needed to reproduce the

signal is on the order of 5 x 10^{10} kg. During the deflationary phase of DI events, the magma reservoir beneath Halema'uma'u must be losing pressure in order to deflate and shrink. It is therefore unlikely that during this time, an increase in density and mass in the summit reservoir would be sufficient to cause a measured increase at the surface over a short time period. It is also difficult to explain how a deflating reservoir can lead to an increase in gravity without significant deformation lowering the elevation of the recording gravimeter.

Oscillation of lava levels in erupting vents on Kīlauea (e.g., Kīlauea Iki, Richter et al., 1970; Mauna Ulu, Swanson et al., 1979) have been frequently observed in the past and attributed to gas-piston activity and drain back. The recent summit vent activity has also been characterized by similar rise and fall events with 10s of meters of displacement. The amount of mass involved to recreate the gravity signal using the modeled rise and fall of the lava surface is 1.4 x 10^{9} kg, two orders of magnitude less then that required by densification of the shallow magmatic system. If deflation is attributable to the draining of the shallow magmatic system, it is also difficult to reconcile any apparent rise in the magma column.

What these simple models do not consider is volatile driven rise. Volatile exsolution could be responsible for a short fluctuation in the magma column height, separate from the ongoing summit deformation. While FLYSPEC measurements of SO_2 flux are inconclusive, they suggest a modest increase in background levels up to 400 t d^{-1} following the VLP and during the gravity anomaly. Mechanisms that may have triggered a rise of volatiles discussed here

include surface processes, shallow magmatic processes and deep reservoir processes.

Immediately following the VLP event, a significant amount of material from the walls of the summit vent collapsed, potentially blocking the vent. The collapse at approximately 12:37 (UTC) could have created a plug of dense material which would have slowed gas escape from the conduit, leading to pressurization until the plug failed and gas could escape freely. This pressure release would cause the trapped, gas rich magma column to rise. The plug would have to be removed in a non-violent manner coincident with the first shallow LP at 00:14 on May 9, 2009, as there were no violent sources recorded by the infrasound network (Fee et al., 2010). There are, however, no direct observations to corroborate this mechanism as a possibility for volatile driven rise in the magma column. It is also unknown how much material collapsed into the vent following the VLP event or whether it would sufficient to create a semi coherent plug.

The DI event could also be responsible for the excess gas necessary to drive a rise in the magma level of the summit vent. Decompression events of Kīlauea's magmatic system have been suggested as the cause of increased gas levels in the summit region (e.g., Johnson, 1992; Poland et al., 2009). While reducing overpressure in a magma chamber to exsolve more volatiles from solution is a recognized process, it does not explain the timing of the event or why it would not have been observed in previous DI events. It is possible that the DI event caused volatiles that had already accumulated at the top of the reservoir to collapse and rise causing the VLP event and observed gravity anomaly.

To explain an increase in the lava column unrelated to deformation observations and surface activity, the source would need to be deeper then the shallow magmatic system. Volatile pulses from depth could potentially rise to the surface without being accompanied by an increase in seismic levels, assuming it does not cause a change in the fluid flow regime (Vergniolle and Jaupart, 1986). In this case, the pressure would cause the magma column to rise in the summit vent until sufficient volatiles had been released and hence would decrease the pressure. There is some circumstantial evidence that supports a volatile pulse originating at depth. At 19:46 on May 8, 2009, the first of three LP events occurred at a depth range of 1.3 to 2.6 km. The calculated depths were located below or at what are thought to be the bottom of the summit reservoir (e.g., Ohminato et al., 1998; Dawson et al., 1999; Battaglia et al., 2003; Cervelli and Miklius, 2003). There have been many LP events since the opening of the summit vent as such are a normal part of activity and not above background levels during this study. The coincidence in timing, however, is impossible to ignore. The shallow LP events that bracket the gravity anomaly in this scenario may represent a volatile pulse from depth reaching the surface. Using reservoir equilibrium values for sulphur of 0.07 wt% (Mangan et al., 1993) and the increase in the average SO_2 flux measurements, a first order approximation of mass increase can be calculated. An increase of 400 metric tonnes per day SO_2 equates to 10^7 kg of equilibrium reservoir magma for the time period of the gravity signal. This value is much smaller than that required to explain the recorded signal for several reasons. First, the magma carrying the increased

volatiles would not have been at reservoir equilibrium. The amount of gas is also unknown as gas measurements are not continuous and contain large sources of uncertainty. Finally, this simple analysis does not account for pressure-induced displacement of material towards the surface, potentially accounting for the apparently missing material. While this deep mechanism can explain most of the volcanic observations, it is unclear how or if a volatile pulse from depth could be connected to the VLP event which occurred almost 2 hours before the anomaly. It is possible that the VLP and the gravity anomaly are not connected given that these events are common and large gravity anomalies are rare. Additionally, there has been no activity similar to the rise and fall described by the gravity data since the measurements were made; suggesting either similar events are rare or that part of the signal is instrumental.

2.7 Conclusion

A continuous gravity anomaly was recorded at Kĩlauea's summit early on May 9, 2009, approximately 85 μGals in amplitude and lasting 90 minutes. While modeling results show that density variation of the shallow magmatic system can reproduce the gravity anomaly, it would require an unknown mechanism to add additional mass during deflation without a resulting elevation change. Rise and fall of magma levels driven by volatile rise does, however, concur with the observed changes of activity in both seismic and SO_2 levels. Shallow seismic LP events bracket the gravity anomaly and an apparent increase SO_2 flux corroborate the gravity data. This short period event gives new insight on

Kīlauea's activity and demonstrates that significant changes can occur over very short periods of time. To further improve upon this hypothesis, a new multi-instrument occupation will be needed with high temporal resolution gas measurements. This could constrain the amount of additional volatiles released in rise and fall events and provide the information for robust modeling. Without having incorporated continuous gravity with the seismic, SO_2 flux, infrasound and deformation data, this event would have been overlooked. This clearly shows the importance of a multi-component approach to any long term volcano monitoring.

2.8 Acknowledgments

Thanks to the U.S. National Park Service for meteorological and logistical support. Thanks also to Albert Eggers and Guillaume Mauri for their insight during scientific discussions. J. Zurek and G. Williams-Jones were supported by a Discovery grant from the National Sciences and Engineering Research Council (NSERC) of Canada and a Jack Kleinman Grant for Volcano Research.

2.9 References

Andò, B., and Carbone, D., 2001, A methodology for reducing the effect of meteorological parameters on a continuously recording gravity meter: IEEE Transactions on Instrumentation and Measurements, v. 50, no. 5, p. 1248-1254.

Andò, B., and Carbone, D., 2004, A test on a Nero-Fuzzy algorithm used to reduce continuous gravity records for the effect of meteorological parameters: Physics of the Earth and Planetarty Interiors, v. 142, p. 37.

Andò, B., and Carbone, D., 2006, A new computational approach to reduce the signal from continuously recording gravimeters for the effect of atmospheric temperature: Physics of the Earth and Planetary Interiors, v. 159, no. 3-4, p. 247-256

Battaglia, M., Gottsmann, J., Carbone, D., and Fernàndez, J., 2008, 4D volcano gravimetry: Geophysics, v. 73, no. 6, WA3-WA18.

Battaglia, J., Got, J., and Oubo, P., 2003, Location of long-period events below Kĩlauea Volcano using seismic amplitudes and accurate relative relocation: Journal of Geophysical Research., v. 108, p. 2553

Boy, J.P., Hinderer, J., and Gegout, P., 1998, Global atmospheric loading and gravity: Physics of the Earth and Planetary Interiors, v. 109, no. 3, p. 161-177.

Branca, S., Carbone, D., and Greco, F., 2003, Intrusive mechanism of the 2002 NE-Rift eruption at Mt. Etna (Italy) inferred through continuous microgravity data and volcanlogical evidences: Geophysical Research Letters, v. 30, no. 20, 2077.

Carbone, D., Buetta, G., Greco, F., and Zuccarello, L., 2007, A data sequence acquired at Mt. Etna during the 2002-2003 eruption highlights the potential of continuous gravity observations a tool to monitor and study active volcanoes: Journal of Geodynamics, v. 43, p. 320-329.

Cervelli, P.F., and Miklius, A., 2003, The Shallow Magmatic System of Kīlauea Volcano: U.S. Geological Survey Professional Paper 1676, p 149-163.

Dawson, P.B., Chouet, B.A., Okubo, P.G., Villaseñor, A., and Benz, H.M., 1999, Three-dimensional velocity structure of the Kīlauea Caldera, Hawaii: Geophysical Research Letters, v. 26, no. 18, p. 2805-2808.

Eggers, A.A., 1983,Temporal gravity and elevation changes at Pacaya Volcano, Guatemala: Journal of Volcanology and Geothermal Research, v. 19, p. 223-237.

El Wahabi, A., Ducarme, B., Van Ruymbeke, M., and d'Oreye, N., 1997, Continuous gravity observations at Mount Etna (Sicily) and correlations between temperature and gravimetric records: Cahiers du Center Europèen de Gèodynamique et de Sèismologie, v. 14, p. 105.

Fee, D., Garces, M., Patrick, M., Chouet, B., Dawson, P., and Swanson, D., 2010, Infrasonic harmonic tremor and degassing bursts from Halema`uma`u Crater, Kīlauea Volcano, Hawaii: Journal of Geophysical Research, v. 115, B11316.

GRAV3D, 2007, A program library for forward modeling and inversion of gravity data over 3D structures: Developed under the consortium research project Joint/Cooperative Inversion of Geophysical and Geological Data: UBC-

Geophysical Inversion Facility,Department of Earth and Ocean Sciences, The University of British Columbia, Vancouver., version 20070309, 2007.

Hautmann, S., Gottsmann, J., Camacho, A.G., Fournier, N., Sacks, I.S., and Sparks, R.S.J., 2010, Mass variations in response to magmatic stress changes at Soufrière Hills Volcano, Montserrat (W.I.): Insights from 4-D gravity data: Earth and Planetary Science Letters, v. 290, no. 1-2, p. 83-89.

Horton, K., Williams-Jones, G., Garbeil, H., Elias, T., Sutton, A., Mouginis-Mark, P., Porter, J., and Clegg, S., 2006, Real-time measurement of volcanic SO_2 emissions: Validation of a new UV correlation spectrometer (FLYSPEC): Bulletin of Volcanology, v. 68, no. 4, p. 323-327.

Jaupart, C., and Vergniolle, S., 1988, Laboratory models of Hawaiian and Strombolian eruptions: Nature, v. 331, no. 6151, p. 58-60.

Johnson, D., J., 1992, Dynamics of magma storage in the summit reservoir of Kīlauea Volcano, Hawaii: Journal of Geophysical Research, v. 97, no. B2, p. 1807-1820

Johnson, D., J., Eggers, A., A., Bagnardi, M., Battaglia, M., Poland, M.P., and Miklius, A., 2010, Shallow magma accumulation at Kīlauea Volcano, Hawai‘i, revealed by microgravity surveys: Geology, v.38 p. 1139-1142.

Mangan, M.T., Cashman, K.V., and Newman, S., 1993, Vesiculation of basaltic magma during eruption: Geology, v. 21, p. 157.

Ohminato, T., Chouet, B.A., Dawson, P., and Kedar, S., 1998, Waveform inversion of very long period impulsive signals associated with magmatic injection beneath Kīlauea Volcano, Hawaii: Journal Geophysical Research, v. 103, p. 23839-23862.

Pesci, A., Fabris, M., Conforti, D., Loddo, F., Baldi, P., and Anzidei, M., 2007, Integration of ground-based laser scanner and aerial digital photogrammetry for topographic modelling of Vesuvio volcano: Journal of Volcanology and Geothermal Research, v. 162, no. 3-4, p. 123-138

Poland, M.P., Sutton, J.A., and Gerlach, T.M., 2009, Magma degassing triggered by static decompression at Kīlauea Volcano, Hawaii: Geophysical Research Letters, v. 36, L16306.

Richter, D.H., Eaton, J.P., Murata, K.J., Ault, W.U., and Krivoy, H.L., 1970, Chronological narrative of the 1959-60 Eruption of Kīlauea Volcano, Hawaii: U.S. Geological Survey Professional Paper 537.

Rymer, H., 1996, Microgravity monitoring. Monitoring and Mitigation of Volcano Hazards: Springer-Verslag, Berlin, p. 169-168.

Rymer, H., 1989, A contribution to precision microgravity data analysis using Lacoste and Romberg gravity meters: Geophysical Journal International, v. 97, no. 2, p. 311-322.

Swanson, D.A., Duffield, W.A., Jackson, D.B., and Peterson, D.W., 1979, Chronological narrative of the 1969-71 Mauna DIu eruption of Kĩlauea Volcano, Hawaii: Geological Survey Professional Paper 1056.

Vergniolle, S., and Jaupart, C., 1986, Separated two-phase flow and basaltic eruptions: Journal of Geophysical Research, v. 91, no. B12, p. 12842-12860.

Vergniolle, S., and Jaupart, C., 1990, Dynamics of degassing at Kĩlauea Volcano, Hawaii: Journal of Geophysical Research, v. 95, no. B3, p. 2793-2809.

Williams-Jones, G., Rymer, H., Mauri, G., Gottsmann, J., Poland, M.P., and Carbone, D., 2008, Toward continuous 4D microgravity monitoring of volcanoes: Geophysics, v. 73, no. 6, p. WA19-WA28.

Wooten, K.M., Thornber, C.R., Orr, T.R., Ellis, J.F., and Trusdell, F.A., 2009, Catalog of tephra Samples from Kĩlauea's summit eruption, March-December 2008: U.S. Geological Survey Open-File Report, 2009-1134.

2.10 Supplementary Material

It is important to try and isolate the effect temperature has on spring gravimeters on a meter by meter basis as each instrument responds differently (Ando and Carbone 2004). The differences in temperature response are attributed to inconsistencies in spring properties and poor environmental seals. Each meter is made with environmental seals which are supposed to isolate the internal sensor from the atmosphere, but over time these seals may leak. This reduces the ability of the meter to insulate the sensor from external temperature

variations and allows changes in humidity to take place within the meter. While there is a heating coil that keeps the sensor and spring at a constant temperature, it may not heat the meter's interior uniformly creating temperature gradients within the sensor.

The meter used in this study (G-127) was tested for temperature effects under 3 different scenarios in Vancouver, British Columbia, Canada. The first was a stable environment where the total temperature fluctuation was less than 1.5˚C. The residual gravity signal from this first test was affected by ocean loading, a linear instrumental drift (supplementary Fig. 2-5 b) and a telesiesm. This test is a good standard to compare how the meter responds to different temperature variations. In the second scenario, G-127 was placed on a balcony and exposed to daily atmospheric oscillations with a diurnal temperature change of 14˚C. Temperature and pressure were recorded by a portable HOBO weather station at 1 minute intervals to match the gravity data. A dual axis tilt meter was also placed beside the gravity meter to characterize any deformation due to thermal expansion. The resulting gravity signal corrected for Earth tides and pressure (supplementary Fig. 2-5 a), displays a diurnal periodic signal that tracks changes in temperature. The measured tilt also tracked with temperature suggesting the balcony is measurably deforming due to thermal expansion. In the last scenario, a rapid increase in temperature to the surrounding area caused an unrecoverable tare in the gravity data (supplementary Fig. 2-5 c). Before and after the increased temperature pulse, the gravimeter was in a stable lab environment with temperature fluctuations less than 1.5˚C.

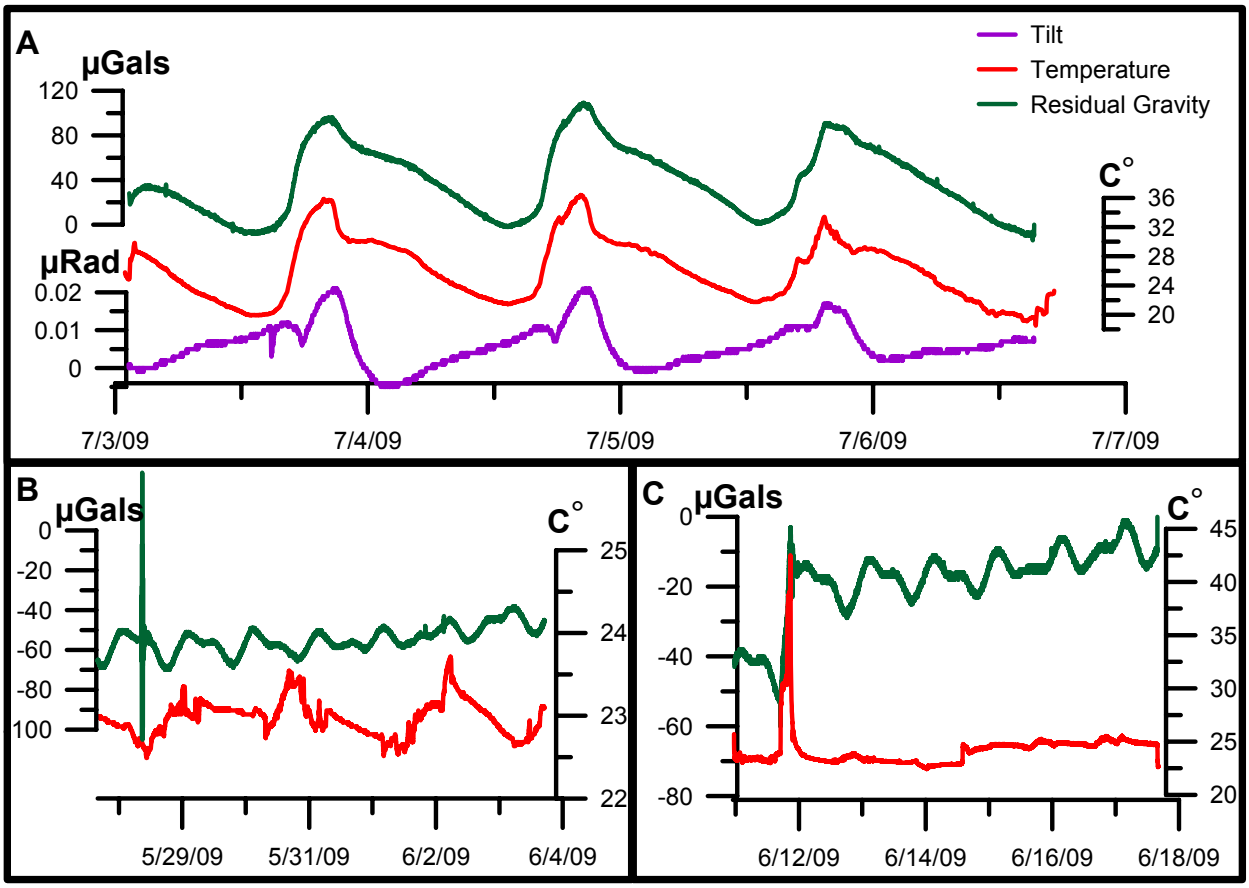

Suplementry Figure 2-5 Residual gravity data (green), temperature (red) and tilt (purple) from a series of meter specific tests. A) The instrument was exposed to atmospheric variations on a balcony. B) The meter was in a stable enviroment where a telesiesm was recorded. C) A forced external temperature spike on the gravimeter.

These tests suggest that large long term (longer than 10s of minutes) temperature variations will cause an apparent gravity change in the meter. What they do not test is the effect of humidity on the meter. Humidity, however, tends to follow temperature closely, and thus any process that would affect atmospheric temperature could be seen to affect humidity as well making it extremely difficult to separate the effect of either on a spring gravimeter. Nevertheless, these three simple tests show that the gravity anomaly presented

is not likely to be an instrumental effect caused by atmospheric changes. The most likely cause of the signal is therefore related to volcanic activity.

With no relationship between temperature and continuous gravity, it is difficult to consider the error associated with these measurements. A first order estimate of the error can, however, be deduced by assuming that the periodic and diurnal signal is completely environmentally and temperature controlled. The amount of temperature forcing at a specific point in time can then be inferred by taking the slope of the signal at the same frequency as the periodicity. To apply this technique to the gravity anomaly observed on May 9, the slopes on either side of the periodic maximum were measured and averaged. The result was 0.4 +/- 0.2 μGal min^{-1} or approximately one fifth the rate of gravity change in the anomaly.

3: SHALLOW MAGMATIC PLUMBING SYSTEMS REVEALED THROUGH BOUGUER GRAVITY AND TOTAL MAGNETIC ANOMALY MAPPING AT KĨLAUEA, HAWAII AND MASAYA, NICARAGUA

Jeffrey Zurek, Glyn William-Jones, Mike Poland, Daniel Dzurisin, Hazel Rymer

3.1 Introduction

Volcanic edifices are often structurally complex with multiple episodes of eruption and dynamic behavior. A volcano's structure is a determining factor for the locations of potential eruptions and as well as type of activity that will occur. Material properties, such as density and magnetic susceptibility, commonly change drastically along structures. The material of a typical volcanic edifice ranges from dense intrusions to relatively low density extrusive materials and has varying magnetic properties based on geothermal heat gradient, hydrothermal alteration and rock chemistry. Potential field surveys, such as Bouguer gravity and total magnetic, have been used in both scientific studies and industry to delineate structures and resources that are not accessible from the Earth's surface. For example, magnetic and gravity surveys have been used together to investigate the large scale volcanic structure at Grímsvötn volcano in Iceland (Gudmundsson and Milsom, 1997) and Aso volcano in Japan (Okubo and Shibuya, 1993). At Aso, magnetic and gravity data were used to identify where buried faults run through the volcano's caldera as well as determine the Currie

point depth. The same surveys were used at the ice covered Grímsvötn volcano and imaged a dense body at 1 to 4 km below the surface, consistent with a magma chamber.

Gravity and total magnetic surveys were completed at Masaya volcano, Nicaragua, and Kĩlauea volcano, Hawaii, to investigate subsurface structure and image the magmatic plumbing system beneath both volcanoes. Inversion of Bouguer gravity anomaly data provides the ability to image density contrasts and large scale structures without relying on prior assumptions of source geometry or substrate homogeneity. Applying this technique with a tightly spaced grid will provide an unparalleled resolution of the magmatic system at even a well studied volcano such as Kĩlauea or Masaya. This data will also be used to test previous dynamic microgravity results (Johnson et al., 2010), deformation (Cervelli and Milkus 2003) and seismic studies (Ohminato et al., 1998; Dawson et al., 1999; Battaglia et al., 2003) that infer the presence of melt at shallow levels within Kĩlauea's caldera. At Masaya the potential field data will add detail to coarse regional survey's (Connor et al., 1989; Metaxian, 1994) to explore shallow vent structures.

Comparing the magmatic plumbing systems at Masaya and Kĩlauea volcano will further the understanding of volcanic process at both of these complex basaltic systems. Both systems are similar as they have had large explosive eruptions (Kĩlauea: e.g., Jagger and Finch 1924; Powers, 1948; Dzurisin et al., 1995, Masaya: e.g., Walker, 1993; Kutterolf et al., 2008; Pérez et al., 2009), repetitive caldera formation, and display similar long term behavior at

their summits. They are also fundamentally different due to their different tectonic environments.

3.2 Geologic Setting and Previous Work

3.2.1 Geologic Setting - Kīlauea

Kīlauea is one of five volcanic edifices that makeup the Big Island of Hawaii, along a hot spot trend in the middle of the Pacific Ocean. Currently, it is the only actively erupting volcano on the Island and has been in a nearly continual state of eruption since 1983; the Pu'U O'o – Kupaianaha eruption began on January 3, 1983 from Kīlauea's East Rift Zone (Fig 3-1a). The East Rift Zone and Southwest Rift Zone intersect at Kīlauea's summit caldera which, until recently, had not seen eruptive activity in 26 years. The current activity at Kīlauea's summit started in March 2008, with the opening of a vent in the summit pit crater, Halema`uma`u, and continues at present. The activity associated with the vent and the lava pond within it has been dominated by vent wall collapse, rise and fall of lava levels, small explosions and passive degassing. Explosions were more common in the early part of the activity, with the largest explosive event on September 2, 2008 (Wooten et al., 2009). Ballistics from these events did not travel more than ~ 150 m away from the vent for all explosions (Wooten et al., 2009). During our study, the volcano was in a nearly steady state with activity at both the summit and at Pu'U O'o. A minor transient deformation event did take place during the magnetic surveys which briefly reduced lava extrusion at the eruption site on the East Rift Zone.

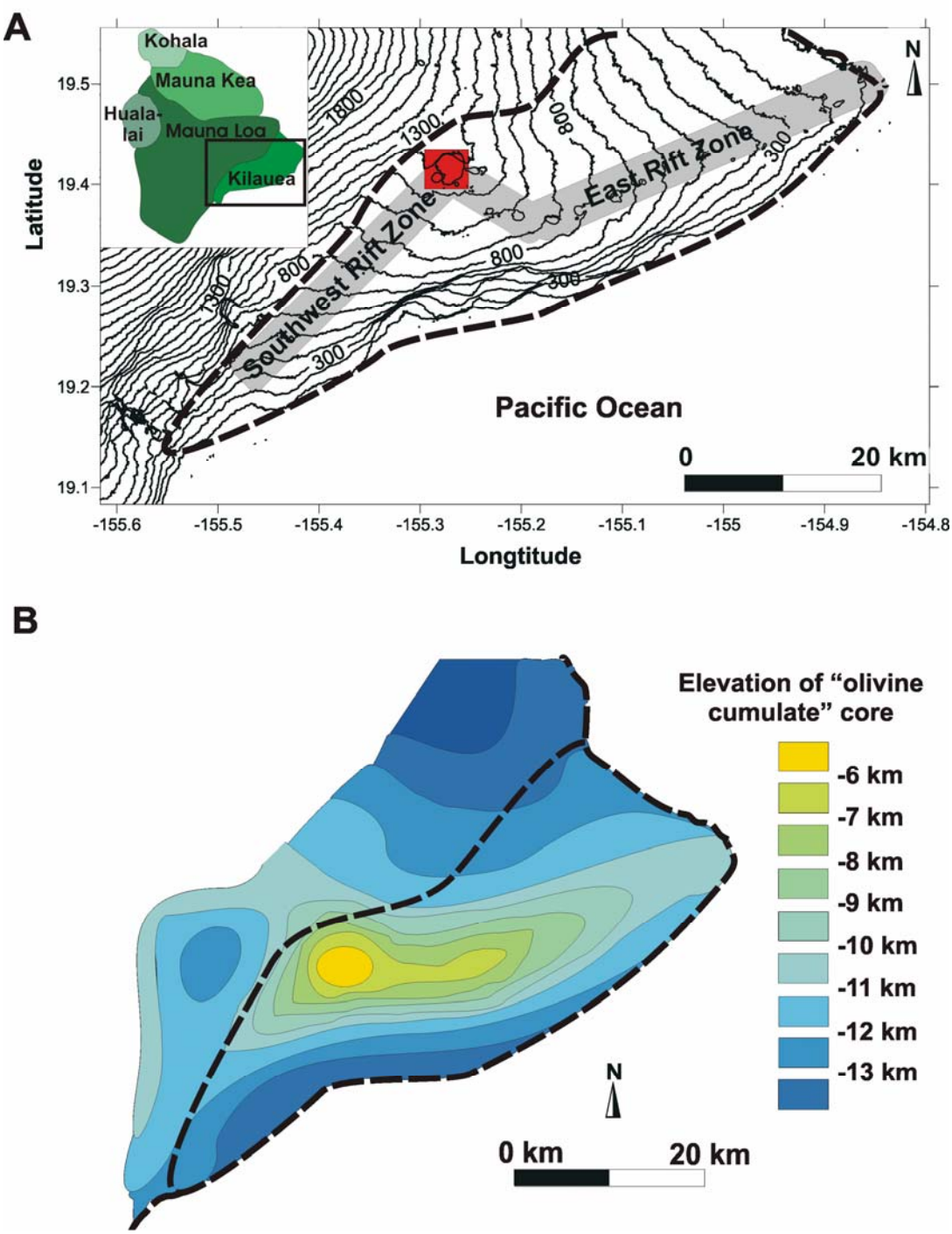

Figure 3-1 A: Topographic map of Kīlauea outlined by the dashed line, the summit caldera and survey area highlighted in orange and both rift zones in grey. Inset: Big Island of Hawaii with the 5 volcanic centres of the island. B: The results of Kauahikaua et al. (2000) Bouguer gravity survey showing the depth to an inferred dense olivine cumulate (3300 kg m^{-3}) core that exists beneath each volcanic edifice on the Big Island of Hawaii.

The summit of Kīlauea has had a complex geologic history and due to much of the evidence being buried by lava, many questions remain unanswered. The formation of Kīlauea's caldera has been narrowed to 540 to 570 years ago through carbon dating and analysis of Hawaiian oral traditions (Swanson, 2008). An older caldera has also been inferred to have existed between 1500 to 2100 years ago and suggests that Kīlauea may have had cycles of effusive filling and collapse (Powers, 1948). Since 1790, there has been a net filling of the caldera leading to almost complete filling of the southern end.

3.2.2 Previous Work - Kīlauea

Gravity survey methods have been utilized occasionally on the Big Island of Hawaii to map areas of high density and provide limits on mass flux at Kīlauea. An island wide Bouguer gravity anomaly study inferred that the core of each volcano consists of dense material approaching a density of an olivine cumulate (3300 kg m^{-3}; Kauahikaua et al., 2000). Through modeling and anomaly wavelength analysis, the depths to the dense core material were calculated for the entire Island with that beneath Kīlauea's summit inferred at 5 to 6 km beneath the surface, becoming deeper away from the summit. The Bouguer anomaly also outlines Kīlauea's rift zones where dense material must exist at an elevated level in the crust (Fig 3-1b). While the spatial coverage of this survey was sufficient for an island wide Bouguer anomaly, the network was insufficient for delineation of shallower density contrasts that should exist due to the presence of Kīlauea's magma chambers. To investigate mass flux within Kīlauea's magmatic plumbing system, microgravity surveys have been periodically performed across a network

of stations in Kīlauea's summit region (e.g., Kauahikaua and Miklius, 2003; Johnson et al., 2010). Surveys prior to and following a 7.2 magnitude earthquake in 1975, showed a significant decrease in the gravitational field around the summit which was interpreted as the creation of 40 – 90 x 10^6 m^3 of void space (Dzurisin et al., 1980). Subsequent surveys measured an increase in the gravitational field centered near Hualema'uma'u with a total magnitude of approximately 450 μGal over 33 years (Bagardi et al., 2008; Johnson et al., 2010). It is suggested that the most likely cause for the gravitational increase would be the filling of 21 - 120 x 10^6 m^3 void space, which is consistent with that inferred to have been created due to the 1975 earthquake. Other models include upward migration of the summit magma reservoir and the settling of olivine to form an olivine cumulate (Bagnardi et al., 2008; Johnson et al., 2010).

There have been two large scale aeromagnetic surveys flown at different elevations across the Big Island of Hawaii (Godson et al., 1981; Flanigan et al., 1986). Hildenbrand et al. (1993) combined these two datasets to further describe the magnetic anomalies displayed by rift zones on Mauna Loa and Kīlauea. They interpret the short wavelength positive anomilies over the rift zones as slowly cooled unaltered intrusions with hydrothermally altered material on either side. However, the results of these airborne surveys have not been ground truthed and as with the island wide Bouguer survey, are too coarse to identify small shallow anomalies in the summit region of Kīlauea.

Deformation and seismic studies have identified at least two zones of magma accumulation beneath Kīlauea's caldera. The deeper magma chamber is

believed to be located 2 to 4 km beneath the southern rim of the caldera (e.g., Delaney et al., 1998; Cervelli and Miklius, 2003). The depth of the shallower magma chamber has been inferred through seismic (Ohminato et al., 1998; Dawson et al 1999; Battaglia et al., 2003), and deformation (Cervelli and Miklius, 2003) studies. Analysis of transient deformation events put the top of the magma chamber at ~400 m beneath the surface (Cervelli and Miklius, 2003) while seismic studies suggest that the shallow chamber is closer to 1 km depth (Ohminato et al., 1998).

3.2.3 Geologic Setting - Masaya

The Las Sierras-Masaya volcanic complex (also referred to as Masaya volcano) is part of the Central America Volcanic Arc stretching from Mexico in the north to Panama to the south. The complex sits within the Nicaraguan depression, which hosts all of Nicraugua's 18 active volcanoes (e.g., Cowan et al., 2002; Girard et al., 2005), and is located at the south end of the Managua Graben (Fig. 3-2). Las Sierras-Masaya consists of a set of nested calderas with the youngest Masaya caldera (6 km by 11 km) being ~6000 yr (Walker et al., 1993) and the oldest Las Sierras caldera ~30,000 yr (Walker et al., 1993). Unlike Hawaiian volcanism, where caldera formation is thought to form through collapse due to flank eruptions draining the summit reservoir, Las Sierras-Masaya's calderas are most likely formed through basaltic Plinian eruptions (e.g., Williams, 1983; Walker et al., 1993). The largest eruption attributed to Masaya caldera took place ~ 6000 years ago with a total volume of 13.5 km^3 (Kutterolf et al., 2008). Two other basaltic Plinian eruptions occurred 2100 and 1800 years ago

with the more recent eruption having an eruptive volume of 6.3 km^3 (Kutterolf et al., 2008; Pérez et al., 2008). Masaya caldera is assumed to have been in its present form since the last large basaltic Plinian eruption.

Within Masaya caldera there are two basaltic cones called Masaya and Nindiri that dominate the landscape (Fig. 3-2). Together they create a basaltic shield from where prehistoric lava flows have partially filled the caldera (Walker et al., 1993). The deepest area of the caldera is in the southeast corner where Lake Masaya (Laguna de Masaya) fills the depression. There are also a number of smaller cinder cones that form a semicircle with Nindiri and Masaya cones at the center of the arc (Fig 3-2). Self potential electrical surveys have identified this area as a structural pathway for hydrothermal fluids (Mauri et al., 2010); the hydrothermal systems do not reach the surface except for one location just northeast of Masaya cone. Historical activity at Masaya has been dominated by degassing cycles with little eruptive products. The last effusive eruption took place in 1772 from a fissure on the north flank of Masaya cone. The pit crater, Santiago, which is nested within Nindiri cone, formed in 1852 and has been the center of activity since (Fig 3-2c). Activity is characterized by at least five degassing cycles with an estimated 10 km^3 of lava degassed (Stoiber et al. 1986). Currently, Masaya is undergoing a degassing crisis that started in 1993**,**

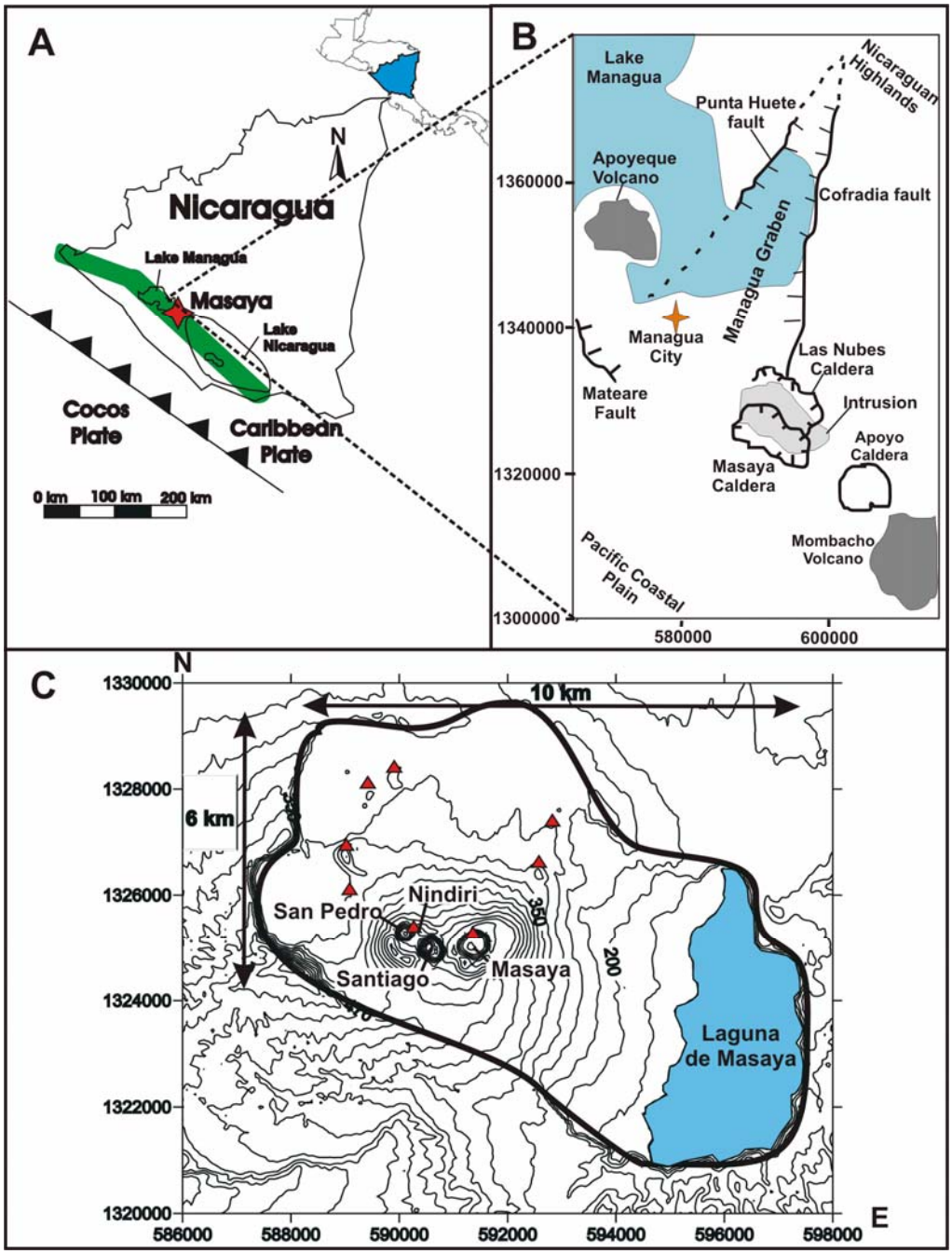

Figure 3-2 A) Map of Nicaragua and the location of Masaya represented by a red star and the Central American volcanic arc highlighted in salmon; map of Central America inset B) Caldera location of the Managua Graben with respect to Las Sierras-Masaya volcanic complex (modified from Girard et al 2005). C) Topographic map centered on Masaya Caldera with each cone represented by an orange triangle.

which has been punctuated with small explosions, vent formation and lava level change as indicated by variable vent incandesance.

3.2.4 Previous Work - Masaya

Over the last two decades, Masaya volcano has been the site of microgravity studies focused on Nindiri cone and its active pit crater, Santiago (Rymer et al., 1998; Williams-Jones et al., 2003). There appears to have been a steady inverse relationship between SO_2 flux and gravity change around Santiago. Williams-Jones et al. (2003) suggest that the most likely explanation for the inverse gas-gravity relationship is fluctuations in the density of the shallow magmatic plumbing system. In times of higher gas flux, the magma in the upper plumbing system contains more gas bubbles and resembles a thick foam layer. This reduces the density beneath Santiago thus reducing the relative amount of mass. In times of low gas flux, there is a decrease in the foam layer thickness increasing the density and mass beneath the surface. Observations of vent formation and collapse in the Santiago pit crater have led to a conceptual model where the upper magmatic plumbing system is defined by pockets of gas-charged magma (Rymer et al., 1998). These pockets, when emptied, provide the space that has facilitated the continual collapse and deepening of Santiago crater.

Masaya has also been the site of two Bouguer gravity studies (Connor et al., 1989; Métaxian, 1994). The first study was a very coarse regional survey that identified a large broad area with an increased gravitational field centered just

north of the caldera (Connor et al., 1989). The broad positive anomaly was interpreted to represent an intrusive body with a depth greater than 500 m and a density contrast of 300 to 500 kg m^{-3}. A more intensive Bouguer study by Métaxian (1994) confirmed the existence of a broad positive anomaly northeast of the caldera and also identified two other significant anomalies in the region

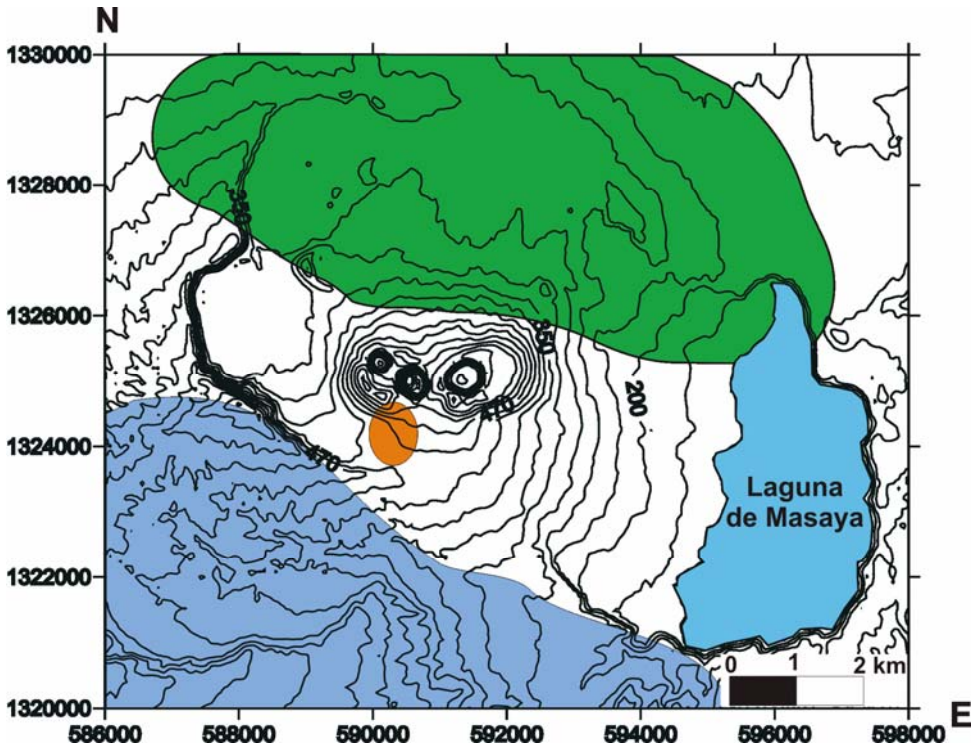

Figure 3-3 Topographic map of Masaya caldera with the locations of the three Bouguer anomalies identified by Métaxian (1994). Green: a broad positive anomaly (15 mGal) interpreted as a deep intrusion. Orange: a large positive (50 mGal) anomaly interpreted as a magma chamber. Blue: a broad negative anomaly (-30 mGal) which was not sufficiently constrained thus not interpreted.

(Fig. 3-3); the largest of which is a positive anomaly just south of Nindiri cone. This large > 50 mGal anomaly has been interpreted to represent a shallow magma chamber with a depth shallower then 3 km (Métaxian, 1994; Pascal, 2008). The other anomaly identified is a broad low, centered southwest of the

caldera, however, this is not constrained and thus no interpretation can be made based on existing datasets (Fig 3-3).

3.3 Methodology

3.3.1 Bouguer Gravity Survey

The Bouguer gravity data collected at both Kīlauea and Masaya followed nearly identical procedures and used the same LaCoste & Romberg meter (G-127). Detailed survey techniques have been extensively discussed in the literature (e.g., Rymer and Brown, 1986; Berrino et al., 1992) and in Appendices A and B, hence they will only be briefly discussed here. Each survey used a base station and periodic station repeats to identify anomalous instrumental drift and data tares. Normal, daily instrumental drift for G-127 is on the order of 1 μGal which is much smaller than the error associated with the survey and hence its effect is ignored. Access for many of the areas surveyed on Masaya and Kīlauea is by foot only reducing the amount of time available to repeat base station measurements and limiting the ability to identify and correct for tares. Base station measurements were used to normalize the data for each survey day and eliminate instrumental drift that can occur over several weeks. The station grid spacing at Kīlauea was 200 by 200 m across the whole caldera and at Masaya where possible stations were surveyed in a 50 by 50 m grid.

To obtain the necessary vertical and horizontal control for each gravity station, a differential GPS system (Leica 500) was used, consisting of a base station receiver and at least one rover unit that records data at each survey station. The base station data used in these surveys was recorded every second

for the entire survey day to provide the necessary overlap with the rover data. Rover GPS data collected at each gravity station is at least 3 minutes in length recorded at 1 second intervals. The amount of time for each rover measurement was dependant on the number and position of satellites at the time of the measurement. At Masaya volcano, there is no surveyed bench mark that can be used as a GPS base station thus a spot was chosen close to the visitor center within the caldera (also used by microgravity studies 1998 - 2010). The position for the GPS base station is then set using the data of the first day of surveying and has a vertical accuracy of ~ 30 cm. Gravity station positions were obtained by post processing the GPS data using the defined base station location. This provides a vertical accuracy to about 2 cm relative to the GPS base station. In Hawaii, to provide accurate positions, data was post processed using one of the continuous GPS station in the summit region. Due to warping of the Earth's geoid in the summit region, the accuracy of these positions is not known, however it is better than 5 cm.

3.3.2 Total Magnetic Survey

To complement the Bouguer gravity data, total magnetic data were collected over approximately the same area as the gravity dataset at both Masaya and Kīlauea volcano. The instrument used was a GEM Overhauser magnetometer, which calculates the magnitude of the Earth's magnetic field by measuring the procession of charged particles in its sensor. Data points were taken approximately every 25 m along lines that were 200 m apart at Kīlauea and 50 m apart at Masaya volcano. Measurement locations were obtained from a

handheld GPS that recorded the operator's position every 5 seconds. The time stamp from the magnetometer was later compared to the GPS to extrapolate a position for each data point. This provided the ability to cover large areas in a single day, however, it reduced the precision of the measurement locations. This is not a problem as there are no corrections that require a high precision in location enable data interpretation.

Unlike gravity measurements, there are few basic corrections that are necessary prior to interpretation of the data. However, there are a large number of analytical techniques that have been used to further the interpretation of magnetic data and have been discussed thoroughly in the literature (e.g., Telford et al., 1990). In the data presented here, no filtering algorithms were applied in an effort to preserve information while processing. The changing intensity of the Sun over a day does affect the local magnetic field by approximately 30 nT. To confirm that the daily variation was 30 nT or less, measurements were taken every 5 seconds for approximately 6 hours spanning a survey day at a single location near the survey area. The diurnal variation is much smaller than expected for the magnetic field across an active volcanic area. While these measurements do not overlap with the survey data, they provide the constraints necessary to characterize the diurnal effect on the data. Highly magnetized intrusions and areas of hydrothermal alteration typically produce contrasts greater than 1000 nT (Telford et al., 1990; Hilderbrand et al., 1993), therefore, diurnal corrections can be ignored. To eliminate the unlikely possibility that that a solar storm was affecting the results, repeat measurements were made

throughout each survey day to verify the stability of the instrument and surrounding magnetic field.

3.4 Results and Modelling

3.4.1 Kīlauea

In total, 420 magnetic measurements and 231 Bouguer gravity measurements were made in and around Kīlauea's summit caldera. The processed and gridded magnetic data show a large magnetic low associated with the southern edge of Halema`uma`u (Fig. 3-4; anomaly A). Two other small, well defined, anomalies are also outlined in Figure 3-4 to the east of Halema`uma`u; both anomalies are about 3000 nT in size and are no more than 500 m across. There are many other short wavelength changes within the survey area, however, these short wavelength fluctuations are not analyzed in detail due to the lack of definition in their magnetic structure or other geological evidence.

Surveys that cover large areas or elevation changes should remove the International Geomagnetic Reference Field (IGRF) so that the entire dataset is at the same base level (Barton, 1997). The change predicted by the IGRF on the dataset due to the horizontal survey extent is less than 40 nT. It also predicts that a 20 m elevation change will cause a 160 to 170 nT variation. The variation in elevation across the survey area is less than 40 m, excluding the pit crater Halema`uma`u, and in general occurs gradually. The vertical accuracy on the positions of the magnetic measurements is approximately +/- 15 m. The poor positional accuracy coupled with relatively flat topography suggests that the error with removing the IGRF outweighs any benefits.

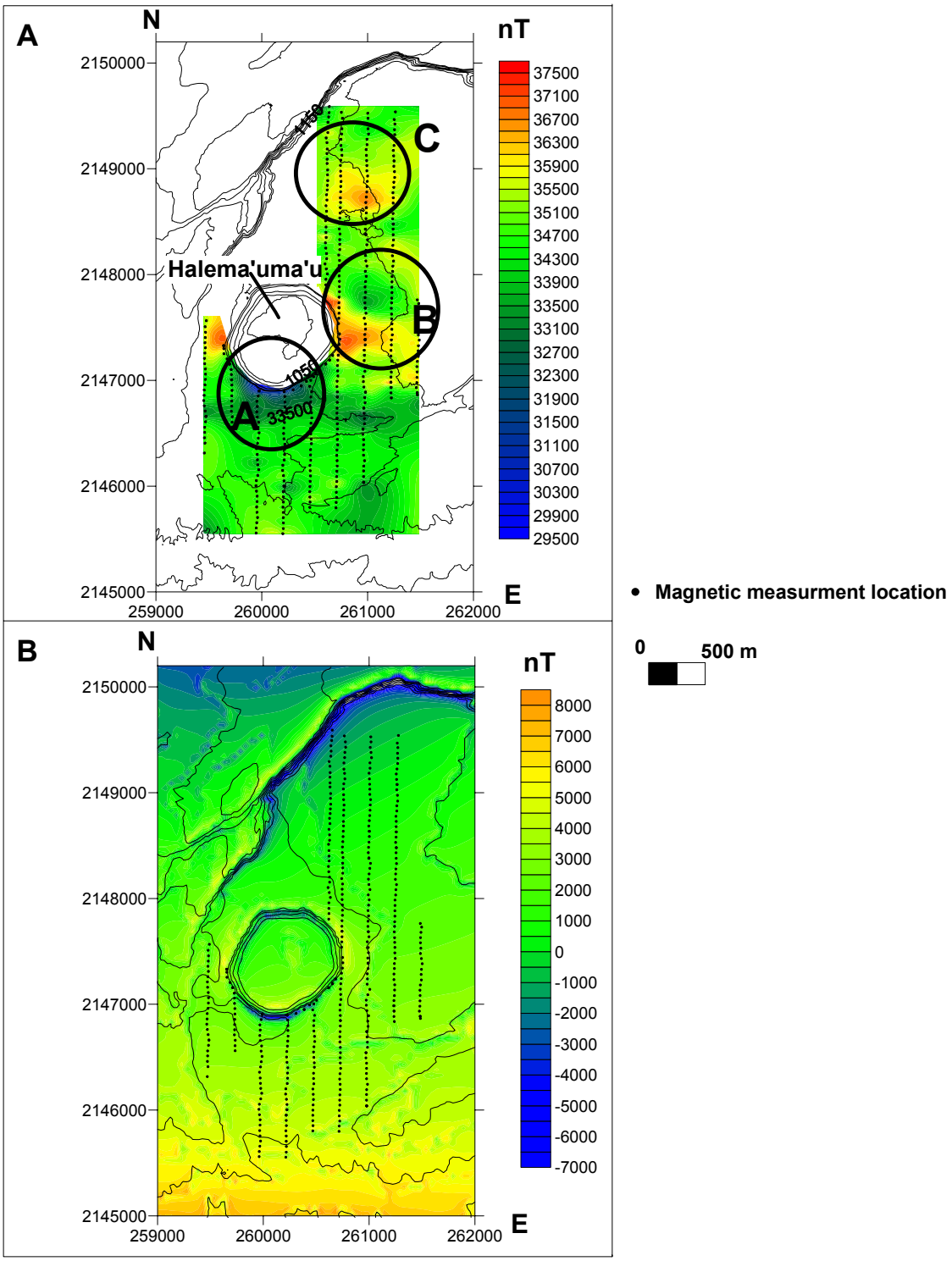

Figure 3-4 A) Total magnetic survey map in Kīlauea caldera with three identifiable short wavelength anomalies outlined by dark circles. B) Theoretical magnetic field strength calculated by using an estimate of the Earth's magnetic susceptibility and magnetic modeling software package MAG 3D (MAG3D, 2007).

In order to interpret the magnetic data, a model was created to test the effect of topography on the measurements (Fig. 3-4) using a DEM (digital elevation model) and a magnetic modeling software package, MAG3D (MAG3D, 2007). The assumed magnetic susceptibility used (7.2 kg m^{-3}) was previously measured by Hildenbrand et al. (1993) from a set of samples gathered from Kīlauea. Fig. 3-4A represents the best estimate of the topographic effect. However, due to uncertainties in the magnetic susceptibility and the DEM, topography is not corrected for in the final dataset.

The Bouguer gravity data covers the entire caldera with a 200 m by 200 m grid of stations (Fig. 3-5). The residual gravity shows a large positive Bouguer anomaly centered northeast of the Halema`uma`u crater, with a long axis that stretches into Halema`uma`u crater near the summit vent. The largest gravity gradient occurs from the center of the anomaly towards the southeast. The error on each measurement is different due to daily survey closures ranging between 8 μGal and 200 μGal; closures were typically less than 100 μGal, however, on three occasions the closures were greater. The long distances traveled carrying the meter over rough ground is the most probable cause for the large closures. Other noise sources include seismic noise from volcanic tremor. At the time of the survey, volcanic tremor was occurring at the summit of Kīlauea increasing the noise in gravity readings near the vent by 5 to 20 μGal (Chapter 2). If the noise is ignored, the smallest wavelength anomaly that can be theoretically resolved without aliasing would be 400 m. For the purposes of modeling and due to a lack

of further constraints, this theoretical value is used for the forward and inversion models. The maximum wavelength that can be described is equal to the dimensions of the survey area or approximately 4 km. The maximum resolvable depth is dependent on both the shape of the density contrast and the maximum wavelength. For an infinite horizontal rod, the depth to the body can be calculated from the anomaly's wavelength such that the depth is one half of its wavelength:

$$X_{1/2} = Z \quad (1)$$

where $X_{1/2}$ is half the anomaly's wavelength and Z is the depth beneath the surface. A sphere has a similar equation to determine the depth to its center where the half-wavelength of the anomaly is multiplied by a factor of 1.3:

$$1.3X_{1/2} = Z \quad (2)$$

If the maximum wavelength is 4 km, then according to these geometries, the maximum depth this dataset can detect is 2 to 2.6 km.

Inverse and forward models were created using a gravity modeling software package, GRAV3D (GRAV3D, 2007). When processing the raw gravity data, an average density of 2330 kg m^{-3} was assumed for all terrain corrections based on previous gravity studies (Watts and ten Brink, 1989; Kauahikaua et al., 2000). Densities displayed in Figures 3-6 and 3-7 are represented as change from this average value. Due to the lack of constraints in reference to the density structure beneath the summit, two general models were created based on different density limits. The first model (Fig. 3-6) assumes that the large positive anomaly in Kīlauea's summit caldera is created only by increases (positive) in

density above the average 2330 kg m^{-3}. The maximum density contrast in this model is set to that of an olivine cumulate (positive 700 kg m^{-3}). This model shows a dense body that begins approximately 790 m a.s.l. (above sea level) or at a depth of 300 m below the topographic surface. The body reaches a maximum size 900 to 1000 m beneath the surface and extends to a depth of approximately 2300 m.

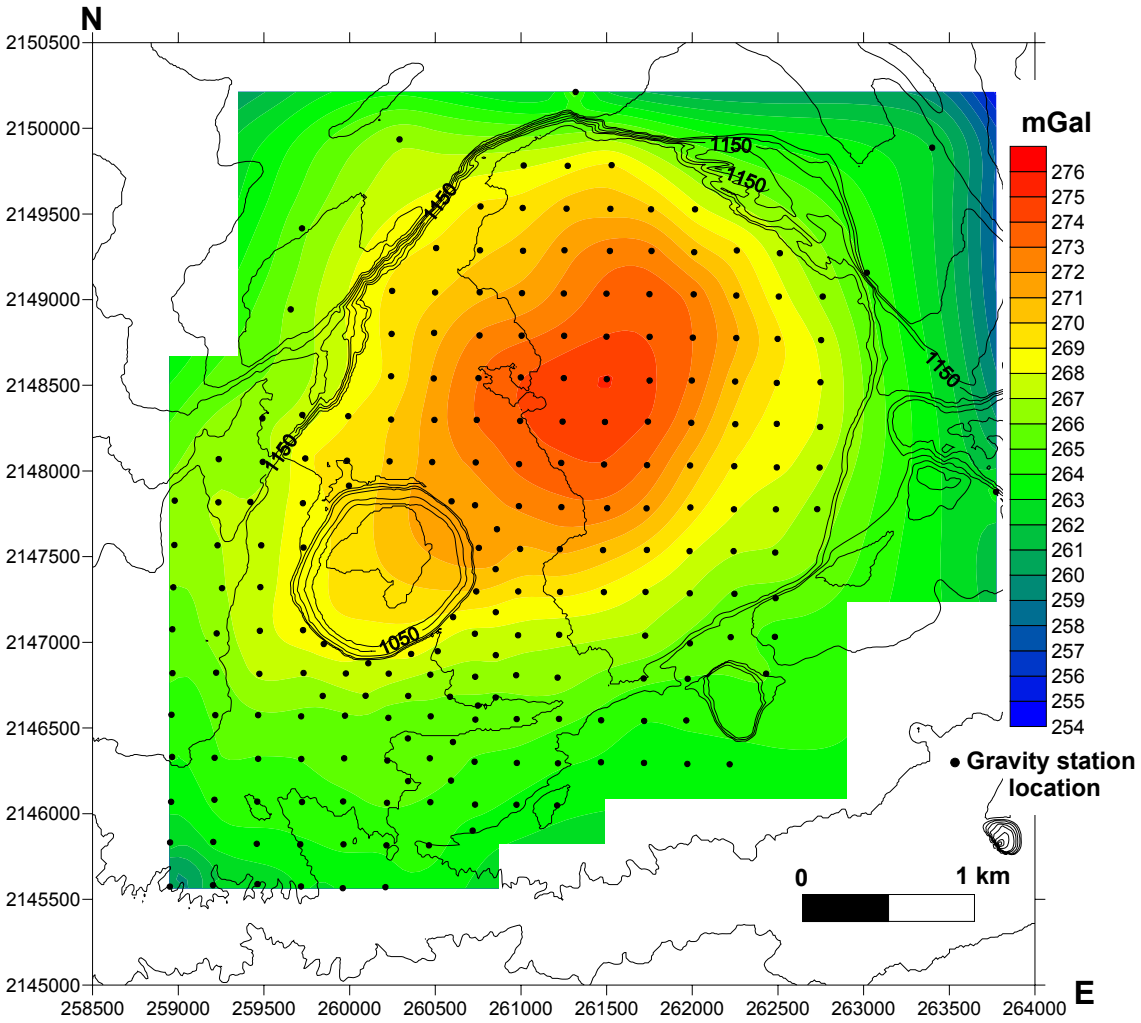

Figure 3-5 Bouguer gravity anomaly map of Kīlauea's caldera overlying topographic 20 m contours.

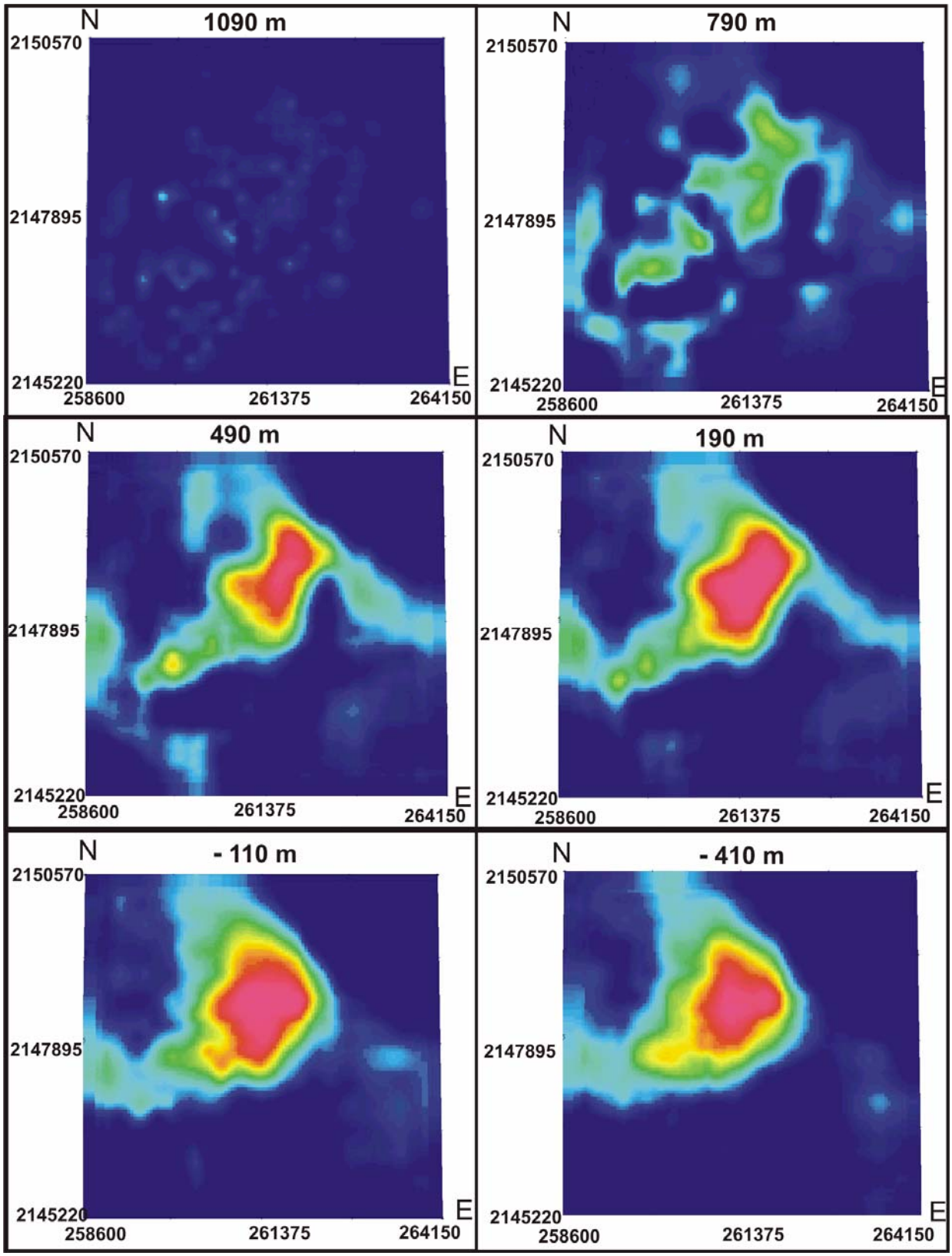
N
1090 m
2150570
2147895
2145220
258600
261375
264150
E
N
790 m
2150570
2147895
2145220
258600
261375
264150
E
N
490 m
2150570
2147895
2145220
258600
261375
264150
E
N
190 m
2150570
2147895
2145220
258600
261375
264150
E
N
- 110 m
2150570
2147895
2145220
258600
261375
264150
E
N
- 410 m
2150570
2147895
2145220
258600
261375
264150
E

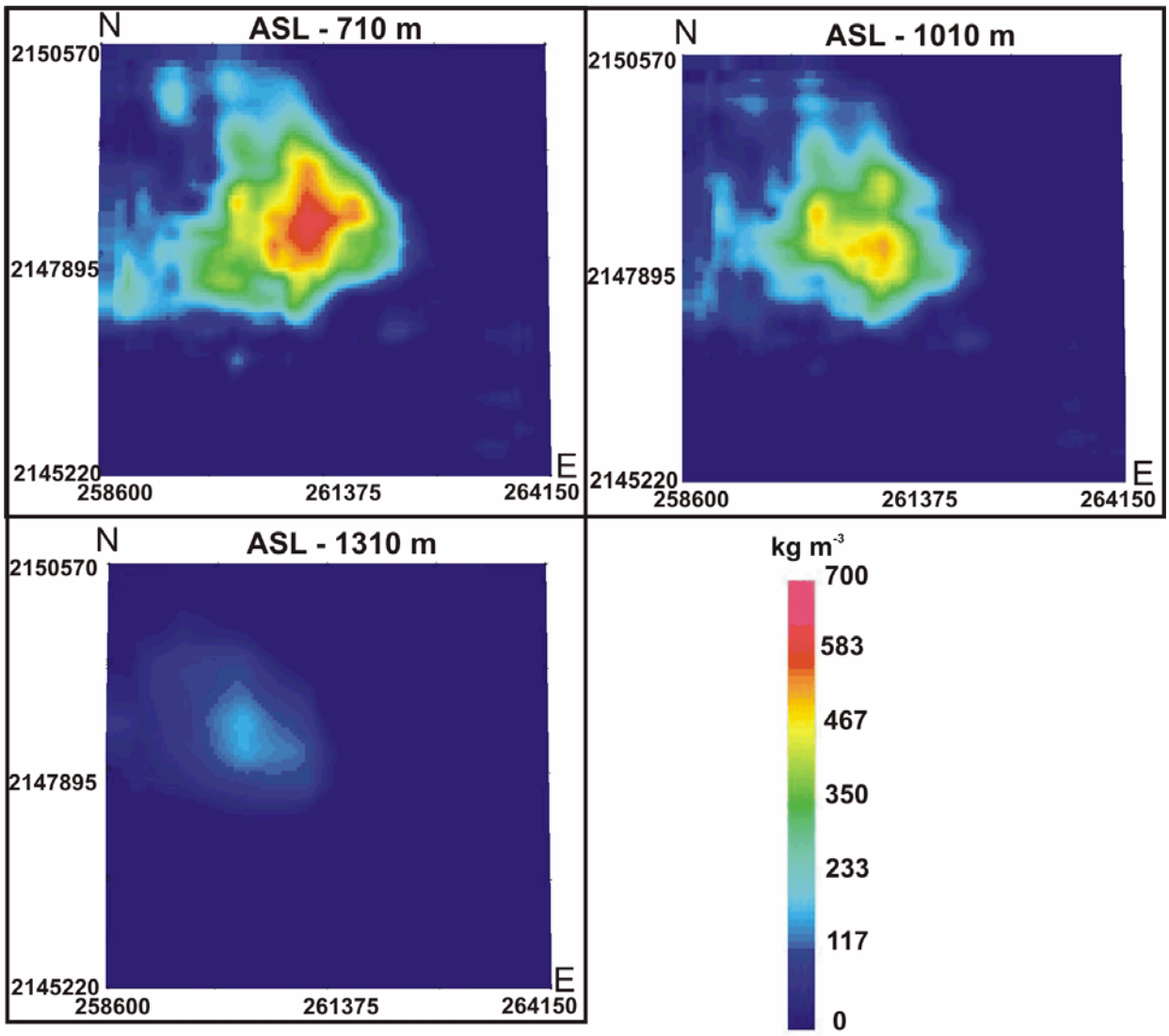

Figure 3-6 Depth slices in 300 m increments of a model from the inversion of the gravity data where the density was forced to be positive. All depths are in metres above sea level.

For the second model, no constraints were used to bound the maximum or minimum density within the model. The resulting inversion (Fig. 3-7) displays different sizes and shapes for density contrasts beneath the summit of Kīlauea than in the first inversion; however, it has the same general characteristics. The second model also displays a dense body beneath Kīlauea, but in general it is deeper. The top of the dense body starts at approximately the same depth

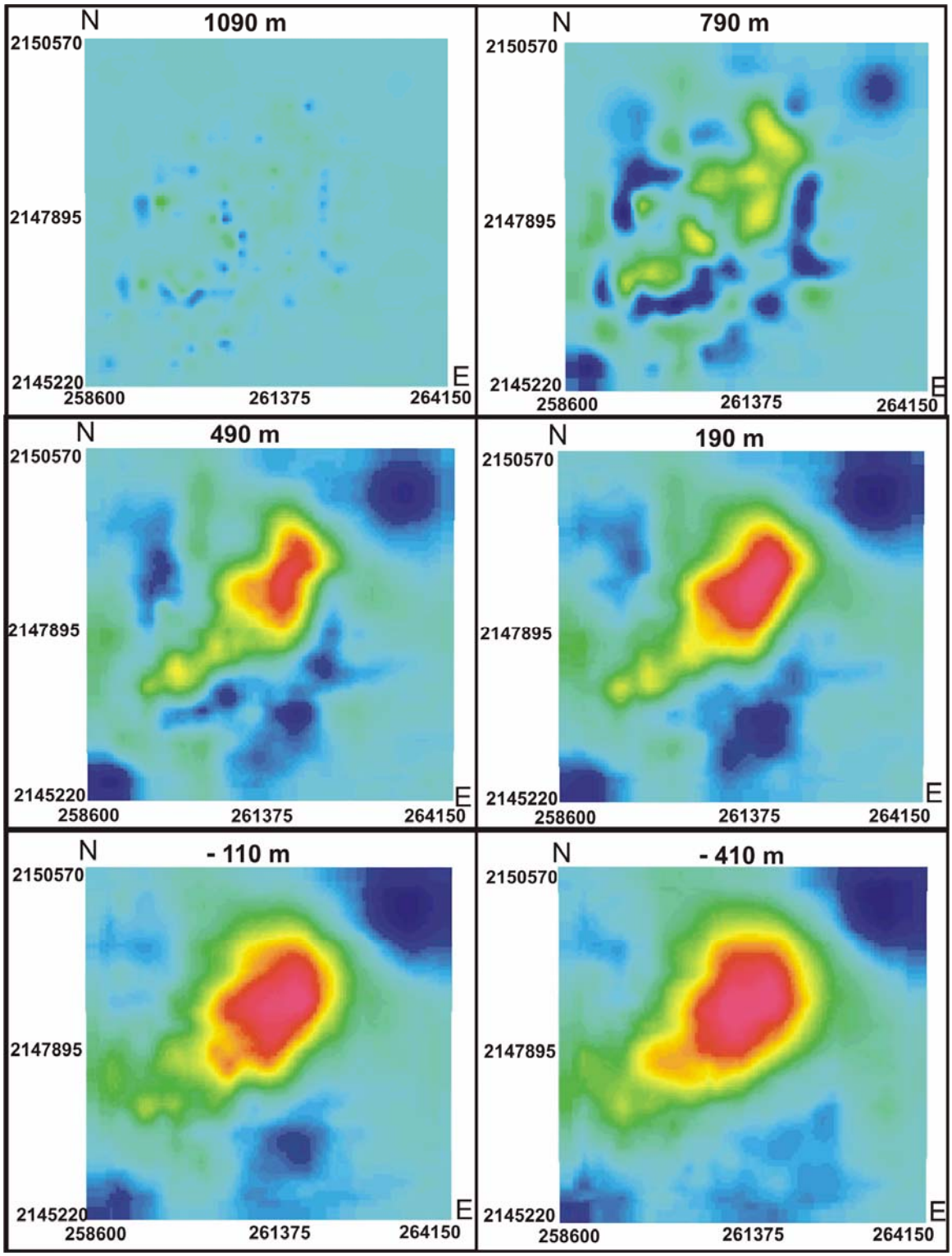
N
1090 m
2150570
2147895
2145220
258600
261375
264150
E
N
790 m
2150570
2147895
2145220
258600
261375
264150
E
N
490 m
2150570
2147895
2145220
258600
261375
264150
E
N
190 m
2150570
2147895
2145220
258600
261375
264150
E
N
- 110 m
2150570
2147895
2145220
258600
261375
264150
E
N
- 410 m
2150570
2147895
2145220
258600
261375
264150
E

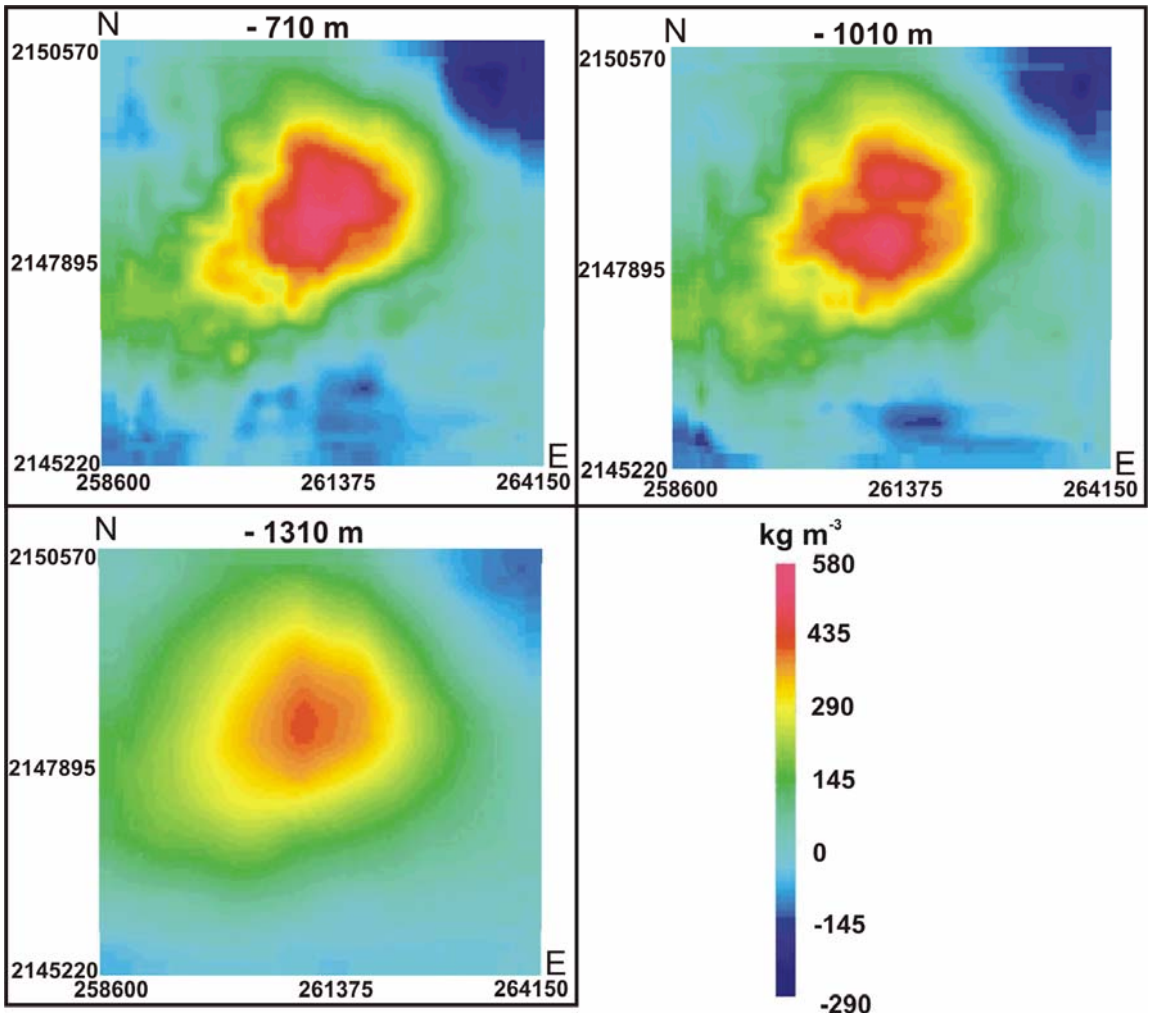

Figure 3-7 Depth slices in 300 m increments of model 2 created from the inversion of the gravity data with no constraints on density. All depths are in meters above sea level.

(300 m); however, its areal extent is smaller and more complex. The bottom of the dense body is not constrained in model 2 and continues deeper than 2400 m beneath the surface or -1310 m a.s.l.

Volume estimates of the dense body beneath Kīlauea's caldera were made by calculating the area underneath a density surface contour of 2680 kg m^{-3}, (+ 350 from the assumed average value) within each model. This density contour was chosen to represent the maximum total volume possible as dyke

densities are typically slightly higher at 2800 to 3100 kg m^{-3}. The model that was restricted to only positive densities has a calculated volume of ~ 15 km^3, while the model with no density constraints has a volume of ~ 5 km^3.

A sensitivity analysis was completed to identify areas containing possible void space beneath Kīlauea's summit. Forward models varied the depth and size of void space to measure the effect on the gravitational field at the surface. A large cavern with a volume of 10^6 m^3 was modeled as void space (density contrast of -2330 kg m^{-3}) at a depth of 200 m. The resulting maximum amplitude of the gravitational field is -300 μGal assuming there are no other factors. The void space was then modeled underlain by a dense (+700 kg m^{-3}) layer at 650 m depth. This had a masking effect where the resulting gravitational field at the surface could then be represented by a number of different models that did not include void space.

3.4.2 Masaya

The data collected on Masaya volcano had a much tighter grid spacing for both gravity and magnetic measurements in comparison to those collected at Kīlauea volcano. The magnetic measurements were spaced approximately 25 m apart along north – south lines 50 m apart (Fig. 3-8). The area inside Nindiri crater has an additional 6 profiles that run east-west to constrain both small scale anomalies and any anisotropic effects on the magnetic field. The elevation range over the survey area is ~150 m. Removing the IGRF from the magnetic dataset is thus important due to this large variation in topography which corresponds to ~ 2000 nT of change in the magnetic field. This is significant as it is greater than

the errors associated with the vertical position of the magnetic measurements. While the elevation component of the IGRF must be removed, the horizontal component is +/- 10 nT over the survey area. This is much smaller than the total error due to removal of the vertical component of the IGRF and is thus ignored. The elevation variation will also create topography induced anomalies based on either missing material near the pit craters or an increase due to excess material near a topographic high. A forward model using a DEM of the craters and an average magnetic susceptibility for basalt of 7 kg m^{-3} was created to characterize the effect of topography on the dataset (Fig. 3-8a). The DEM used was of only moderate resolution with a horizontal accuracy of ~60 m and vertical accuracy of ~10 m (Pascal, 2008). Furthermore, without obtaining a large number of rock samples, it is impossible to fully characterize the magnetic susceptibility around the craters, as the magnetic susceptibility can vary by an order of magnitude in basaltic rocks. Both of these problems are difficult to overcome as there is no publically available DEM with a better accuracy and exporting large amounts of volcanic material from Nicaragua has been logistically difficult. With this in mind, the topography model cannot completely characterize the induced topographic field. Therefore, attempting to remove it directly could obscure other features within the data and thus it is used only to aid in interpretation of the magnetic data.

The corrected magnetic data show large magnetic lows on the south side of both San Pedro and Santiago pit craters. The northern section of the survey

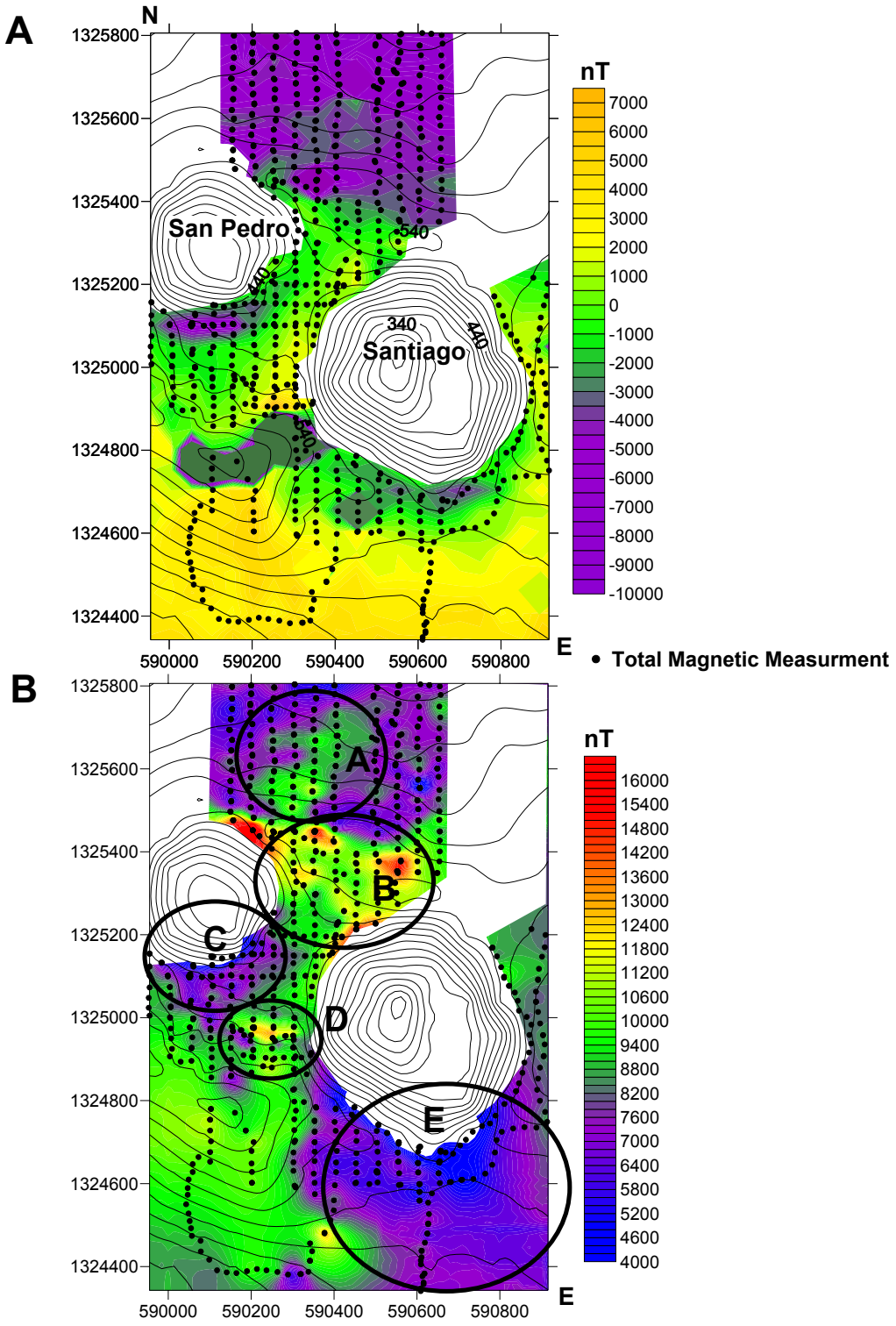

Figure 3-8 A: Theoretical magnetic field created by topography at Masaya. B: Residual magnetic data with anomalous areas labelled A -E. The data in both A and B are overlain on 25 m topography contours.

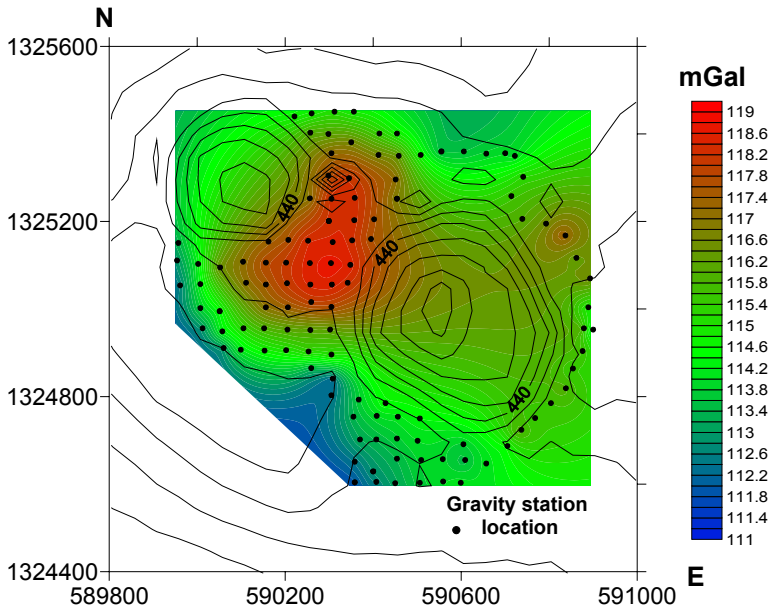

Figure 3-9 Residual Bouguer gravity anomaly map at Masaya. Topography contours are 40 m.

area shows interconnected pockets of higher (green; Fig. 3-8) magnetic field strength pinched off by lows. The north rim of Nindiri crater has a higher magnetic field strength than the rest of the survey area, with the highest point along the crater rim near San Pedro. One other area where the magnetic field strength is particularly high is along a cliff on the south west part of Nindiri crater. This short linear high is well displayed in the data in Fig 3-8 as anomaly D.

The residual Bouguer gravity anomaly map (Fig. 3-9) shows that the floor of Nindiri crater between San Pedro and Santiago has a higher field strength then the rest of the survey area. The southwest edge has a marked decrease of 8 mGal from the center of the high in Nindiri crater. As the data were not collected in a grid, determining the true resolution and maximum depth that the

dataset can infer is non-trivial. Within the lava plain bounded by San Pedro and Santiago craters, the smallest wavelength that can be completely captured would be 100 m and the maximum wavelength would be ~ 400 m. Applying Eq 1 and Eq 2 gives a depth range of 200 and 260 m. Taking the whole survey area into account, the maximum wavelength would be ~ 800 m and the maximum depth information that can be inferred is between 420 and 520 m. The depth to the floor of Santiago and San Pedro is ~ 300 m which is close to the maximum depth the survey can resolve.

Due to inconsistent closures, the errors on each data point vary similarly to the gravity data presented for Hawaii. While there are no closures above 150 μGal, there is still significant variation with the maximum at 95 μGal and the minimum at 10 μGal. Seismic noise from Santiago crater is also prevalent in the Bouguer gravity dataset. Given the behaviour of G-127, the magnitude of the noise measured by the meter was less than what was experienced near Kilauea's summit vent. While the error within the gravity dataset is not rigorously constrained, we assume that is less than 100 μGal.

3.5 Discussion

It is important to note that the forward and inverse models developed to interpret both gravity and magnetic data cannot provide unique solutions. Instead they provide only possibilities of what may occur at depth. When combined with other geologic and geophysical evidence, one can limit the possibilities to a few reasonable options.

3.5.1 Kīlauea

The total magnetic data show three anomalies within the survey area (Fig. 3-4a). Anomaly A, is a broad low located on the southern edge of Halema`uma`u. The magnetic model created to show the theoretical effect of topography on the data, also shows an anomalous low on the southern edge of Halema`uma`u (Fig. 3-4b). This suggests that anomaly A is due entirely to topographic effects and not related to volcanic structures. The low and high points of anomaly B are situated near fissures that erupted between 1954 and 1982 and strike northeast from Halema'uma'u (Fig. 3-10). Forward modeling suggests that the simplest geometry that can reproduce the anomalous field is a dyke that becomes shallower towards the east. Assuming that the anomaly is created by the eruptive fissures, the source for the eruption is most likely beneath Halema`uma`u. Anomaly C is located in the northern area of the caldera away from any visible fissure or eruptive landform (Fig. 3-4a). This area is covered by lava flows that were erupted in 1919 (Holcomb, 1980) suggesting that the source of anomaly C is buried beneath (Fig 3-10). The signature of the anomaly is complex and difficult to reproduce with forward models. The high part of the anomaly is approximately 2000 nT above the background field strength and has a small low associated with it to the southeast. Due to the large magnetic inclination angle around the summit of Kīlauea (39.9˚), no simple geometry can reproduce the measured high and corresponding small low to the south. It is possible that the magnetic low for anomaly C could be just outside the survey area to the north, or

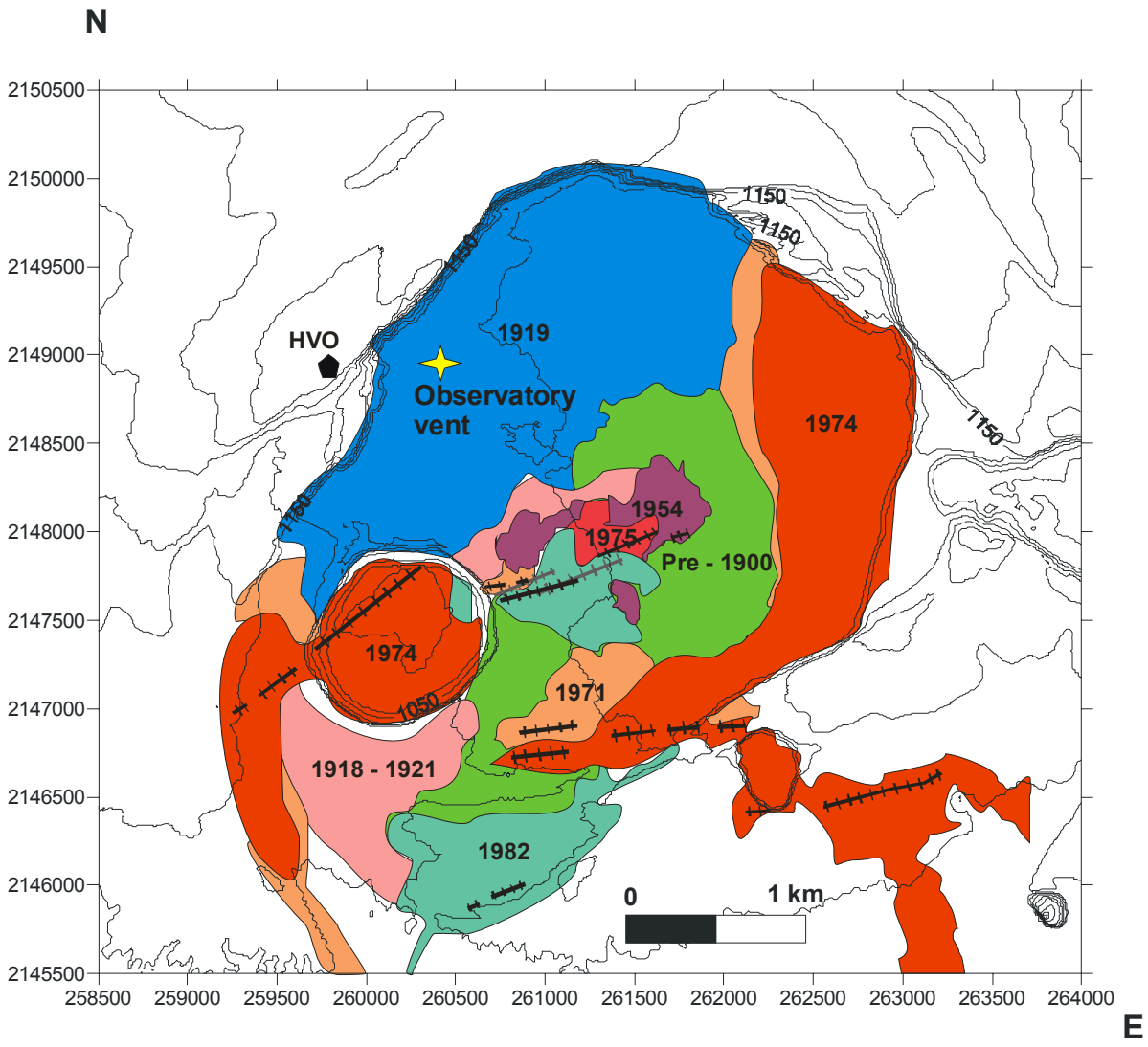

Figure 3-10 Geologic map of Kīlauea's summit caldera with visible eruptive fissures represented as black lines and buried fissures shown in grey. Modified from Holcomb (1980) and Neal and Lockwood (2003). The inferred location of the Observatory vent inferred by Holcomb (1987) is represented by a yellow star and the Hawaiian Volcano Observatory (HVO) by a black square.

perhaps the survey does not have sufficiently dense coverage to define it. If the corresponding low is outside the survey area, the source of the anomaly would need to be buried at sufficient depth to produce a large anomaly wavelength. Regardless of the size of the anomaly, the source is sufficiently complex that

further modeling will not provide more information. Previous geologic mapping by Holcomb (1980; 1987) does, however, suggest that a long lived prehistoric eruptive center, called the Observatory vent, was approximately 1 km east of the Hawaiian Volcano Observatory due to flow direction indicators (Fig. 3-10). The Observatory flows formed a large shield at the summit and created a 4 km wide band that flowed from the summit area down the northwest margin of Kīlauea to the ocean (Holcomb 1980). The ages of the observatory flows are not well constrained due to limited carbon samples and a lack of detailed mapping away from the summit, but are estimated at between 250 and 350 years before present (Holcomb, 1980). While there is no evidence to confirm whether anomaly C was indeed created by the inferred Observatory vent, a long lived eruptive site should have a complex magnetic signature associated with it. To accurately describe and model the source of this anomaly at depth, an expanded survey to the north and west along with infill lines to tighten spatial controls would be required.

Kauahikaua et al. (2000) imaged a dense core to Kīlauea which is much deeper than imaged here; their study was unable to image any shallow bodies. Likewise, the data presented here does not image any of the deeper anomalies due to a smaller spatial coverage limiting the information from depth. Combining the results suggests that Kīlauea's dense core starts with the shallow magmatic system and follows it deep within the volcano.

Inversions of our gravity dataset show a dense body covering an area that has been inferred to be a shallow summit magma reservoir. The volume of the entire dense body beneath the summit is between 5 and 15 km^3 as calculated

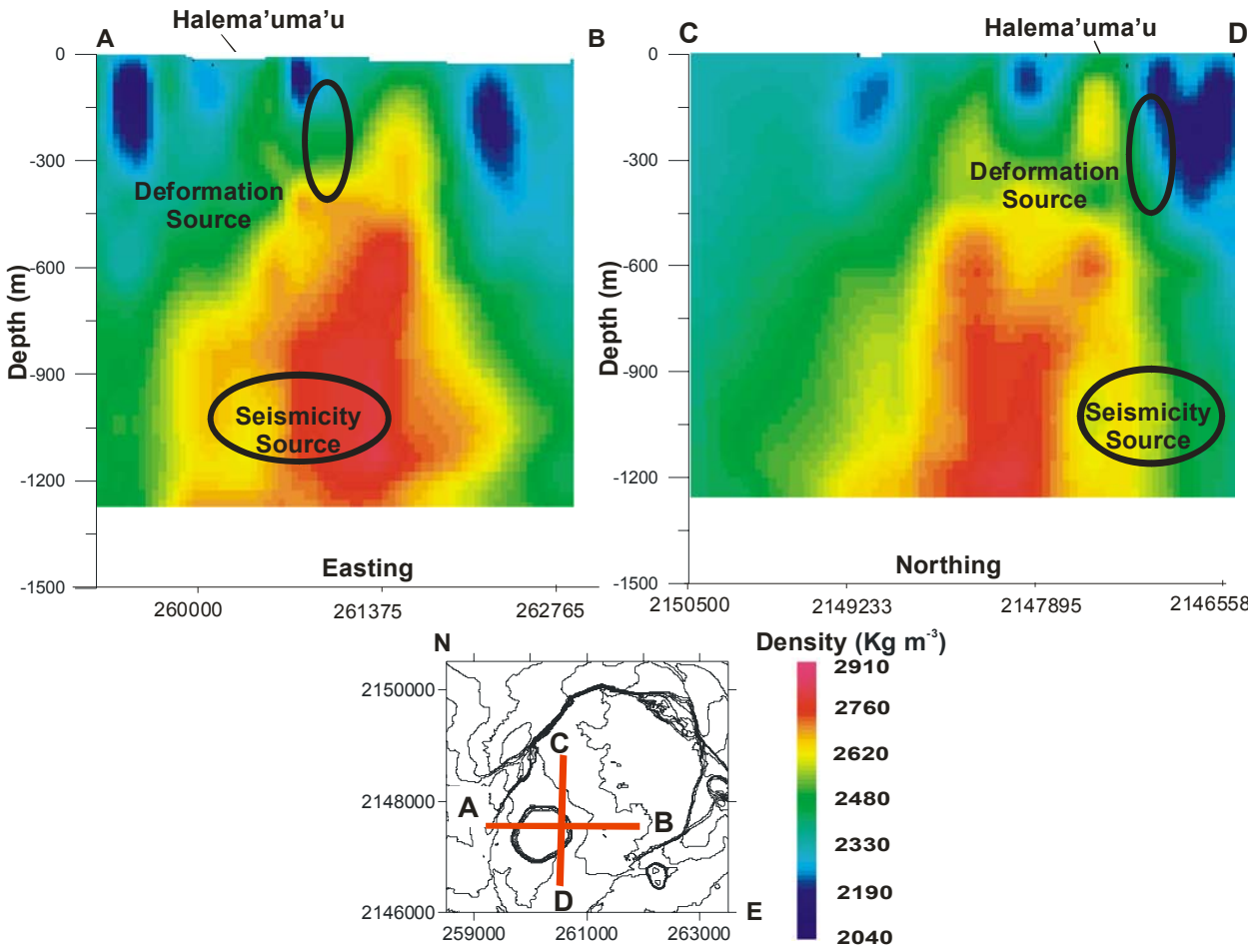

Figure 3-11 Cross-sections from inverse model 2 plotted with seismicity and deformation sources that have been used to infer melt at depth

from the two inversion models presented here. This volume is too large to consist entirely of melt as a magma chamber of this size and situated shallowly would have long ago been described by deformation and seismic data. While the gravity data can infer density contrasts, it cannot constrain the amount of melt at depth. Therefore, the majority of the dense body at depth is most likely an intrusive complex consisting of dense solid rock with a density between 2800 to 3300 kg m^{-3}. Both gravity inversions agree well with published deformation and

seismic results (Fig. 3-6, 3-7, 3-11). Tilt data from individual transient deformation events (Cervelli and Milkus, 2003) provide a source depth range from 130 to 450 m below the surface. Due to error within the tilt data, the events were stacked to provide a single source at 350 m. Both of the gravity inversions show that the intrusive complex could begin as little as 200 m below the surface, which could represent the top of the melt-filled volume. Seismic studies have inferred that melt exists beneath the northeast edge of Halema`uma`u at approximately 1 km depth (Ohminato et al., 1998; Almendros et al., 2002; Fig. 3-11). The intrusive complex as defined by the gravity inversions continues deeper than 1 km beneath the surface and can easily accomodate the range of depths inferred by the different surveys. The most recent conceptual model of the Halema`uma`u magma reservoir is a set of interconnected melt filled dykes and sills (Pietruszka and Garcia, 1990). The gravity data indirectly supports this model as the dense material at depth probably consists of mostly dykes and sills rather than melt.

Although it is impossible to constrain the amount of melt, inferences can be made by combining historical eruptive records and previous deformation studies. Transient deformation events have occurred intermittently with periods of regularity since 2000, centered just east of Halema`uma`u (Cervelli and Miklius 2003; Poland et al., 2009). The center of the deformation field should represent the greatest concentration of melt at depth; however, it is not centered over inferred intrusive complex. Historical eruptive vents within the caldera (Fig. 3-10) show that eruptions have taken place closer to the southwestern edge of the Bouguer anomaly than the northeastern edge. With so little dynamic activity

recorded beneath the northeastern section of the caldera, this means that either our ability to detect melt is lacking or there is a very little to no magma in this area of the caldera. Kīlauea is extremely well monitored with extensive seismic and deformation networks, thus it is unlikely that a significant amount of melt exists shallowly beneath the northern section of the caldera without evidence. The most probable reason for the lack of historical or recent dynamic activity is that this area is an old melt accumulation zone. The reason why the majority of the inferred intrusive complex is inactive could take a number of different forms. It is possible that there have been many magma chambers that have been abandoned through time. The most likely possibility takes into account volcanic rifting that has long been documented to occur at Kīlauea (Delaney et al., 1998). The forced injection of material from depth and the fact that the south flank of Kīlauea is mobile and slowly moving seaward (Denlinger and Okubo, 1995), creates extensional rifting that could cause a slow migration of a shallow magma chamber. If volcanic rifting is the principal mechanism responsible for the growth of the intrusive complex, then it is to be expected that the youngest section would be currently active. The gravity data and the location of historical vents provide some circumstantial evidence for this with the positive Bouguer anomaly elongated in the direction of Halema`uma`u. However, the stretching towards Halema`uma`u could also represent structures at depth such as a conduit that may connect to the deeper magma chamber in the southern caldera.

Another goal of this study was to test the results from Johnson et al. (2010) which suggested that 20 to 120 x 10^6 m^3 of void space beneath the

caldera filled over 33 years. Due to the non-uniqueness of interpreting potential fields, there is no way to directly quantify the amount of void space within the summit region. However, tests were done to investigate how large caverns may be represented within the gravity data. Through forward modeling, it is clear that large caverns of void space can exist, which might not be identified in the summit region through gravity analysis. If there is a high density body above or below an area of void space, it masks the resulting signal. While the gravity data does not provide the ability to constrain void space as caverns or small interconnected cracks within the caldera, it is still difficult to conceptualize this amount of void space. One other possibility that could explain the observed mass increase is volcanic rifting causing a slow addition of mass to the summit region. To fully explore this idea requires future study of the spreading forces and how they might propagate from depth to the surface.

3.5.2 Masaya

The residual magnetic data (Fig. 3-8) shows a set of complicated anomalies with large magnitudes. While it is not unusual to have a variation of 3 to 4000 nT in the magnetic field across volcanic terrain, the approximately 12,000 nT variation across the survey is much greater then what is typically seen. The theoretical magnetic field created from forward models also show large contrasts across the survey area. This suggests that topography is probably a controlling mechanism causing many of the large magnetic variations occur across the survey area. There are several assumptions that have been used to create the topography model, the largest of which assumes an average magnetic

susceptibility of 7 kg m^{-3} without taking into account remnant magnetism. The topography model is thus only used as a tool to determine which of the anomalies identified in Figure 3-8 are most likely due to topography effects. Anomalies C and E exist on the south side of the San Pedro and Santiago pit craters, and correspond to the lows identified in the topography models. Anomaly C is most likely completely created by San Pedro crater, however, anomaly E extends far enough from Santiago crater to, in part, be caused by something else. The one small profile which extends the magnetic map south is over a set of flows with a large network of lava tubes (Fig. 3-8). Lava tubes represent missing material thereby creating a low when measured on the ground surface above. The extent of the magnetic low is likely not as large as depicted in the anomaly map as it is based on essentially one profile in the southeastern part of the survey area. Anomaly D is a short linear high that follows a small 10-15 m fault scarp in Nindiri crater. Next to the bottom of this fault scarp, magnetic readings jumped significantly and are most likely due to the material beside and above the sensor increasing the observed magnetic field instead of a fault or some other structure. The area of high field strength identified as anomaly B does not appear in the theoretical topographic model and must thus represent a material property change. This area is structurally complex with multiple faults present and thus it is difficult to identify any individual structure responsible for the high field strength. The area also undergoes heavy surface alteration due to prevailing winds carrying acidic volcanic gases from Santiago; however, the degree of alteration with depth is unknown. It is thus difficult to build a

reasonable model with no constraints on magnetic contrasts at the surface or at depth. Detailed mapping of faults and cracks with magnetic susceptibility and remnant magnetism measurements would be necessary to truly attempt to analyze the magnetic signature within this area. The last anomaly in Figure 3-8 (anomaly A), is located on the north slope of Nindiri cone. This high area approximately outlines a lobe of the 1670 flow that issued from Nindiri crater and suggests that the flow has stronger magnetic properties than its surroundings. Unfortunately there is no direct way to build upon this map without investing a significant amount of time and resources to characterize the magnetic properties of the rocks in each location. To expand and produce a magnetic map of the whole caldera through ground surveys is not realistic due to topography and dense vegetation in some areas. Airborne magnetic surveys are an alternative and, although costly, could provide a robust map to identify areas of anomalous magnetic field strength to ground truth and increase resolution.

The Bouguer gravity data increases the visible resolution relative to the work by other researchers (Connor et al., 1989; Metaxian, 1994). While no new anomalies have been identified, it is clear there is no large gravity low associated with the either of the craters. An anomalous low would be expected if there were large caverns of void space below the floor of Santiago crater. Since 1986, the formation of void space and subsequent collapse has been observed and documented (Rymer et al., 1998) within Santiago crater. This could imply one of three things: 1) the void space is relatively small and compartmental as it is destroyed shortly after being created and is thus too small to detect using the

gravity data; 2) the gravity survey does not cover a large enough area to identify any broad shaped lows that could represent void space; 3) there was no void space at the time of survey as it had been recently filled or destroyed. At the time of the survey, there was no incandescence visible from the active vent within the Santiago crater, suggesting that there was some space between the magma column and the vent. Also, there was no anomalous collapses before the survey, making option 3 the least likely. Due to the unknown structure with depth, it is difficult to determine if the void space is too small to be directly inferred or if the survey area was too small to identify it. Increasing the survey area would likely solve the problem and provide more information. Having a dataset with the size and spacing as Kīlauea would be ideal, although impractical due to vegetation and access problems. The ability to image the density contrasts within the Bouguer anomalies that have been identified by past researchers (Connor et al., 1989; Metaxian, 1994) would greatly increase the knowledge of the plumbing system of Masaya.

3.5.3 Kīlauea vs Masaya

Both Masaya and Kīlauea are baslaltic caldera systems, with long periods of continuous activity at their summits. However, their Bouguer gravity anomalies are drastically different. The gravity anomaly at Kīlauea is centered near Halema'uma'u, the focus of current summit activity. This gravitational high probably formed over a long period of time through repeat intrusions. In contrast, no analogous high density body was detected beneath Santiago crater at Masaya volcano. Masaya's caldera was created through a series of basaltic

Plinian eruptions over the last 6000 years, which may have led to a change in the eruptive center. If the center of activity changed, there may not have been enough time to develop a detectible intrusive complex. There is a gravitational high north of Nindiri cone (Métaxian, 1994) interpreted as most likely being a magma chamber; however it could also represent a relict intrusive body over an older center of activity. No comparisons are made based on the magnetic data due to the Masaya data being dominated by topographic effects such that it is impossible to make rigerous comparisons.

3.6 Conclusion

The magnetic survey at Kīlauea identifies two large non topography anomalies within the caldera. The first is likely created by a set of fissures which include the historical eruptions from 1954 to 1982 and strike northeast; magnetic field modeling suggests these fissures deepen towards Halema'uma'u. The second anomaly is probably due to a long lived eruptive center that is older than 200 years called the Observatory vent (Holcomb 1987). This data expands the current knowledge of the structures within the caldera and provides the basis for further investigations which might be able to identify other buried fissure zones or long sustained eruptive vents. The best explanation for the positive Bouguer gravity anomaly centered within Kīlauea's caldera is a large shallow intrusive complex. The volume of the whole intrusion is between 5 and 15 km^3 and is likely much larger than the amount of melt stored at depth. Other gravity studies (Kauahikaua et al., 2000) have suggested that the majority of the dense material beneath Kīlauea could have a density that approaches that of an olivine

cumulate. This would require the intrusion's maximum modeled volume of 15 km^3 which is probably too large and not realistic. Void space was also investigated to determine how much currently exists in the summit region. No constraints were obtained due to the non-uniqueness of potential fields where void space could be masked by denser material above or below. The center of the gravity anomaly is offset from the majority of historical eruptions. Volcanic rifting is one possible explanation for this phenomenon causing a slow south westward migration of the intrusive complex. It could also explain previous dynamic microgravity results without relying on a large amount of void space near Halema'uma'u. Future work is needed to fully investigate the effect of volcanic rifting on magma chamber growth to distinguish between rifting or void space.

The magnetic and gravity data collected at Masaya volcano reflect changes in the superficial geology and not volcanic structures. The lack of a strong Bouguer anomaly centered over the focus of historical activity is most likely due to the edifice's age being less than 6000 years old rather than a fundamental difference in processes occurring at Masaya and Kīlauea. Currently, there are ongoing studies that will increase the gravity station density within Masaya's caldera. This should provide the ability to image the density structures in much greater detail.

Magnetic and gravity survey data can be used to image subsurface structures where no direct observations are possible. These are potential field techniques and thus are non-unique, however, when integrated with other

datasets like seismic and deformation, it becomes possible to more fully characterize the processes and evolution of volcanic activity at volcanoes.

3.7 References

Almendros, J., Chouet, B., Dawson, P., and Bond, T., 2002, Identifying elements of the plumbing system beneath Kīlauea Volcano, Hawaii, from the source locations of very-long-period signals: Geophysical Journal International, v. 148, no. 2, p. 303-312

Bagnardi, M., Eggers, A.A., Battaglia, M., Poland, M.P., and Johnson, D., J., 2008, Mass intrusion beneath Kīlauea Volcano, Hawaii, constraints from gravity and geodetic measurements: American Geophysical Union, Fall Meeting 2008.

Barton, C.E., 1997, International Geomagnetic Reference Field: The seventh generation: Journal of Geomagnetism and Geoelectricity, v. 49, no. 2-3, p. 123-148.

Battaglia, J., Got, J., and Okubo, P., 2003, Location of long-period events below Kīlauea Volcano using seismic amplitudes and accurate relative relocation: Journal of Geophysical Research, v. 108, p. 2553.

Berrino, G., Rymer, H., Brown, G.C., and Corrado, G., 1992, Gravity-height correlations for unrest at calderas: Journal of Volcanology and Geothermal Research, v. 53, no. 1-4, p. 11-26.

Cervelli, P.F., and Miklius, A., 2003, The Shallow Magmatic System of Kīlauea Volcano: U.S. Geological Survey Professional Paper 1676, p 149-163.

Clague, D. A., 1987, Hawaiian xenolith populations, magma supply rates, and development of magma chambers: Bulletin of Volcanology, v. 49, no. 4, p. 577-587

Connor, C.B., Williams, S.N., Lawe, D.K., and Draper, G., 1989, Interpretation of gravity anomalies, Masaya Caldera Complex, Nicaragua: Transactions of the 12th Caribbean Conference, St. Croix, v. 12, p. 495-502.

Cowan, H., Prentice, C., Pantosti, D., de Martini, P., Strauch, W., and Workshop Participants, 2002, Late Holocene earthquakes on the Aeropuerto Fault, Managua, Nicaragua: Bulletin of the Seismological Society of America, v. 92, no. 5, p. 1694-1707.

Dawson, P.B., Chouet, B.A., Okubo, P.G., Villaseñor, A., and Benz, H.M., 1999, Three-dimensional velocity structure of the Kīlauea Caldera, Hawaii: Geophysical Research Letters, v. 26, no. 18, p. 2805-2808

Decker, R., 1963, Magnetic studies on Kīlauea Iki lava lake, Hawaii: Bulletin of Volcanology, v. 26, no. 1, p. 23-35

Delaney, P.T., Denlinger, R.P., Lisowski, M., Miklius, A., Okubo, P.G., Okamura, A.T., and Sako, M.K., 1998, Volcanic spreading at Kīlauea, 1976–1996: Journal of Geophysical Research, v. 103, p. 18003-18023.

Denlinger, R.P., and Okubo, P., 1995, Structure of the mobile south flank of Kīlauea Volcano, Hawaii: Journal of Geophysical Research, v. 100, p. 24499-24507.

Dzurisin, D., Anderson, L.A., Eaton, G.P., Koyanagi, R.Y., Lipman, P.W., Lockwood, J.P., Okamura, R.T., Puniwai, G.S., Sako, M.K., and Yamashita, K.M., 1980, Geophysical observations of Kilauea Volcano, Hawaii, 2. Constraints on the magma supply during November 1975–September 1977: Journal of Volcanology and Geothermal Research, v. 7, no. 3-4, p. 241-269.

Dzurisin, D., Lockwood, J.P., Casadevall, T.J., and Rubin, M., 1995, The Uwekahuna Ash Member of the Puna Basalt: product of violent phreatomagmatic eruptions at Kīlauea volcano, Hawaii, between 2800 and 2100 14C years ago: Journal of Volcanology and Geothermal Research, v. 66, no. 1-4, p. 163-184

Ellis, W., 1823, A naritive of tour through Hawaii: London, p. 367.

Flanigan, V.J., Long, C.K., Rohret, D.H., and Mohr, P.J., 1986, Aeromagnetic map of the rift zones of Kīlauea and Mauna Loa volcanoes, Island of Hawaii, Hawaii, United States Geological Survey Field Investigation Map, v. MF-1845A.

Girard, G., and van Wyk de Vries, Benjamin, 2005, The Managua Graben and Las Sierras-Masaya volcanic complex (Nicaragua); pull-apart localization by

an intrusive complex: results from analogue modeling: Journal of Volcanology and Geothermal Research, v. 144, p. 37-57.

Godson, R.H., Zablocki, C.J., Pierce, H.A., Frayser, J.B., Mitchell, C.M., and Sneddon, R.A., 1981, Aeromagnetic map of the Island of Hawaii, scale 1:250,000, U.S. Geol. Surv. Geophys. Invest. Map, v. GP-946.

GRAV3D, 2007, A program library for forward modeling and inversion of gravity data over 3D structures: developed under the consortium research project Joint/Cooperative Inversion of Geophysical andGeological Data: UBC-Geophysical Inversion Facility,Department of Earth and Ocean Sciences, The University of British Columbia, Vancouver., version 20070309, 2007.

Gudmundsson, M.T., and Milsom, J., 1997, Gravity and magnetic studies of the subglacial Grímsvötn volcano, Iceland: Implications for crustal and thermal structure: Journal of Geophysical Research, v. 102, no. B4, p. 7691-7704.

Hildenbrand, T.G., Rosenbaum, J.G., and Kauahikaua, J.P., 1993, Aeromagnetic Study of the Island of Hawaii: Journal of Geophysical Research, v. 98, no. B3, p. 4099-4119.

Holcomb, R.T., 1980, Preliminary geologic map of Kilauea Volcano, Hawaii: U.S. Geological Survey Open-File Report 81-796.

Holcomb, R.T., 1987, Eruptive History and long-term behavior of Kĩlauea volcano: U.S. Geological Survey Professional Paper 1350, p. 261-350.

Jagger, T.A., and Finch, R.H., 1924, The explosive eruption of Kĩlauea in Hawaii: American Journal of Science, v. 8, no. 5, p. 353-374.

Johnson, D.J., Eggers, A.A., Bagnardi, M., Battaglia, M., Poland, M.P., and Miklius, A., 2010, Shallow magma accumulation at Kīlauea Volcano, Hawai‘i, revealed by microgravity surveys: Geology, v.38 p.1139-1142.

Kauahikaua, J., Hildenbrand, T., and Webring, M., 2000, Deep magmatic structures of Hawaiian volcanoes, imaged by three-dimensional gravity models: Geology, v. 28, no. 10, p. 883-886

Kutterolf, S., Freundt, A., and Peréz, W., 2008, Pacific offshore record of Plinian arc volcanism in Central America: 2. Tephra volumes and erupted masses: Geochemistry, Geophysics, Geosystems, v. 9, no. 2, p. Q02S02

MAG3D, 2007, A program library for forward modeling and inversion of magnetic data over 3D structures: developed under the consortium research project Joint/Cooperative Inversion of Geophysical andGeological Data: UBC-Geophysical Inversion Facility,Department of Earth and Ocean Sciences, The University of British Columbia, Vancouver., v. version 20070309.

Mauri, G., Williams-Jones, G., Saracco, G., and Zurek, J.M., 2010, The hydrothermal complex of Masaya volcano, Nicaragua., Journal of Volcanology and Geothermal Research, Submitted.

Metaxain, J.P., 1994, Etude sismologique et gravimetrique d'un volcan actif. Dynamisme interne et structure de la Caldeira Masaya Nicaragua. PhD. thesis Université de Savoie, France (unpublished).

Neal, C.A., and Lockwood, J.P., 2003, Geologic Map of the Summit Region of Kĭlauea Volcano, Hawaii: U.S. Geological Survey: Geologic Investigations Series, I–2759.

Ohminato, T., Chouet, B.A., Dawson, P., and Kedar, S., 1998, Waveform inversion of very long period impulsive signals associated with magmatic injection beneath Kĭlauea Volcano, Hawaii: Journal Geophysical Research, v. 103, p. 23839-23862

Okubo, Y., and Shibuya, A., 1993, Thermal and crustal structure of the Aso volcano and surrounding regions constrained by gravity and magnetic data, Japan: Journal of Volcanology and Geothermal Research, v. 55, no. 3-4, p. 337-350

Pascal, K., 2008, 3D Modelling of multi-parameter geophysical data from Masaya volcano, Nicaragua: BSc Honors Thesis, University of Leeds, Leeds, West Yorkshire, England.

Pérez, W., Freundt, A., Kutterolf, S., and Schmincke, H., 2009, The Masaya Triple Layer: A 2100 year old basaltic multi-episodic Plinian eruption from the Masaya Caldera Complex (Nicaragua): Journal of Volcanology and Geothermal Research, v. 179, p. 191-205.

Pietruszka, A.J., and Garcia, M.O., 1999, The size and shape of Kĩlauea Volcano's summit magma storage reservoir: a geochemical probe: Earth and Planetary Science Letters, v. 167, no. 3-4, p. 311-320.

Poland, M.P., Sutton, J.A., and Gerlach, T.M., 2009, Magma degassing triggered by static decompression at Kĩlauea Volcano, Hawaii: Geophysical Research Letters, v. 36, p. L16306.

Powers, H.A., 1948, A chronology of explosive eruptions of Kĩlauea: Pacific Science, v. 2, p. 278-292.

Rymer, H., and Brown, G.C., 1986, Gravity fields and the interpretation of volcanic structures: Geological discrimination and temporal evolution: Journal of Volcanology and Geothermal Research, v. 27, no. 3-4, p. 229-254.

Rymer, H., van Wyk de Vries, B., Stix, J., and Williams-Jones, G., 1998, Pit crater structure and processes governing persistent activity at Masaya Volcano, Nicaragua: Bulletin of Volcanology, v. 59, no. 5, p. 345-355.

Stoiber, R.E., Williams, S.N., and Huebert, B.J., 1986, Sulfur and halogen gases at Masaya Caldera Complex, Nicaragua: total flux and variations with time: J.Geophys.Res., v. 91, p. 12215-12231.

Swanson, D.A., 2008, Hawaiian oral tradition describes 400 years of volcanic activity at Kīlauea: Journal of Volcanology and Geothermal Research, v. 176, no. 3, p. 427-431.

Telford, W.M., Geldart, L.P., and Sheriff, R.E., 1990, Applied geophysics (2nd ed.): New York, U.S.A., Cambridge University Press, 770 p.

Walker, G.P.L., 1993, Basaltic-volcano systems: Geological Society London, Special Publications, v. 76, no. 1, p. 3-38.

Walker, J.A., Williams, S.N., Kalamarides, R.I., and Feigenson, M.D., 1993, Shallow open-system evolution of basaltic magma beneath a subduction zone volcano: The Masaya Caldera Complex, Nicaragua: Journal of Volcanology and Geothermal Research, v. 56, no. 4, p. 379-400.

Watts, A.B., and ten Brink, U.S., 1989, Crustal structure, flexure, and subsidence history of the Hawaiian Islands: Journal of Geophysical Research, v. 94, p. 10473-10500.

Williams, S.N., 1983, Plinian airfall deposits of basaltic composition: Geology, v. 11, no. 4, p. 211-214.

Williams-Jones, G., Rymer, H., and Rothery, D.A., 2003, Gravity changes and passive SO2 degassing at the Masaya caldera complex, Nicaragua: Journal of Volcanology and Geothermal Research, v. 123, no. 1-2, p. 137-160.

Wilson, D., Elias, T., Orr, T., Patrick, M., Sutton, J., and Swanson, D., 2008, Small Explosion From New Vent at Kilauea's Summit: EOS American Geophysical Union Transactions, v. 89, no. 22, p. 203.

Wooten, K.M., Thornber, C.R., Orr, T.R., Ellis, J.F., and Trusdell, F.A., 2009, Catalog of tephra Samples from Kīlauea's summit eruption, March-December 2008: U.S. Geological Survey Open-File Report 2009-1134.

4: CONSTRAINING VOLCANIC INFLATION AT THREE SISTERS VOLCANIC FIELD IN OREGON, U.S., THROUGH MICROGRAVITY AND DEFORMATION MODELING.

Jeffrey Zurek, Glyn William-Jones, Daniel Dzurisin, Dan Johnson, Al Eggers, Mike Poland

4.1 Introduction

Large-scale deformation events are common at active volcanoes and are most often detected using seismic or deformation techniques (e.g., Dzurisin et al., 1990). While these methods can provide information about the volume and shape of the source, they do not constrain the change or redistribution of mass at depth. However microgravity surveys, when used in conjunction with deformation data can provide constraints on the mass flux at depth and source density (e.g., Berrino et al., 1992; Rymer, 1996; Battaglia et al., 2003).

Microgravity has been utilized on numerous volcanic systems including Yellowstone (USA) and Campi Flegei (Italy) calderas to constrain and investigate the properties of deformation sources. At both calderas, changes in the associated hydrothermal systems have been postulated by several authors (e.g., Dzurisin et al., 1990, 1994; Bonafede et al., 1998; Orsi et al., 1999; Gottsmann et al., 2006) as a possible source of the observed deformation and gravity change. Microgravity provides the possibility to distinguish between a magmatic source

and a hydrothermal source by determining a density based on depth and volume information obtained from deformation analysis. Natural systems are usually complex and can have multiple deformation sources. For example, Gottsmann et al. (2006) indicate that it is more realistic to model the deformation and gravity data at Campi Flegei as a combination of magmatic and hydrothermal sources. When determining the nature of a deformation event, it is also important to consider the possibility that the Earth's crust may be deforming viscoelastically; an elastic deformation model can result in unrealistic overpressures needed to reproduce the observed uplift (e.g., Berrino et al., 1984). Furthermore, volcanic areas generally consist of incoherent material produced from eruptions and a high crustal heat flow (e.g., Bonafede et al., 1986), which produces a lower effective viscosity for the crust and thus requires the consideration of its inelastic properties.

Integrating deformation and microgravity has become the standard approach to determine source parameters (e.g., Battaglia, 2008) and it is also important for process identification and forecasting volcanic behaviour (e.g., Rymer and Williams-Jones, 2000). This study combines time series data from microgravity measurements (2002 to 2009) and deformation data (Dzurisin et al., 2006, 2009) at Three Sisters Volcanic Field (Oregon, USA) in order to further constrain source parameters of the inferred intrusion at depth.

4.2 Geologic setting

The Three Sisters Volcanic Field is located in central Oregon and is part of the Cascade Volcanic arc which stretches from northern California to south-

western British Columbia (Fig 4-1). The Juan de Fuca plate, at the Oregon coast, is subducting beneath North America obliquely at a rate of ~ 3 cm yr^{-1} (Riddihough, 1980; Bates et al., 1981). The central Oregon section of the volcanic arc has produced more Cenozoic vents and lava than any other part of the arc, while historically producing very few seismic events (Guffanti and

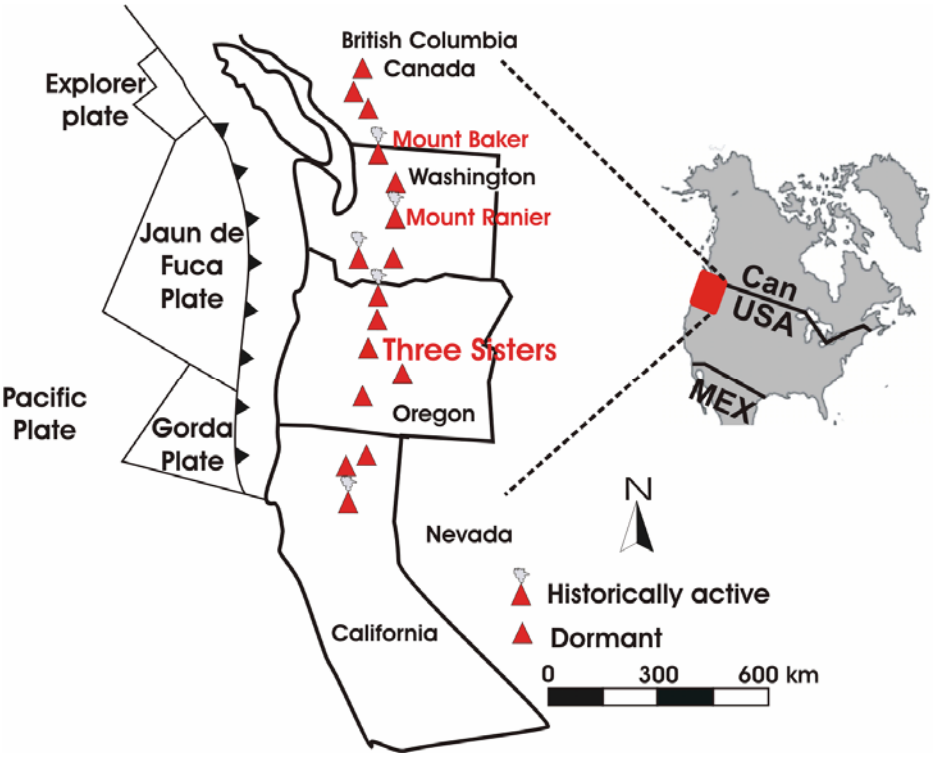

Figure 4-1 The subduction of the Juan de Fuca, Gorda and Explorer plates off the west coast of North America; red triangles represent major volcanic centers in the Cascade Volcanic arc. Inset: North America with the highlighted area in red representing the Cascade Volcanic arc.

Weaver, 1988; Priest, 1990; Sherrod and Smith, 1990). The cause of the region's aseismic behaviour is likely due to a change in tectonic stresses from compression to extension, as well as an increased heat flow gradient (Blackwell et al., 1982, 1990).

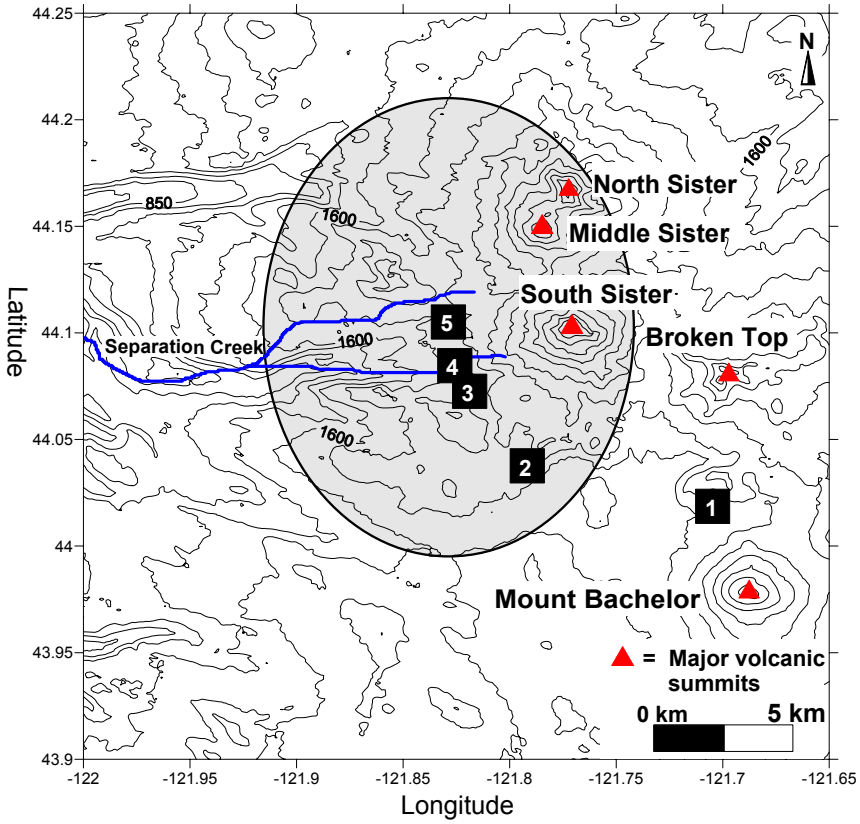

Figure 4-2 Topographic map of the Three Sisters Volcanic Field with the grey circle representing the approximate area affected by the current deformation event. Five large Quaternary cones are indicated with red triangles. The gravity network stations are displayed as black squares and numbered: 1) BASE, 2) BUGS, 3) BRUCE, 4) CUT and 5) CENTER.

The region's extensional stresses are a by-product of rotation as southern Washington and Oregon rotate away from the rest of North America (e.g., Magill et al., 1981). A possible tectonic cause for the apparent rotation is the increase in the obliqueness of subduction along the Oregon coast over the course of the last 40 Ma (Verplank and Duncan, 1987). The amount of obliqueness has increased by a factor of 7 over this time (Verplank and Duncan, 1987) and more recently, the plate convergence may have slowed (e.g., Riddihough, 1980; Magill

et al., 1981). A paleomagnetic study by Magill and Cox (1980) suggests that the rocks in the Western Cascades, Oregon, have been rotated 27˚ clockwise. It is possible that this rotation away from the rest of North America is responsible for the high regional heat flow and gravity anomaly observed in the central Oregon Cascades (Blackwell et al., 1982, 1990). Blackwell et al. (1982, 1990) show that the regional heat flow in the central Oregon arc averages over 100 mW m^{-2} in comparison to 60 mW m^{-2} in the Washington section of the arc. This combination of high heat flow and extensional tectonic forces may be the cause for the increase in Cenozoic vents and eruptive output in the last 3.9 Ma (Priest, 1990; Sherrod and Smith, 1990).

There are few constraints on the ages of the volcanic cones in the Three Sisters Volcanic Field, however, based on pyroclastic deposits it has likely been a center of volcanic activity for longer than 700,000 years (Scott et al., 2001). There are five large Quaternary age cones that dominate the area including: North Sister, Middle Sister, South Sister, Broken Top, and Mount Bachelor (Fig. 4-2). The youngest, South Sister, erupted rhyolite tephra and lava flows approximately 2000 years ago (Taylor, 1978; Wozniak, 1982; Clark, 1983; Scott, 1987). This long lived volcanic center has also had considerable eruptive activity away from the main cones with 10s of vents erupting over the last 4000 years (Scott et al., 2001). The most recent eruptive event away from the main cones took place approximately 1500 years ago, north of South Sister, with an eruption of basaltic and andesitic lavas (Fierstein et al., 2003).

Eruptive products, from basaltic to rhyolite, and different vent locations have led to a variety types of eruption styles at the Three Sisters Volcanic Field in the past (Scott et al., 2001). Large explosive eruptions are rare but have occurred at least 4 times in the last 700,000 years (Scott et al., 2001), however, at this time, there is no evidence of a magma chamber of sufficient size to drive a large Plinian volcanic eruption. The vent locations in the area and their link to tectonic stresses and general eruptive behavior have been discussed by Bacon (1985), who suggests that the last silicic eruptive episode was fed from a small deep reservoir on the south side of South Sister. The current unrest and deformation takes place west of South Sister and appears to have no relation to the most recent events.

4.3 Previous work

Wicks et al. (2002) discovered that an area west of South Sister was deforming and that it likely started as early as 1996. The results of this study show that from 1998 to the autumn of 2000, the deformation was steady with 3 to 5 cm yr^{-1} of uplift. Modelling of the early results indicated a source depth for the inferred intrusion at 6.5 km based on a point source model (Wicks et al., 2002). Since the discovery of uplift in the Three Sisters region, further deformation (Dzurisin et al., 2006, 2009) and water geochemistry surveys (Evans et al., 2004) have been completed to better characterize the deep seated processes responsible for this activity.

Spring geochemistry of the Three Sisters area was first investigated by Ingebritsen et al. (1994) who showed that there was a mantle-derived component

of CO_2 prior to the start of the current deformation event in the Separation creek drainage system. The study also showed that there was an anomalous chloride load of 10 g s^{-1} suggesting that hydrothermal fluids were being incorporated into the springs that drain into Separation creek. Further data were collected at the center of the deforming area in 2001 and 2002 (Evans et al., 2004). This later study shows that there was no change in the chloride load or in the temperature of the water flowing in Separation creek, suggesting that previous intrusive heat sources were controlling the hydrothermal system near the center of uplift.

Dzurisin et al. (2006, 2009) refined the original deformation models of Wick et al. (2002) with a longer time series and more data from continuous and campaign GPS, as well as tilt levelling surveys. Using 95% confidence levels, these deformation models describe the intrusion as a prolate spheroid with a depth of ~ 5 km. From the deformation models, Dzurisin et al. (2009) also calculated bounds on the volume change for the whole event by extrapolating the uplift decay rate and suggest the total volume may reach approximately 44.9 to 51.6 x 10^6 m^3. They put forward three conceptual models that could explain the current deformation event: 1) hydraulic or instantaneous response of the crust to continued intrusion at depth; 2) pressurization of the hydrothermal system in the area of Three Sisters and 3) continued viscoelastic response of the crust due to an intrusion emplaced at depth.

4.4 Methodology

4.4.1 Microgravity

Mass flux and redistribution at depth can be constrained using a combination of microgravity and high resolution deformation surveys. The dynamic microgravity surveys implemented at Three Sisters measure small changes in the gravitational field over time and space across a network of stations. The application and theory of this technique is discussed thoroughly in the literature (e.g., Eggers 1987; Rymer and Brown, 1986; Rymer, 1996) and hence, will only be summarized here.

The gravity network at Three Sisters consists of 5 stations spanning the deforming area (Fig. 4-2). The station locations were chosen such that there was less than 1 mGal difference from the reference station outside the deforming area with respect to the rest of the network. This was accomplished by utilizing both a topographic map to identify areas of equal elevation along the trail and field testing of these sites with a La Coste & Romberg gravity meter (G-209). Each station consists of three metal rods drilled into bedrock and made flush with the ground. The rods are arranged such that the 3 leveling screws on a LaCoste-Romberg G-meter rest on them to eliminate the need for a base plate while ensuring precise positioning. The stations from the edge of the deforming area to the center are: BASE, BUGS, BRUCE, CUT, and CENTER (Fig. 4-2). CENTER is approximately located at the center of the deforming area near Separation creek; BASE is on the edge of the deformation zone and is used as the reference station as it is not expected to vary appreciably over the period of study.

To maximize accuracy, data were collected by completing three station loops or surveys over a period of 3 to 6 days; the exception is 2008 and 2009 where only one loop was completed. After corrections on each survey are performed, surveys which are completed over a single week are grouped and averaged to represent one data point. Two gravity meters were also used on each survey to eliminate any bias due to anomalous results from instrumental malfunction or noise. Each loop repeats every station at least twice, except CENTER, in order to pinpoint and correct for tares. The surveys typically start at BASE and measure at each station until CENTER, where the stations are measured in reverse until BASE is repeated. Only surveys in 2002 and 2004 have data that were not collected in this way. In an effort to more accurately describe the gravitational field at a particular station, station loops were shortened such that stations could be repeated more frequently. Table 4-1 shows the three different survey sequences that were used during this study.

First station								Last station
BASE	BUGS	BRUCE	CUT	CENTER	CUT	BRUCE	BUGS	BASE
BASE	BUGS	BRUCE	BUGS	BASE	BUGS	BRUCE		
BRUCE	CUT	CENTER	CUT	BRUCE	CUT	CENTER	CUT	CENTER

Table 4-1 Different possible survey loop combinations for data collected throughout this study. The most common survey starting and ending with BASE was also the only one used in 2005, 2008 and 2009.

The raw gravity data in this study was first corrected for the effects of Earth tides. The calculation of Earth tides, based on the recorded time of a gravity

measurement, has an accuracy better than 2 μGal (Quick Tide Pro; Micro-g Lacoste). Changes in a station's vertical position were corrected by multiplying the height change with the theoretical free air gradient (-306.8 μGals m^{-1}) and subtracted. The vertical position of each station was obtained from deformation models produced by Dzurisin et al. (2009); the model has been shown to fit the deformation data within 95 % confidence levels. Instrumental factors such as drift can be ignored as the meters used in this study were stable and the instrumental drifts were thus negligible over the course of a single survey.

After corrections, the data are then normalized to the base station; BASE's closure was averaged and then subtracted from each other measurement in the survey. In surveys that did not close with BASE, the data were normalized to BASE using a normalized value of BRUCE. This was obtained from other survey days in the same grouping where both BRUCE and BASE were collected. With each station normalized and repeated in a survey, it is easy to identify when a data tare occurred. However, correcting and removing the effects of tares is usually non trivial and increases the uncertainty of the data. It is thus preferable to not use tare-corrupted data, especially when attempting to obtain precise values. The redundancy in the data, by having three surveys with two meters for each data point in time, allows for strict quality control and as such, the data were not corrected for tares. If an unrecoverable tare occurred, either the data from the whole survey with that meter was discarded or only the data leading up to the tare were used. If there was a recoverable tare such that the meter did not display an offset following it, measurements were thrown out until a reasonable

closure between stations was obtained (less than 25 μGals). The upper limit for closures from the first to last measurement of the survey is 60 μGals if no specific tare can be identified. Averaging the results from both meters and the whole survey group significantly reduces the effect of any larger closures.

With each station within 1 mGal of the next, calibration between meters is less of a concern after normalizing each survey to the reference station. The two meters that were used most frequently were G-209 and G-127. G-209, G-248 and D-52 were analogue (with optics and calibration dial) and to be consistent, each analogue meter had the same operator making the measurements at each station. Meter G-127 and D-17 utilize a digital Aliod feedback system to record and collect field measurements. This system allows a 100 mGal dynamic range and removes the necessity for a surveyor to manually null the meter. It also streams the data to a serial device at 2 Hz; each reading in the survey was averaged over one minute to further reduce noise. The change in the calibration factor for the each G meter is on the order of 0.01 for each 100 mGal of field strength change; therefore, a change of less than 1 mGal is of the order of $1x10^{-4}$. The calibration between G-127 and G-209 has been determined to be .09899 or approximately 10.1 μGals for every 1 mGal of change. This allows for the data of multiple meters to be used and merged together without having to carefully calibrating each meter to one another.

4.4.2 Viscoelastic and gravity modelling

In order to test the validity of the hypotheses purposed by Dzurisin et al. (2006, 2009), modelling of both gravity and viscoelastic forces was preformed. A gravity forward modelling program (GRAV3D, 2007) was used in conjunction with volumetric results (Dzurisin et al., 2009) to predict the gravitational field caused by an intrusion at depth. The gravity model examines the change in the gravitational field from 2002 to 2009. In this simple gravity model, the volume is calculated from deformation results (Dzurisin et al., 2009) and given a basaltic melt density based on compositions of known past eruptive vents in the area (e.g., Wozniak 1982; Taylor, 1987). Dzurisin et al. (2006) calculated the yearly volumetric change using their deformation model to be 3.5×10^6 to 6.5×10^6 m^3 yr^{-1}. Extrapolating from 2002 to 2009 would bring the total expected volume change to 24.5×10^6 m^3 to 45.5×10^6 m^3. In a later study, deformation models were updated with more data and a different source geometry (Dzurisin et al., 2009). In this study, the volume change from August 2001 to August 2006 was calculated to be 21.45×10^6 m^3 for a prolate vertical spheroid. The newer models fall between the original maximum and minimum volumetric bounds. To eliminate any bias or uncertainty in the possible model geometries, the larger original range is used for gravity modelling here. The forward gravity model will provide the expected gravitational field change due to continual injection of material at depth.

Deformation modelling with a geomechanics software package called FLAC 5.0 (Fast Lagrangian Analysis of Continua; Itasca Consulting Group, 2005) was used to test the possibility that viscoelastic response of the crust is the

controlling factor in the observed deformation. FLAC 5.0 allows for the analysis of stress fields through elastic, viscoelastic and viscoplastic modelling in two dimensions. It has been used previously in volcanic studies, however, only in application to slope stability and flank collapse (e.g., Apuani et al., 2005, 2008; Casagli et al., 2009). In this study, only elastic and Maxwell viscoelastic materials were considered when attempting to model the deformation event at Three Sisters Volcanic Field. There are very few constraints available to obtain realistic properties for crustal material thus assumptions about viscosity, density, bulk and shear modulus have to be made. Due to the wide range of eruption types, geologic processes and heterogeneity, it is impossible to represent the crust accurately in the Three Sisters area. Therefore, a simple model with the elastic properties of basalt was used (Table 4-2), as basalt to basaltic andesite volcanics are the most common eruptive products near the center of uplift (e.g., Wozniak 1982; Taylor, 1987) and old intrusions at depth would presumably also be basaltic in composition. Previous studies (e.g., Bonafede et al., 1986; Folch et al., 2000; Newman et al., 2006) have investigated the possibility that the crust in volcanic areas can behave in a viscous manner due to high heat flow and incoherent materials. The results of these studies suggest that viscous deformation cannot be ignored in volcanic areas; however, they do not provide a rigorous method to constrain viscosity. The only measurements of crustal viscosities that have been inferred are derived from post seismic deformation and isostatic rebound for the upper mantle and the lower crust (e.g., Wdowinski and Axen, 1992; Ueda et al., 2003). Values from these studies range from 3×10^{17} to

1 x 10^{18} Pa s for the upper mantle and 1 x 10^{18} to 1 x 10^{23} for the lower crust.

Density	2700 kg m^{-3}
Bulk modulus	3.32 x 10^{10} Pa
Shear modulus	1.32 x 10^{10} Pa

Table 4-2 Average elastic properties for basalt which were used in viscoelastic modelling of the crust at Three Sisters.

The FLAC 5.0 model used consists of a single two dimensional viscous unit 6 km by 6 km, with the inferred intrusion at 5 km depth. The intrusion is represented by a constant vertical force applied at 5 km depth across a small 100 m long surface. The side and bottom boundaries of the model are fixed to stop the edges from deforming outward, while the top is allowed to deform freely.

4.5 Results

4.5.1 Microgravity

The gravity network was established in the summer of 2002 and the first surveys were completed in fall 2002. D. Johnson collected all data between 2002 and 2005, with surveys in 2008 and 2009 completed in collaboration with the United States Geological Survey (Table 4-3). In total, 35 surveys were completed from August 2002 to September 2009 consisting of 12 survey groups each containing 3 surveys; the exceptions are 2008 and 2009 only one survey, each.

Survey Group	Normalized Gravity (Each Survey Station in μGal)					Instrument
	BASE	BUGS	BRUCE	CUT	CENTER	
Aug. 2 – 8, 2002	0.0	0.0	0.0	0.0	0.0	G-209 & G-248
Sept. 2 – 4, 2002	0.0	-17	2	-25	-4	G-209 & G-248
Sept. 17 – 19, 2002	0.0	-35	-8	-19	-15	G-209 & G-248
Jul. 15 – 18, 2004	0.0	-24	TARE	TARE	TARE	G-209 & D-17
Jul. 30 – Aug. 1, 2004	0.0	-25	TARE	-13	TARE	G-209 & D-17
Aug. 23 – 26, 2004	0.0	-67	TARE	-6	-5	G-209 & D-17
Sept. 24 – Oct. 1, 2004	0.0	-22	-41	-4	16	G-209 & G-127
Jun. 28 – Jul. 1, 2005	0.0	-12	5	11	-12	D-52 & G-127
Aug. 22 – 24, 2005	TARE	TARE	TARE	TARE	TARE	G-209 & D-52
Sept. 26 – 28, 2005	0.0	-74	TARE	TARE	32	G-209 & D-52
Oct. 12, 2008	TARE	TARE	TARE	TARE	TARE	G-209 & G-127
Sept. 1, 2009	0.0	17	-48	-148	-52	G-209 & G-127

Table 4-3 Each survey group with the gravity data normalized to the first set of data collected in August 2002. Where the normalized gravity value is referred to as "TARE", there was too much high frequency noise to obtain a data point.

It is possible to obtain measurement accuracies of ± 10 μGal in volcanic areas if strict survey procedures are used (e.g., Rymer and Brown, 1986; Rymer, 1989). However, the Three Sisters station network is not in an ideal environment for measuring gravity. The major difficulty with processing this dataset is the

presence of tares, particularly in 2005 (Table 4-3). In 2004 and 2005, D meters were used and frequently had large tares. In addition to sensitive meters, the trail used to access the gravity network is approximately 21 km in length and takes 10 to 12 hours to complete on foot over rugged ground. The constant jostling of walking, even with the spring clamped, can create tares (e.g., Crider et al., 2008). The data collected in 2002 is some of the cleanest in this study, with very few obvious tares corrupting the surveys. High frequency noise throughout the survey is, however, still prevalent, as the closures reached up to 56 μGals (Table 4-2). By using repeats and redundant data, much of the noise is averaged out through multiple surveys; as a result, no data were excluded in 2002. The data collected in 2004, 2005 and 2008, however, had many large tares and in some cases, the data was completely unusable. In 2004, 40% and in 2005, 50% of the data were unusable due to tares. There were 24 survey loops (12 surveys) completed in each of these years, so although large amounts of the data were unusable, there is no loss of information about the gravitational field. The data collected in 2008 had to be thrown out completely, while a tare-free survey was collected in 2009. The standard deviation is taken as the estimated error for each data point averaged from a survey group. Where there are insufficient measurements to effectively calculate the standard deviation, an error of 25 μGals is assumed. The normalized residual gravity through time does not change appreciably as the majority of the measurements are within one standard deviation (Fig. 4-3). The station BUGS has one point which is lower than the error bounds in 2005, while all other stations have a lower outlier in 2009.

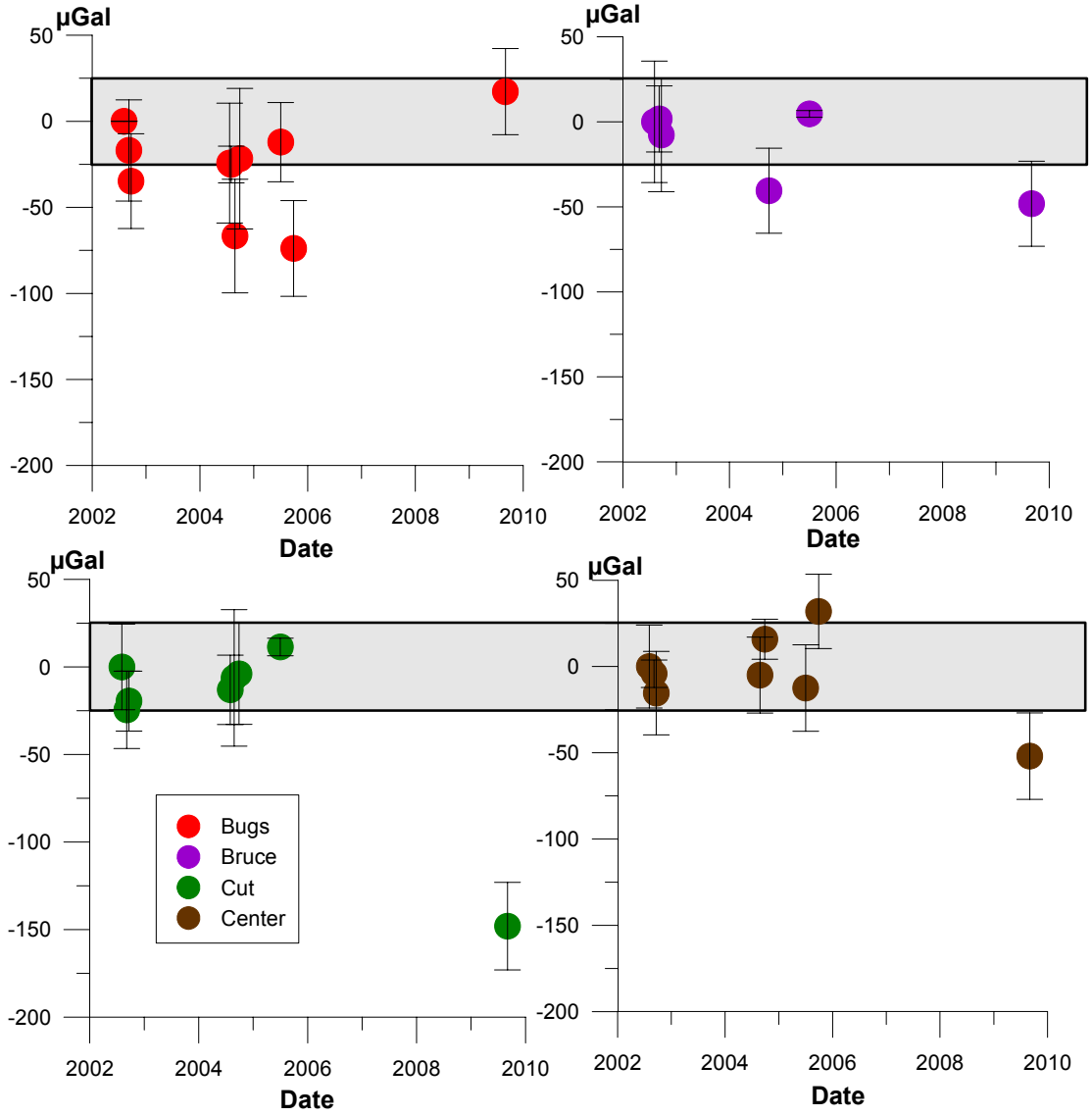

Figure 4-3 Residual gravity data for BUGS (red), BRUCE (purple), CUT (green), and CENTER (brown) from 2002 to 2009. The error bars are the standard deviation of each point and the highlighted region is +/- 25 µGals from 0.

4.5.2 Modeling

To investigate the likelihood that the continual injection of material is responsible for the deformation at Three Sisters Volcanic Filed, forward

modelling of the gravitational field was performed (Grav3D, 2007; Fig. 4-4). The intrusion was modelled at 5 km depth with a volume of 2.4 to 7.5 x 10^7m and a density from 2500 to 2900 kg m^{-3}. While the modelled density range is large, a basaltic melt density is more likely based on the basaltic eruptive vents mapped in the area of Separation creek and north of South Sister (Wozniak, 1982; Taylor, 1987). The addition of material to the system is modelled as an increase in mass with no deformation. Since the gravity model does not take into account vertical deformation, direct comparisons to the gravity data must be done only on data that has been corrected for vertical change.

Using the volume range defined by Dzurisin et al. (2006, 2009), the models result in a 15 to 30 μGal increase in the gravitational field near the station CENTER. It predicts that the maximum magnitude of the gravity increase will fall away from CENTER, with CUT having an increase of 24 μGal and BRUCE of 16 μGal. A sensitivity analysis of the intrusion's shape and density was performed to test what affect initial assumptions have on the modelling results. Modelling the intrusive source as rectangular or spherical shape made no appreciable difference in the resulting gravitational field.

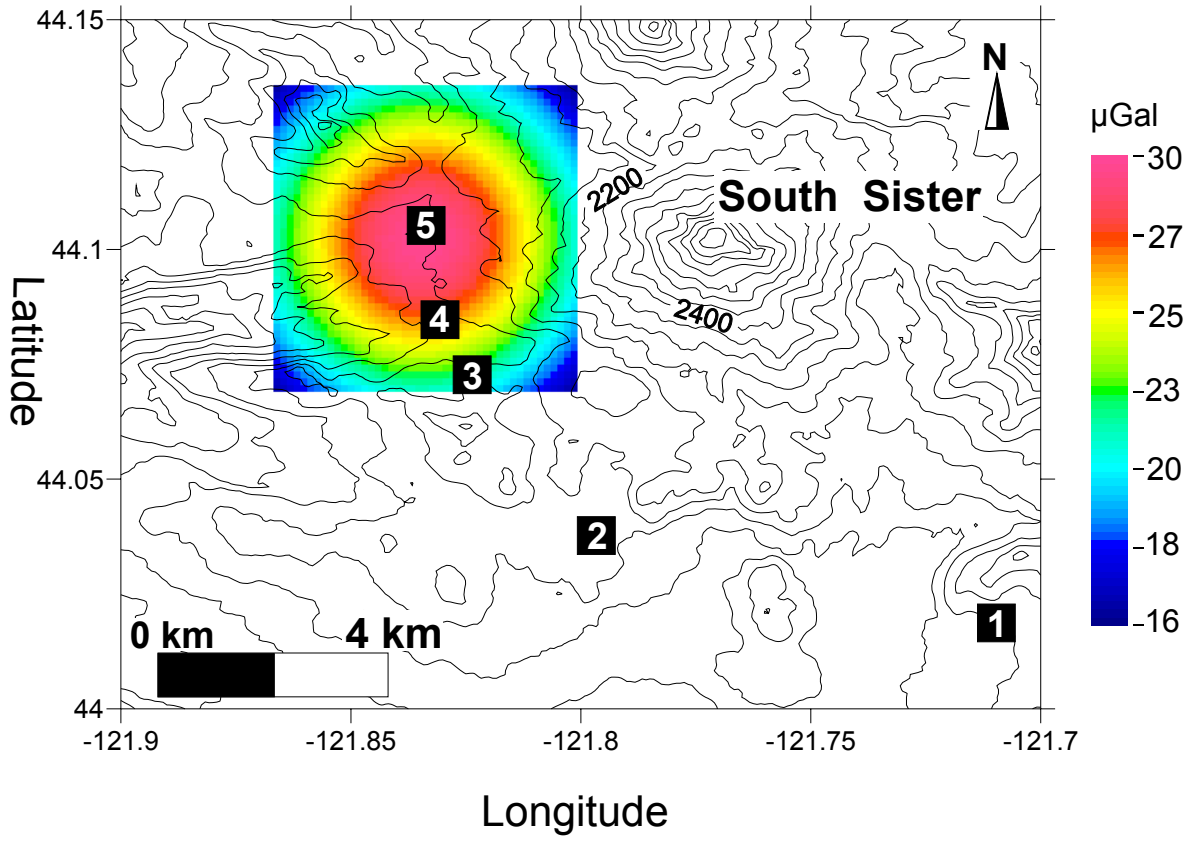

Figure 4-4 A forward gravity model using 2900 kg m^{-3} as the melt density, overlain by 100 m topography contours. Numbered black squares represent gravity stations: 1) BASE; 2) BUGS; 3) BRUCE; 4) CUT; 5) CENTER.

To test the possibility that viscoelastic forces could be responsible for controlling the deformation over the gravity study, the geomechanics code FLAC 5.0 (Itasca Consulting Group, 2005) was used to model the effect of an upward force at a depth of 5 km. The models have a viscosity range of 10^{18} to 10^{20} Pa s and show two end members of the deformation response (Fig. 4-5). Models with viscosities 10^{20} Pa s or higher are dominated by a nearly instantaneous elastic deformation with a very small viscoelastic component, while models with viscosities on the order of 10^{18} Pa s are dominated by a linear viscoelastic response. Results show that a viscosity of 10^{18} Pa s can produce an uplift of 4.3

cm yr^{-1} after the elastic response has ceased with 5 x 10^{10} N of force. However, for a viscosity of 10^{20} Pa s, there is essentially no viscoelastic response, thus it cannot produce the continual deformation at rates observed.

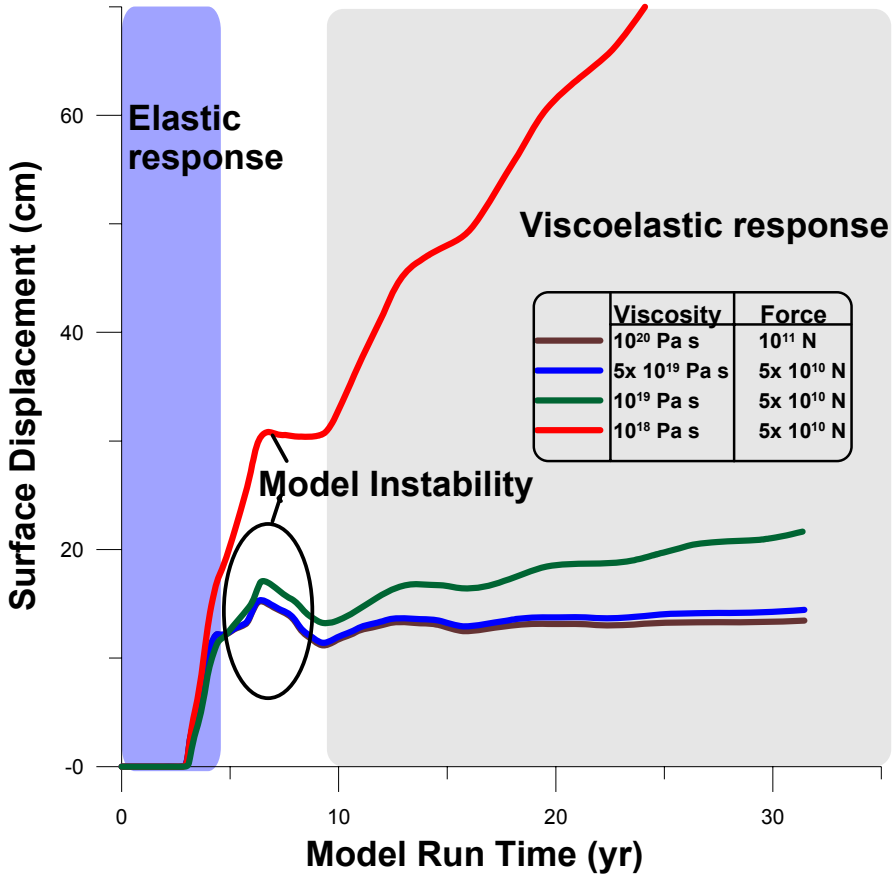

Figure 4-5 Modelled viscoelastic responses of the ground for different viscosities with their corresponding applied force. In each case, the elastic properties were that of basalt.

Regardless of viscosity, each model displays short lived instability immediately following the elastic component of the deformation due to the application of an instantaneous force at depth. The instantaneous force causes a wave that propagates through the model representing the elastic response of the medium. When this wave of force reaches the boundaries of the model it is

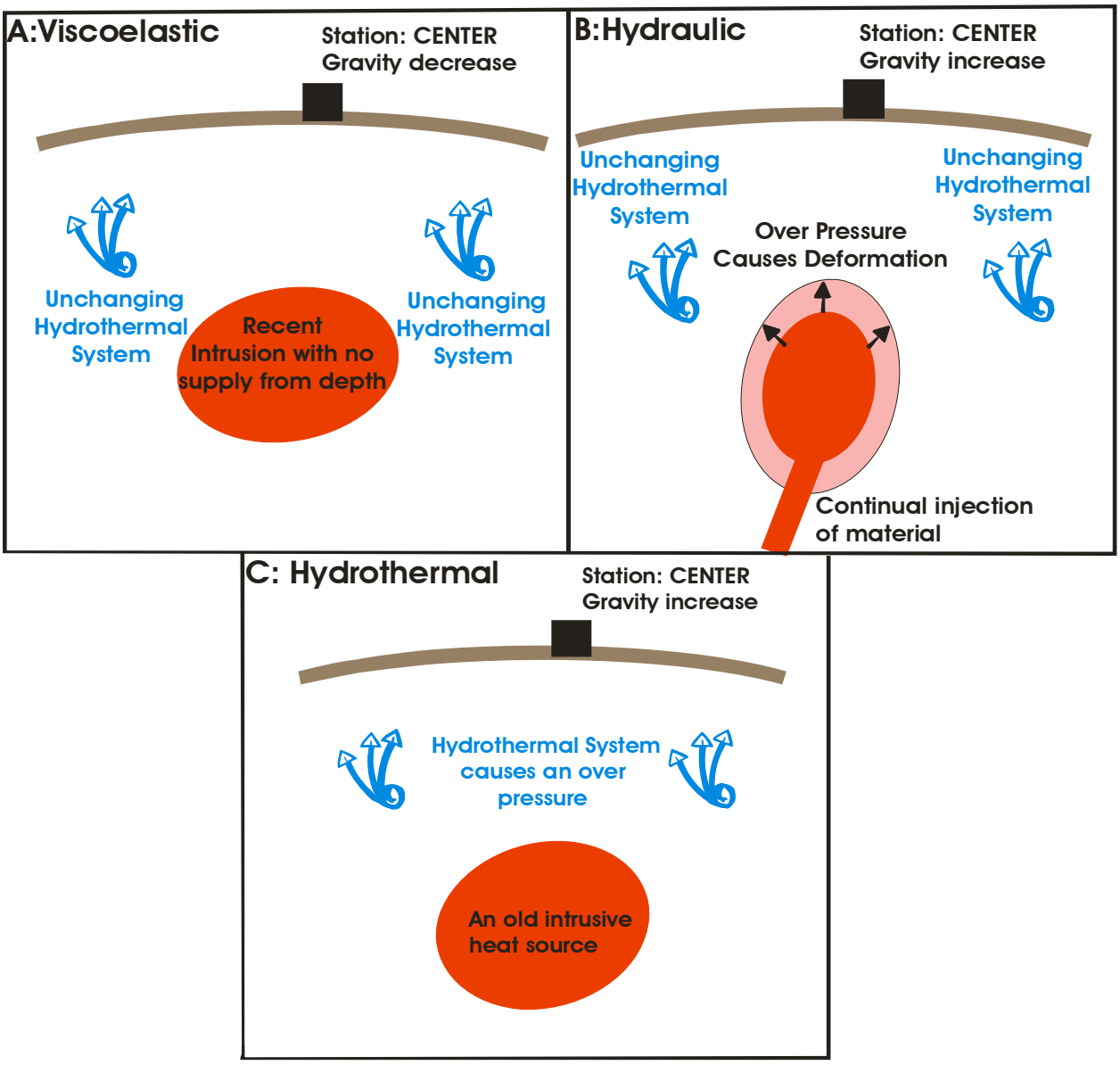

Figure 4-6: Schematic model to explain the activity to the west of South Sister. A) Viscoelastic model with a continual reaction of the crust to past over pressure. B) Hydraulic model with a continual reaction of the crust to pressure from intrusive injection of material. C) Hydrothermal pressurization causing continual uplift.

reflected causing instabilities. The amplitude of the reflected force within the model is greater with higher viscosities and higher intrusive force. To reduce this effect, damping within the model was increased to dissipate any reflected waves

of force as it has no effect on the amplitude of the viscoelastic or elastic response at the surface of the model.

4.6 Discussion

The deformation episode at the Three Sisters began in 1997 (Dzurisin et al. 2009) and continues at a declining rate to the present. Previous work has outlined three possible end member models that can explain the deformation event. 1) Continuous injection of material where the magma flow rate from the lower crust is proportional to the pressure causing uplift. 2) Instantaneous pressurization of the crust and the time dependant response of a Maxwell fluid causing continued uplift at the surface. 3) Pressurization of hydrothermal fluids due to the injection of magmatic volatiles from a previous crustal magma body. Each of these possibilities are discussed below with reference to the expected gravitational field and models.

In order to use the microgravity data spanning the deforming area at Three Sisters for interpretation, the effect of water table fluctuations must be addressed. The surveys performed in 2004 and 2005 occurred from early summer into fall, in an effort to characterize the seasonal effects in ground water levels. However, the large number of tares and loss of data limit the effectiveness of this approach. Instead, it is better to analyze the data as a whole in conjunction with monthly precipitation as it is more robust and less sensitive to a single anomalous survey. The precipitation data in Fig. 4-7 shows that 2004 had more rain than any other year during the survey months. If water tables are a controlling factor, it would be expected that the gravity measurements made in

2004 would be greater than those in any other year. The corrected data in Fig. 4-3 show no change throughout the dataset greater then estimated error for the surveys. There is, however, an exception where small gravity decreases were measured at stations CUT and CENTER in 2009. The precipitation in 2009 is comparable to that in 2002 and thus a gravity decrease from 2002 to 2009 based on water table changes is not expected. Since the gravity signal has no mesurable change outside the estimated error in both 2004 and 2005, changes in ground water tables have no obvious influence on the gravity data set.

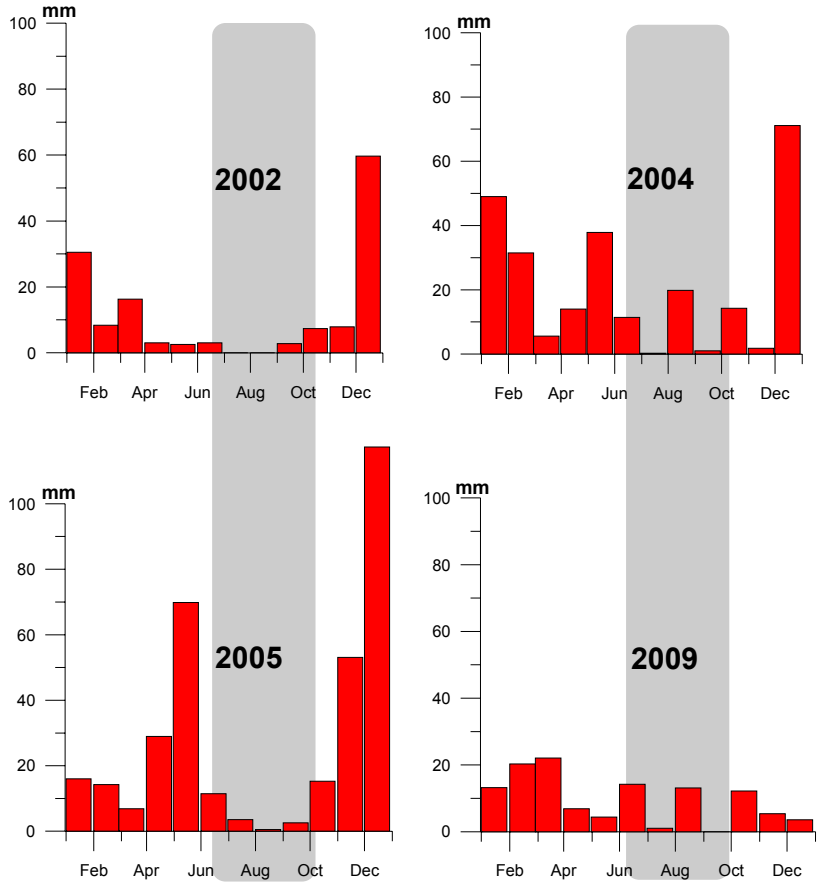

Figure 4-7 Monthly rainfall for Bend, Oregon. The highlighted months represent when surveys were completed starting in late June and repeated throughout the summer until early October (Oregon State Climate Center, 2010).

Within the microgravity dataset, there are 4 points that fall outside the estimated error, 3 of them in 2009. Each outlier shows a smaller gravitational field than what was originally measured in 2002. Although unlikely, the 2009 decrease at CUT could be partly attributed to mass wasting as the station is near a small cliff. This cannot, however, explain a smaller decrease at both BRUCE and CENTER stations in 2009. It seems improbable that the entire amplitude of the decrease is real as it is not likely due to water tables or a change in the deformation event. However, it is clear that it does not represent an increase in the gravitation field due to a positive mass flux.

The deforming area is approximately 10 x 20 km and the gravity network consists of only a single transect. Measuring only a single profile reduces our ability to describe the source of the event, however, it does cover from the edge to the center of the deformation zone. While this is far from ideal, it is the only feasible way to monitor the gravitational field across a network of stations due to the remoteness of the area. Repeat measurements in part overcome the poor special coverage.

The data collected by Evans et al. (2004) show that the geochemical anomalies in the Separation creek drainage are most likely caused by previous intrusions and not directly connected with the current event. If hydrothermal pressurization is the main cause of deformation then it would also be expected to increase the amount of hydrothermal fluids at depth. Residual gravity would then increase as hydrothermal fluids add mass to the system. However, depending on the volume and depth, this mass increase may be too small to detect above the

noise in the gravity data. The steady-state nature of the geochemical results suggests that any hydrothermal pressurization would have to be deep enough not to interact with groundwater. The inferred depth of the deformation source at 4.9 km by Dzurisin et al. (2009) is sufficiently deep that there is essentially 0% porosity, suggesting that at this depth, hydrothermal fluids cannot be the cause of uplift. While the models and data presented do not sufficiently constrain the deformation and mass flux to rule out hydrothermal pressurization as a possible cause, they do suggest that this is the least likely conceptual model to explain the current deformation event at the Three Sisters Volcanic field.

Gravity forward modeling shows that the expected increase in the gravitational field is between 15 to 30 μGals. Field measurements, however, do not show any increase and may suggest a decreasing gravitational field near CENTER and CUT. The lack of gravitational increase suggests that a continual flow of material at depth into an intrusion is not responsible for the deformation. The amplitude of the modelled gravitational field, however, straddles the error levels within the microgravity dataset. Hence, it is not possible to completely rule out the possibility that the crust is behaving hydraulically as material is injected continuously at depth. It does suggest, though, that it is unlikely to be the dominant process.

The increased heat flow for the central Oregon section of the Cascade arc could play a dominant role in determining how the crust is responding to the inferred deep-seated source. Blackwell et al. (1990) made measurements of heat flow throughout much of Oregon and although the measurements do not cover

the Three Sisters region, they do provide an estimate of the heat flow and the geothermal gradient. An average of 65 ^{o}C km^{-1} was obtained along arc near volcanic centers but the values could be much higher near the main cones, to as much as 100 ^{o}C km^{-1} (Blackwell et al., 1982; 1990). This would suggest that the crust around the inferred intrusion at 5 km depth could be between 325 and 500 ^{o}C. The strength of quartz greatly decreases at temperatures greater than 350 ^{o}C (e.g., Buck, 1991) and incoherent material can reduce the effective viscosity (Bonafede et al., 1986). While these properties are known, there have been no rigorous studies to obtain a crustal viscosity in local areas of high heat flow. Therefore, any viscosity used is conjecture based on studies that infer lower crustal viscosities from post seismic relaxation (e.g., 4 x 10^{18} Pa s, Japan; Ueda et al., 2003). The temperature may be similar in volcanic areas to that in the lower crust; however, the confining pressure is significantly less.

Furthermore, there is also a conspicuously low level of seismic activity in the central Oregon part of the Cascade Volcanic Range (Weaver and Michaelson, 1985). This includes the current deformation event at Three Sisters as there have been very few seismic events associated with it apart from a seismic swarm in 2004 that consisted of over 300 seismic events (Dzurisin et al., 2006). High heat flow, low levels of seismic activity, and the presence of incoherent material suggest it is not unreasonable that the crust beneath the Three Sisters could have viscosities lower than 10^{20} Pa s.

If the observed deformation from 2002 to 2009 is primarily caused by a viscoelastic response due to an intrusion, the results of the microgravity data

would show no net change after being corrected for changes in elevation. Furthermore, viscoelastic models provide limited bounds on the expected viscosity and investigate the possibility that the deformation event is a hybrid of viscoelastic response and continual injection. FLAC modeling shows that it is possible to obtain the observed rate of deformation with a nearly instantaneous intrusion of magma if the crustal viscosity beneath the Three Sisters is on the order of 1 x 10^{18} Pa s. Viscosities that are an order of magnitude higher have a strong elastic component to the deformation and hence would require some magmatic injection to continue while also deforming viscoelasticly. The gravity data does not rule out this possibility as material injected in this way would be below the detection limits of the survey. If viscosities reach 10^{20} Pa s, the modelled deformation is nearly all elastic and would require continual injection of material. The gravity data does not show an increase hence it does not support continual injection as the sole cause of the continuing deformation event as previously discussed. The viscosity, as determined from these simple models for the ground beneath the Three Sisters, is most likely between 5 x 10^{19} Pa s and 10^{18} Pa s with the deformation being either dominated by a viscoelastic response or a combination of elastic and viscoelastic. This agrees with those determined for the lower crust (e.g., Wdowinski and Axen, 1992).

4.7 Conclusion

Three general conceptual models have been suggested by past studies (Dzurisin et al., 2006; 2009) to explain the cause of the deformation event at the

Three Sisters Volcanic complex: 1) viscoelastic response of the crust due to instantaneous pressurization from an intrusion; 2) continual intrusion of material at depth causing constant deformation; 3) overpressure caused by many shallow hydrothermal sources. Spring geochemistry studies have indicated that there has been no measurable change in the hydrothermal system after the start of the deformation event (Ingebritsen et al., 1994; Evans et al., 2004) suggesting that model 3 is the least likely. Models 2 and 3 require a positive mass flux to drive uplift from 2002 to 2009 whereas viscoelastic deformation (model 1) does not. Furthermore, the event has been generally aseismic suggesting that viscoelastic deformation probably plays a major role. Microgravity surveys were completed to constrain the deformation process by determining if any mass was added beneath the deforming area. Gravity results show no change, within error, in the mass flux across the deforming area suggesting that the crust is deforming viscoelastically. While it is impossible to quantify the amount of deformation that could be attributed to viscoelastic response due to noise within the gravity surveys, it is possible to provide some constraints on the crustal viscosity in the Three Sisters region. Viscosities greater than 5×10^{19} Pa s have a very weak viscoelastic component requiring the constant addition of material to drive deformation, however, if the crustal viscosity is 10^{18} Pa s then it is possible to continue the deformation event from a single instantaneous pressurization. The most likely cause of this deformation event is the combination of hydraulic and viscoelastic responses due to a magmatic intrusion with average crustal viscosities beneath the Three Sisters between 5×10^{19} Pa s and 10^{18} Pa s. This

agrees with previous studies that the most likely cause of the deformation event is the intrusion of magma at depth. To further ground truth both the geothermal gradient and viscosity, a set a drill holes could be made, or an active seismic survey could be used. This would provide better constraints for building a comprehensive model of this continual process, however, the area is a protected wilderness and these approaches are not viable. Unless there is reactivation with a larger intrusion to reverse the decaying deformation trend, this event is extremely unlikely to lead to an eruption.

4.8 References

Apuani, T., and Corazzato, C., 2008, Numerical model of the Stromboli volcano (Italy) including the effect of magma pressure in the dyke system: Rock Mechanics and Rock Engineering, v. 42, no. 1, p. 53-72.

Apuani, T., Corazzato, C., Cancelli, A., and Tibaldi, A., 2005, Stability of a collapsing volcano (Stromboli, Italy): Limit equilibrium analysis and numerical modelling: Journal of Volcanology and Geothermal Research, v. 144, no. 1-4, p. 191-210.

Bacon, C.R., 1985, Implications of silicic vent patterns for the presence of large crustal magma chambers: Journal of Geophysical Research, v. 90, p. 11,243-11,252.

Bates, R.G., Beck, M.E., and Burmester, R.F., 1981, Tectonic rotations in the Cascade Range of southern Washington: Geology, v. 9, no. 4, p. 184-189.

Battaglia, M., Gottsmann, J., Carbone, D., and Fernàndez, J., 2008, 4D volcano gravimetry: Geophysics, v. 73, no. 6, p. WA3-WA18.

Battaglia, M., Segall, P., and Roberts, C., 2003, The mechanics of unrest at Long Valley caldera, California. Constraining the nature of the source using geodetic and micro-gravity data: Journal of Volcanology and Geothermal Research, v. 127, no. 3-4, p. 219-245.

Berrino, G., Corrado, G., Luongo, G., and Toro, B., 1984, Ground deformation and gravity changes accompanying the 1982 Pozzuoli uplift, Springer Berlin / Heidelberg, 187 p.

Berrino, G., Rymer, H., Brown, G.C., and Corrado, G., 1992, Gravity-height correlations for unrest at calderas: Journal of Volcanology and Geothermal Research, v. 53, no. 1-4, p. 11-26.

Blackwell, D., Bowen, R., Hull, D., Riccio, J., and Steele, J., 1982, Heat flow, arc volcanism, and subduction in Northern Oregon: Journal of Geophysical Research, v. 87, no. B10, p. 8735-8754.

Blackwell, D., Steele, J., Frohme, C., Murphey, G., Priest, G.R., and Black, G., 1990, Heat flow in the Oregon Cascade Range and its correlation with regional gravity, Curie point depths, and geology: Journal of Geophysical Research, v. 95, no. B12, p. 19475-19493.

Bonafede, M., Dragoni, M., and Quareni, F., 1986, Displacement and stress fields produced by a centre of dilation and by a pressure source in a viscoelastic half-space: application to the study of ground deformation and seismic activity at Campi Flegrei, Italy: Geophysical Journal of the Royal Astronomical Society, v. 87, no. 2, p. 455-485.

Bonafede, M., and Mazzanti, M., 1998, Modelling gravity variations consistent with ground deformation in the Campi Flegrei caldera (Italy): Journal of Volcanology and Geothermal Research, v. 81, no. 1-2, p. 137-157.

Buck, W.R., 1991, Modes of Continental lithospheric extension: Journal of Geophysical Research., v. 96, p. 20161-20178.

Casagli, N., Tibaldi, A., Merri, A., Del Ventisette, C., Apuani, T., Guerri, L., Fortuny-Guasch, J., and Tarchi, D., 2009, Deformation of Stromboli Volcano (Italy) during the 2007 eruption revealed by radar interferometry, numerical modelling and structural geological field data: Journal of Volcanology and Geothermal Research, v. 182, no. 3-4, p. 182-200.

Clark, J.G., 1983, Geology and petrology of South Sister volcano, High Cascade Range, Oregon: Ph.D. Thesis (unpublished) University of Oregon, Eugene.

Crider, J.G., Hill Johnsen, K., and Williams-Jones, G., 2008, Thirty-year gravity change at Mount Baker Volcano, Washington, USA: Extracting the signal from under the ice: Geophysical Research Letters, v. 35, no. 20, p. L20304.

Dzurisin, D., Lisowski, M., and Wicks, C.W., 2009, Continuing Inflation at Three Sisters volcanic center, central Oregon Cascade Rand, USA, from GPS, leveling, and InSAR observations: Bulletin of Volcanology, v. 71, no. 10, p. 1091-1110.

Dzurisin, D., Lisowski, M., Wicks, C.W., Poland, M.P., and Endo, E.T., 2006, Geodetic observations and modeling of magmatic inflation at the Three Sisters volcanic center, central Oregon Cascade Range, USA: Journal of Volcanology and Geothermal Research, v. 150, no. 1-3, p. 35-54.

Dzurisin, D., Savage, J.C., and Fournier, R.O., 1990, Recent crustal subsidence at Yellowstone Caldera, Wyoming: Bulletin of Volcanology , v. 52, no. 4, p.247-270

Dzurisin, D., Yamashita, K.M., and Kleinman, J.W., 1994, Mechanisms of crustal uplift and subsidence at the Yellowstone caldera, Wyoming: Bulletin of Volcanology, v. 56, no. 4, p. 261-270.

Eggers, A.A., 1987, Residual gravity changes and eruption magnitudes: Journal of Volcanology and Geothermal Research, v. 33, no. 1-3, p. 201-216.

Evans, C.W., Soest, v.C.M., Mariner, h.R., Hurwitz, S., Ingebritsen, S., Wicks, C.W., and Schmidt, M., E., 2004, Magmatic intrusion west of Three Sisters, central Oregon, USA; the perspective from spring geochemistry: Geology, v. 32, no. 1, p. 69-72.

Fierstein, J., Calvert, A., and Hildreth, W., 2003, Two young silicic sisters at Three Sisters volcanic field, Oregon [abs]: Programs- Geological Society of America, v. 35 (6).

Folch, A., Fernández, J., Rundle, J.B., and Martí, J., 2000, Ground deformation in a viscoelastic medium composed of a layer overlying a half-space: a comparison between point and extended sources: Geophysical Journal International, v. 140, no. 1, p. 37-50.

Gottsmann, J., Folch, A., and Rymer, H., 2006, Unrest at Campi Flegrei: A contribution to the magmatic versus hydrothermal debate from inverse and finite modeling: Journal of Geophysical Research, v. 111, no. B07203.

GRAV3D, 2007, A program library for forward modeling and inversion of gravity data over 3D structures: developed under the consortium research project Joint/Cooperative Inversion of Geophysical andGeological Data: UBC-Geophysical Inversion Facility,Department of Earth and Ocean Sciences, The University of British Columbia, Vancouver., v. version 20070309.

Guffanti, M., and Weaver, C.S., 1988, Distribution of late Cenozoic volcanic vents in the Cascade Range: Volcanic arc segmentation and regional tectonic considerations: Journal of Geophysical Research, v. 93, p. 6513-6529.

Ingebritsen, S., Mariner, H.R., and Sherrod, D.R., 1994, Hydrothermal Systems of the Cascade Range, north-central Oregon U.S.: Geological Survey Profesional Paper 1044-L, p. 86.

Itasca Consulting Group, 2005, FLAC modelling code version 5.00: http://www.itascacg.com/flac/index.php.

Magill, J., and Cox, A., 1980, Tectonic rotation of the Oregon Western Cascades: Department of Geology and Mineral Industries, Portland, Oregon, v. 10, p. 67.

Magill, J., Cox, A., and Duncan, R., 1981, Tillamook Volcanic Series: Further Evidence for Tectonic Rotation of the Oregon Coast Range: Journal of Geophysical Research, v. 86, no. B4, p. 2953-2970.

Newman, A.V., Dixon, T.H., and Gourmelen, N., 2006, A four-dimensional viscoelastic deformation model for Long Valley Caldera, California, between 1995 and 2000: Journal of Volcanology and Geothermal Research, v. 150, no. 1-3, p. 244-269.

Orsi, G., Petrazzuoli, S.M., and Wohletz, K., 1999, Mechanical and thermo-fluid behaviour during unrest at the Campi Flegrei caldera (Italy): Journal of Volcanology and Geothermal Research, v. 91, no. 2-4, p. 453-470.

Priest, G.R., 1990, Volcanic and Tectonic Evolution of the Cascade Volcanic Arc, Central Oregon: Journal of Geophysical Research, v. 95, no. B12, p. 19583-19599.

Riddihough, R.P., 1980, Gorda plate motions from magnetic anomaly analysis: Earth and Planetary Science Letters, v. 51, no. 1, p. 163-170.

Rymer, H., 1994, Microgravity change as a precursor to volcanic activity: Journal of Volcanology and Geothermal Research, v. 61, no. 3-4, p. 311-328

Rymer, H., 1996, Microgravity monitoring; In Scarpa, R., and Tilling, R.I. (eds), Monitoring and Mitigation of Volcano Hazards: Springer-Verslag, Berlin, p. 169-168.

Rymer, H., and Brown, G.C., 1986, Gravity fields and the interpretation of volcanic structures: Geological discrimination and temporal evolution: Journal of Volcanology and Geothermal Research, v. 27, no. 3-4, p. 229-254

Rymer, H., 1989, A contribution to precision microgravity data analysis using Lacoste and Romberg gravity meters: Geophysical Journal International, v. 97, no. 2, p. 311-322.

Rymer, H., and Williams-Jones, G., 2000, Volcanic eruption prediction: Magma chamber physics from gravity and deformation measurements: Geophysical Research Letters, v. 27, no. 16, p. 2389-2392.

Scott, W.E., 1987, Holocene rhyodacite eruptions on the flanks of South Sister volcano, Oregon, In Fink, J.H., ed., The emplacement of silisic domes and lava flows: Geological Society of America Special Paper, v. 212, p. 35-53.

Scott, W.E., Iverson, R.M., Schilling, S.P., and Fisher, B.J., 2001, Volcano hazards in the Three Sisters Region, Oregon: U.S. Geological Survey Open-File Report 99-437.

Sherrod, D.R., and Smith, J.G., 1990, Quaternary extrusion rates of the Cascade Range, Northwestern United States and Southern British Columbia: Journal Geophysical Research, v. 95, no. B12, p. 19465-19474

Taylor, E.M., 1978, Field geology of the SW quarter of the Broken Top quadrangle, Oregon: Special Paper Oregon Department of Geology and Mining Industry, v. 2, p. 1-50.

Taylor, E.M., 1981, Central High Cascades roadside geology, Bend, Sisters, McKenzie Pass, and Santiam Pass, Oregon In Johnston, D.A., and Donnelly-Nolan, Julie, eds., Guides to some volcanic terrains in Washington, Idaho, Oregon, and Northern California: U.S. Geological Survey Circular 838, p. 55-58.

Taylor, E.M., 1987, Field Geology of the northwestern quarter of the Broken Top 15 minute quadrangle, Oregon: Special Paper Oregon Department of Geology and Mining Industry, p. 1-20.

Ueda, H., Ohtake, M., and Sato, H., 2003, Postseismic crustal deformation following the 1993 Hokkaido Nansei-oki earthquake, northern Japan: Evidence for a low-viscosity zone in the uppermost mantle: Journal of Geophysical Research., v. 108, no. B3, p. 2151

Verplanck, E., and Duncan, R., 1987, Temporal variations in plate convergence and eruption rates in the western Cascades, Oregon: Tectonics, v. 6, no. 2, p. 197-209.

Wdowinski, S., and Axen, G.J., 1992, Isostatic rebound due to tectonic denudation: A viscous flow model of a layered lithosphere: Tectonics, v. 11, no. 2, p. 303-315.

Weaver, C.S., and Michaelson, C., 1985, Seismicity and volcanism in the Pacific Northwest: Evidence for the segmentation of the Juan De Fuca Plate: Geophysical Research Letters, v. 12, no. 4, p. 215-218.

Wicks, C.W., Dzurisin, D., Ingebritsen, S., Thatcher, W., Lu, Z., and Iverson, J., 2002, Magmatic activity beneath the quiescent Three Sisters volcanic center, central Oregon Cascade Range, USA: Geophysical Research Letters, v. 29, no. 7, p. 1122.

Wozniak, K.C., 1982, Geology of the northern part of the southeast Three Sisters quadrangle: M.S. Thesis (unpublished). Oregon: Corvallis, Oregon State University.

5: GENERAL CONCLUSIONS

5.1 Overview

The purpose of this thesis was to expand upon the understanding of magma transport systems and structures at active volcanoes. This was done using gravity surveys to measure mass flux and density variations spatially and temporally at Kīlauea, Masaya and Three Sisters volcanoes. The principal conclusions from these studies are described briefly below.

5.2 Conclusions

5.2.1 Kīlauea

- Significant short term volcanic changes can occur in the shallow magmatic plumbing system beneath Halema'uma'u over 10s of minutes. To understand these perturbations it is important to include measurements of mass flux which can potentially provide density constraints.
- To fully understand a volcanic system, it is necessary to include as many disparate data sets as possible. Volcanic systems like Kīlauea are very complex and require information about different parameters, such as density and volatile content, to build a complete picture and move our understanding forward.

- Ground based total magnetic surveys can be used in volcanic areas to identify structures regardless of surface exposure. At Kīlauea, magnetic surveys identified two anomalies, the first of which is a set of fissures that strike northeast from Halema'uma'u. This anomaly may be completely created by historical fissure eruptions from 1954 -1982, or include older buried eruptive sequences. The second anomaly identified most likely belongs to a long lived ancient eruptive center called the Observatory vent which has been inferred to exist approximately 1 km east of the Hawaiian Volcano Observatory.
- Beneath Kīlauea caldera, a large dense body exists from ~300 m to at least 2 km beneath the surface and is centered in the northeast quadrant of the caldera. The body has a large volume, between 5 and 15 km^3, and most likely represents an intrusive complex. The size of the intrusive complex and historical rates of summit eruptions suggests that this complex must be quite old.
- The center of the intrusive complex inferred to exist beneath Kīlauea's summit is not centered over Halema'uma'u. One possible way to explain this is by volcanic rifting due to the south flank being mobile, moving south away from the summit of Kīlauea. While there are no constraints on the effect this would have on Kīlauea's magma chambers, it is unrealistic to assume they would not be affected.

5.2.2 Masaya

- There is no gravity low centered over Santiago crater suggesting that the amount of void space beneath the crater floor is small. This means that the void space that has been observed and created throughout the most recent degassing crisis is probably destroyed shortly after it is formed through collapse.
- There is no large positive Bouguer gravity anomaly over the historical center of volcanic activity at Masaya; this suggests the main cone is young. Time is required for repeating dyke intrusions to create a high density intrusive complex similar to that at Kĩlauea.

5.2.3 Three Sisters

- There was no measurable increase of gravity associated with the deformation at Three Sisters Volcanic Field. If the deformation is driven by the continual injection of magma or hydrothermal fluids at depth, gravity measurements at the center of the deforming area should increase. This suggests that viscoelastic deformation plays an important role in the ongoing, decaying deformation taking place at the Three Sisters Volcanic Field.
- Simple models looking at the elastic vs. viscoelastic response of the crust with varying viscosities, suggests that the viscosity of the crust beneath the Three Sisters is between 5×10^{19} to 1×10^{18} Pa s. These

values are not unrealistic as volcanic material is often incoherent and there is high heat flow throughout the Cascades in central Oregon.

5.3 Future Work

The studies within this thesis do not represent the end of these ideas. It is important to reflect and further build upon the understanding of each study.

5.3.1 Kīlauea

- Monitoring the active, open vent in Halema'uma'u using continuous gravimeters would provide a new dataset and new perspective into Kīlauea. It should provide the means to look at the physical properties of gas slugs and other process associated with the shallow vent activity.
- A complete study on how volcanic rifting can affect the summit and rift zone magma chambers is needed. How does the deformation field from the mobile south flank of Kīlauea change with depth? To be able to complete this study, it would be necessary to build a 3D numerical model which could solve for the effects of gravity, given input parameters of fault planes and viscosities. Repeat microgravity measurements will supply the mass flux information that that can be used to test the validity of the numerical deformation model.

5.3.2 Masaya

- Long term microgravity stations over the inferred magma chamber just north of Nindiri could perhaps provide a better measure of long term mass flux to Masaya which has not had an effusive eruptive episode since 1770.
- Bouguer gravity data that covers more of the caldera with sufficient station density would increase the ability to identify intrusive bodies which could represent the plumbing system. Imaging these density contrasts might help solve the question of where the degassed magma goes since it is not erupted.
- Masaya sits at one end of a large Graben; it is unknown how this tensile structure affects the volcanism at Masaya volcano. Deformation studies should be performed to investigate whether the structure could represent rifting at depth, and possibly growth of a large magma chamber.

5.3.3 Three Sisters

- Further modeling with realistic crustal divisions and pressure inputs from an intrusion at 5 km are necessary to further constrain crustal properties that are controlling the deformation.
- The Three Sisters area is a protected wilderness which makes access exceedingly difficult. To obtain more data that can constrain crustal parameters, such as viscosity, would require heat flow measurements

and seismic surveys. Obtaining either dataset is unrealistic due to the necessity of drilling or active seismic sources which are not allowed in the protected area.

APPENDICES

Appendix A: Gravity Methods

Introduction

The physical properties of the Earth in volcanic areas can change over short distances or small amounts of time. There is, however, no practical way to directly observe what is occurring beneath the ground. Geophysical techniques can be used to remotely gather information about Earth properties such as, but not limited to, density, magnetic susceptibility, conductivity and resistivity. Measuring the Earth's gravitational field can identify mass changes beneath the ground either temporally or spatially. The Earth's gravitational field obeys Newton's law of universal gravitation (Eq. 1), where the force due to gravitational acceleration (F) between two objects is proportional to the masses ($M_{1,2}$), the gravitational constant (G), and inversely proportional to the square of the distance (R) from the center of each.

$$F = \frac{GM_eM_1}{R^2} \qquad (1)$$

Measuring the vertical gravitational field at the Earth's surface is effectively a measurement of the amount of mass between a point on the surface and the center of the Earth. Spatial changes will, therefore, reflect differences in density within the Earth, while temporal changes must be related to movements of mass in the vicinity of the measurement location. In a volcanic region, temporal change could be associated with magma movement, density changes due to degassing or a precursor to an eruption (e.g., Rymer, 1994; Williams-Jones et al., 2003, 2008; Battaglia et al., 2008). Many of the gravity survey techniques used here were first developed for the mining and oil and gas sectors to identify subsurface

density differences that correspond to natural resources (Telford et al., 1990). The same gravity techniques developed for resource exploration have been applied and modified for volcano monitoring and research.

Basic Corrections

Gravity measurements are affected by a number of different variables that can obscure the desired data. There are two corrections that need to be dealt with in all gravity surveys before interpretations can be made (Telford et al., 1990). The first correction accounts for tidal forces due to the gravitational force from the Moon and the Sun. The distance of the Moon and Sun to a point on the Earth's surface will change as the Earth and Moon rotate through their orbits. Therefore, based on equation 1, the gravitational attraction due to the Moon and Sun will change (Earth tides). Computer programs are used to calculate the correction used to remove Earth tides from the dataset. Tidal forces also affect the ocean creating high and low tides that are offset in time from the maximum (Earth) tidal force due to the momentum of the water. The changing mass of water (ocean loading) can significantly affect gravity surveys that are performed near an ocean or large body of water. Ocean loading can also be calculated and corrected for, however, the error associated with this is significantly higher due to poor constraints on ocean bathymetry (e.g., Hautmann et al., 2010).

The second important factor that all gravity surveys must account for is elevation change or a change in the distance to the center of the Earth. The rate at which the Earth's gravitational attraction decreases with distance from its center is called the free air gradient (FAG). To correct for elevation, a global

average value of -308.6 μgal m^{-1} is used unless directly measured. The real value can be up to 40% different due to topography and/or density variations beneath the ground (e.g., Rymer and Brown , 1986; Berrino et al., 1992). It is thus important to obtain the actual FAG by making a series of measurements first at ground level and then some distance off the ground (~1 m) using a tripod. The change in gravity between the two measurements is then divided by the change in height to obtain the local FAG. Every measurement within a survey must be corrected for deformation so each data point represents the same distance from the centre of the Earth (Telford et al., 1990). This is usually accomplished through differential GPS occupations at every station; however, it can also be done through leveling surveys and interferometric synthetic aperture radar (InSAR) data.

Instruments

Spring and absolute gravimeters are the two general types of devices that are used to measure the Earth's gravitational field in research applications. Absolute gravimeters precisely measure the Earth's acceleration due to gravity at a single point. They can obtain a precision of 1 x 10^{-9} m s^{-2} by measuring the speed of a free falling object in a vacuum tube with a laser interferometer and an atomic standard clock (Sasagawa et al., 1995). An absolute gravimeter requires 3-4 hours to set up on a single point and then 24 hours to collect enough data for a precise measurement. This is not practical in a survey that needs to cover a large area with a large number of points. In addition to long set up times, strong volcanic tremor can make absolute measurements impossible due to vibrations.

The other more common option for gravity surveys instrumentation is spring gravimeters (also called relative or zero length spring gravimeters). As the name implies, they utilize springs to measure gravity. Figure A-1 shows a schematic of a La Coste & Romberg gravimeter that measures the force of gravity by measuring extension of a “zero length” spring. In a “zero length spring” gravimeter, the force required to stretch and contract the spring in normal surveying conditions obeys Hooke’s Law (Eq. 2):

$$F = -kx \quad (2)$$

Hooke’s Law states that the force (F) applied to the spring is negatively proportional to the amount of stretching (x) multiplied by a characteristic spring constant (k). The term “zero length spring” refers to the physical property that if the spring were physically able to contract to a length of zero, then the force acting on it would also be zero.

The advantages of a spring meter over an absolute meter are that they are less expensive, portable, relatively easy to use, and require less time to obtain a precise measurement (2-10 minutes). Disadvantages of these gravimeters pertain to how their physical spring measures gravity, as measurements are relative to the meter being used. The spring of each instrument will have a slightly different spring constant, thus measurements with different meters at a location will be different (e.g., Rymer, 1989). This is not a problem if the gravity measurements are being used to detect changes in the Earth’s mass distribution rather than for an absolute value of the Earth’s gravitational field. To combine the data from two different meters, a calibration

needs to be obtained by repeating measurements with both instruments over a range of values (Carbone and Rymer, 1999). This is typically done by making a traverse that covers significant elevation gain and loss. It is however, better to keep instrumentation consistent throughout a survey to avoid this problem. Besides causing a gravimeter's measurement to be relative, the spring's properties will also slowly drift over time. As time passes, a gravimeter's spring will change its length and in newer meters, this relaxation is faster while in older meters it is often unnoticeable over a survey (e.g., Rymer, 1989) Instrumental drift is corrected using a linear fit between measurements at the same location. Each meter used in this thesis was stable such that the amount of drift was negligible in a single day of surveying.

The spring in a relative meter is also susceptible to rapid changes that can cause data corruption and potentially cause a day worth of surveying to be unusable (e.g., Rymer, 1989). A high frequency noise spike or tare is caused by a change in a gravimeter's spring due to moving the meter violently, or changes in the internal temperature of the meter. Tares can manifest as either a simple offset that the meter never recovers from, or a spike that the meter recovers from slowly. Simple offset tares can be corrected for by removing the permanent offset, however, it is not possible to correct a recoverable tare. It is possible to remove only the affected data points and keep the rest of the uncorrupted data. Tares that occurred in the gravity data collected in Hawaii and Nicaragua were smaller then the anomalies such that they do not affect the data set. The gravity measurements from the Three Sisters Volcanic Complex, however, contained

many large tares. For this dataset no attempt was made to correct tares as it was difficult to pinpoint the time they occurred and whether they involved a simple offset.

While individual instruments may have upgrades to their functionality that change the measurement procedure, the upgrades will not change how the instrument measures gravity. Examples of instrumental upgrades would be a self leveling meter or an onboard software package able to correct the data in real time. In analogue LaCoste & Romberg G and D meters, the operator must use the meter's optics to level and read the measurement, adding a possible element of human error. To provide constant readings, it is preferable that only one person operates a meter during the survey. The instrument used to obtain Bouguer and continuous gravity measurements at Kīlauea and Masaya was a LaCoste & Romberg gravimeter, G127. This meter has an Aliod feedback system upgrade which streams gravity data at 2 Hz to an external Palm PDA. This functionality allows for quicker reading and removes human error from reading an instrument's optical gauges (Gottsmann et al., 2004). The microgravity data collected at the Three Sisters Volcanic Field was done with several meters, only two of which were equipped with the Aliod upgrade.

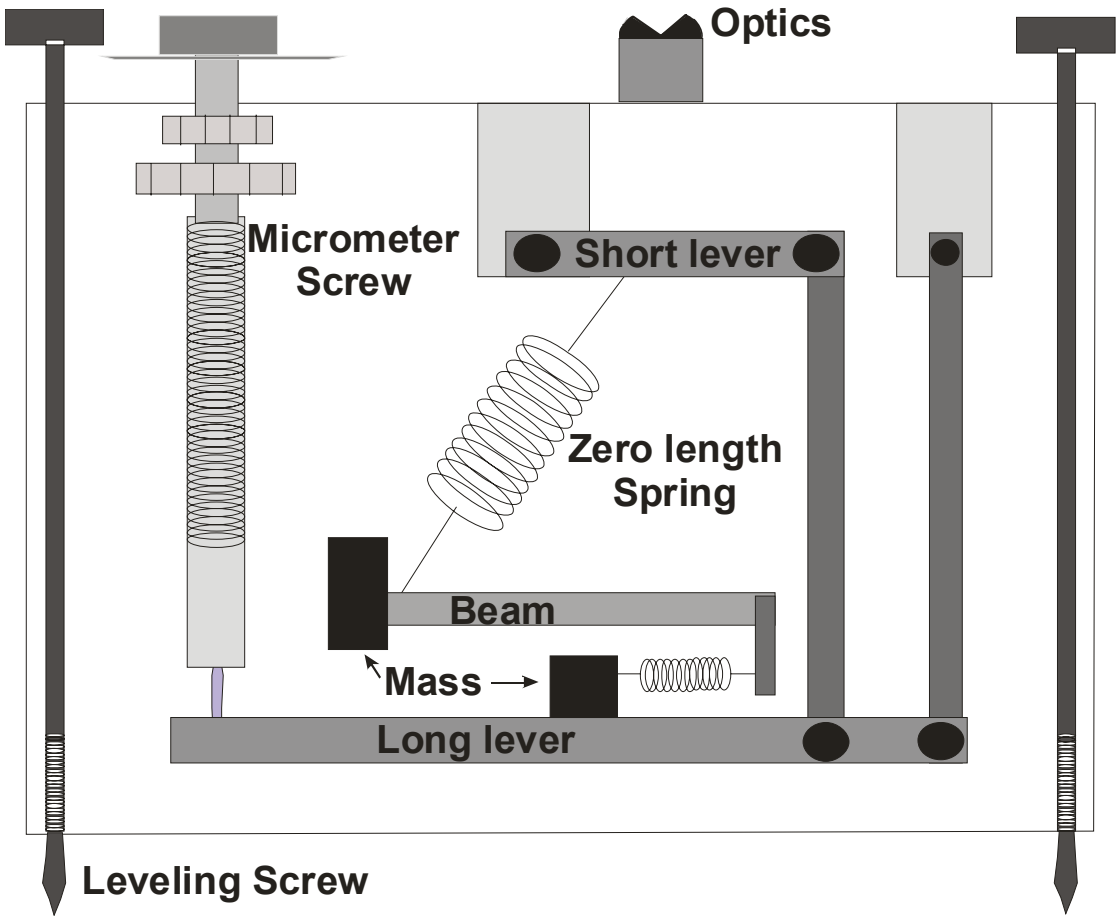

Figure A-1 Schematic of a LaCoste & Romberg G or D meter

Surveys

Bouguer, dynamic microgravity and continuous are three general gravity survey types which are used in research and volcano monitoring. While each survey technique is treated and interpreted differently, they all have to be corrected for Earth tide, ocean loading, elevation change, and instrumental drift. Bouguer surveys were completed at Masaya volcano (Nicaragua) and Kīlauea

volcano (Hawaii, U.S.A.) to map density contrasts near their active summit vents. Continuous gravity measurements were also collected at Kīlauea to investigate short term dynamic behavior of the summit vent and shallow plumbing system. Dynamic microgravity data were collected at Three Sisters volcanic complex in Oregon, USA, to further describe a deep seated deformation process. The following sections summarize the procedure, gravity corrections, and processing of each survey as used within this thesis.

Bouguer Survey

Bouguer surveys aim to map out density differences at depth beneath the Earth and are commonly used to define shallow dense ore bodies, the location and size of kimberlite pipes, and the extent of large scale regional structures (Telford et al., 1990). The survey is typically conducted over days to weeks covering an area of 100s m^2 to 10s km^2. Ideally, the survey would consist of measurements in a grid over the area of interest to create an even spatial data set; however, in volcanic and mountainous areas, it is often difficult to achieve this due to safety concerns. The data sets from both Kīlauea and Masaya volcanoes were able to utilize a grid for the survey but have large holes in the grid due to the presence of summit pit craters.

Proper survey procedure requires that the operator take repeat measurements at a common point or base station before and after surveying each day. Primarily, this is done to correct any instrumental drift and identify data tares between two readings. With only one repeated measurement, it is difficult to pinpoint when a tare occurred and thus it is preferable to repeat station

measurements periodically throughout each survey day. Most often, there is no ideal gravity station location at a predetermined grid point. The soil may be soft causing the gravimeter to lose level or force the operator to be as still as possible not to upset the meter. This increases the noise in the reading thus it is best to take repeat measurements to average out error. Surveys completed on Kĩlauea and Masaya had a minimum of three repeat measurements for each station.

After removing the effects of Earth tides and the difference in elevation between two gravity station locations, there are several different terrain corrections that should be applied. While the FAG removes the gravitational difference due to elevation, the effect of the associated mass that has created the change in elevation (the Bouguer correction) must be removed (Telford et al., 1990). The Bouger anomaly correction uses an infinite slab of an assumed density to remove the effect of an increase (or decrease in the case of elevation loss) of material at higher elevations. The effect of terrain on the gravitational field will always cause an apparent gravitational decrease. The simplest example is measuring gravity at the top and bottom of a cliff. If measuring by the edge of a cliff, there is empty air below; this empty space represents missing material that is not providing a force towards the center of the earth. Likewise, when measuring gravity at the base of a cliff, the material above provides a force upwards decreasing the vertical component of the gravitational field. The two general terrain corrections that remove the effect of terrain features like a cliff are the near terrain and far terrain corrections. For the near terrain correction, slope measurements are taken in different ranges, varying from 2 m to 50 m with either

a clinometer or a range finder (Telford et al., 1990). The slopes are then used to calculate the effect of the missing or additional mass close to gravity station. The relatively flat survey areas of both Kīlauea and Masaya volcanoes are punctuated with pit craters and do not allow for accurate and meaningful slope measurements. To remove terrain from the data, the far terrain correction, using an accurate DEM of most of the volcano, is relied upon. The far terrain correction attempts to remove the gravitational effect of all terrain outside a set exclusion distance, based on either on the areal extent of the near station terrain correction or the accuracy of the DEM, whichever is greater. One consideration with implementing the far terrain correction is that it requires a significant amount of computer power, especially with a large and high resolution DEM. Latitude and Bullard corrections are the last of the effects that Bouger anomaly datasets are routinely corrected for (Telford et al., 1990). The latitude correction is only important for large surveys as it removes the effect that the Earth is not a perfect sphere. The Bullard correction adds the effect of the curvature of the Earth to the infinite slab used by the Bouger anomaly correction. After the measurements are corrected, the data is normalized to the base station. With each measurement normalized to the base station, data collected on different days can be merged even when there is significant drift separating them.

Bouguer gravity anomalies within a volcanic region typically fall into a range of 1 to 50 mGals (Rymer and Brown, 1989). This is much greater than the sensitivity for spring gravimeters (1 μGal; Rymer, 1989); therefore, the dataset is less susceptible to being corrupted by error due to tares or inaccurate

corrections. Due to the lack of precision in applying terrain corrections, a Bouguer dataset will have an estimated error of at least 50 μGal. In most cases, the error is greater than 50 μGal as it is difficult to accurately measure and calculate the effect of terrain across the survey area. This, however, does not affect the interpretation of typical volcanic Bouguer anomalies.

Dynamic microgravity

Dynamic microgravity surveys are used to quantify local changes in the Earth's gravitational field due to mass movements beneath the Earth over time. To accomplish this, surveys are repeated periodically across a network of stations. This technique has been used on many different volcanoes for research and monitoring purposes to quantify mass flux in dynamic processes such as dyke intrusion, magma recharge, and fluid-gas density variations (e.g., Rymer and Brown, 1986; Eggers, 1987; Williams-Jones et al., 2003). Studies often investigate small changes in the gravitational field and hence require that care is taken to reduce noise and error within the data. In perfect survey conditions, it is possible to obtain accuracies better than +/- 10 μGal (e.g., Rymer, 1994; Battaglia et al., 2008). An active volcanic region is not a laboratory environment and volcanic tremor and rough terrain can create high frequency noise (data tares). Stringent survey procedures such as multiple repeat measurements at different times can isolate tares and reduce noise. To compare surveys taken years or months apart, each survey must use a common base station, which is outside the assumed dynamic area. Each survey is normalized to the base station to remove any effects of instrumental drift between surveys.

The surveys completed at the Three Sisters Volcanic Field measured stations in a loop so that every station was repeated. The loops were also repeated three times over the course of a week and averaged to provide one data point. Using data redundancy and averaging, the errors caused by tares induced by the 17 km hike across the Three Sisters Wilderness were significantly reduced.

Under ideal circumstances the basic gravity corrections are all that is required prior to interpretation, however, mass wasting, anthropogenic modifications, and meteorological variations are different factors that can cause a gravitational field change unrelated to changes in volcanic activity. Of these factors, only water table fluctuations due to changes in rain fall will leave no trace at the surface to explain a measured change in the gravitational field. Constraining the effect of water tables on a dataset can be difficult without accessible wells in the survey area. To minimize the effect, surveys are usually repeated at the same time of year with comparison to typical rain fall levels (e.g., Rymer, 1989; Battaglia et al., 2003, 2008). Surveys at the Three Sisters Volcanic Field were completed from early summer into fall. By stretching the observational period through summer, it is possible to monitor the effect of water tables separate from volcanic influences; assuming the ground water rise and fall is faster than any volcanic process. Overall, greater care is required to obtain the precision needed to describe many dynamic volcanic processes that are often 30 to 100s μGal in amplitude (Rymer, 1994). For instance, an anomaly of 15 μGal between surveys could be caused by a small deformation of only 5 cm instead of material moving closer to the surface. Accurate deformation data collected

through differential GPS, leveling or InSAR are then necessary to describe a gravity change. The data can then be used to quantify the mass flux or provide bounds on the density of material that is causing a change in volcanic activity (e.g., Battaglia et al., 2003; Gottsmann et al., 2006).

Continuous

Persistently active volcanoes often have small interruptions to their background activity that involve a significant amount of mass. Events of this nature have been observed in Hawaii in the form of gas pistoning and lava level rise and drain back (e.g., Swanson, 1979). These events occur over short time scales that cannot be observed in a microgravity data set. By deploying a gravimeter to record continuously, it is possible to capture short period events while also allowing for near real time volcano monitoring.

Continuous gravity is rarely measured due to the logistical complications involved with installing and running a gravimeter continuously on an active volcano (e.g., Battaglia et al., 2008; William-Jones et al., 2008). Volcanoes are most often in remote areas creating a challenge in providing enough power to run the gravimeter for long periods of time and transmitting the data from the site. It can also be an inhospitable environment with corrosive gas, earthquakes, ground deformation, and possible volcanic eruptions which can destroy or unlevel the instrument. To provide protection, supply power and easy access to the meter for upkeep, infrastructure needs to be built to house the meter in a volcanic area. If the deployment is meant to be permanent, it is also important to insulate the meter from the atmosphere as meters are susceptible to temperature and

humidity changes (El Wahab et al., 1997). Pressure changes need to be recorded at the instrument site as changes in the mass of the air column above the instrument can affect the gravity reading. The data can be corrected by simply using a theoretical factor of -3.06 μGal $mbar^{-1}$ (Boy et al., 1998). Temperature and humidity changes, however, are not easily described and corrected for. Each gravity meter has its own thermostat and environmental seals that should keep the internal sensors isolated from temperature and humidity, however, these seals can become leaky. Changes in humidity could add or remove weight to the spring due to condensation of moisture causing an uncorrectable anomalous drift (El Wahab et al., 1997; Boy et al., 1998). Although the thermostat will correct for external temperature differences, a temperature gradient can still occur across the sensor causing expansion and contraction of the spring. While there is no way to quantify the effect of humidity, there are a number of mathematical algorithms that have been developed that can remove the effect of temperature on a gravity dataset (e.g., Ando and Carbone, 2001,2004). The algorithms, however, require a long standing dataset and are different for each meter and location. This limits their usefulness in short term deployments. Continuous data collected on Kĩlauea volcano was corrected for the effects of Earth tides, ocean loading and atmospheric pressure. Ambient temperature was not corrected for as this was a short term deployment thus pervious algorithm routines are not usable on the dataset.

Conclusion

Regardless of the survey type, gravity measurements provide information of the density and/or mass flux. The instruments used in this thesis are relative meters, hence; do not provide absolute measurements of the Earth's gravitational field. They do, however, still provide the ability to characterize it. Surveys can be designed to provide information about temporal processes or map out structures through density contrasts.

Bouguer gravity surveys are static pictures that provide information about density contrasts beneath the Earth's surface and it is impossible to obtain mass flux from the dataset. This information can then be inverted and provide a best fit to what the subsurface may hold in the way of structures, magma bodies, and intrusive complexes. Chapter 3 uses this survey technique to provide information about the subsurface geology at Masaya volcano and image a large intrusive complex at Kĩlauea.

Examples of surveys that incorporate a temporal component are continuous and dynamic microgravity surveys. These provide measurements of mass flux within the system. When incorporating volume constraints from deformation measurements it is possible to also obtain density. These two techniques typically require a sacrifice of station density to be able to realistically complete the study. Chapter 2 used a continuous deployment to observe short term perturbations in the shallow magma plumbing system at Hawaii. In Chapter 4, dynamic microgravity surveys are utilized to provide constraints on ongoing deformation at Three Sisters Volcanic Field. Ongoing volcano gravity research is

developing and refining techniques to provide mass flux constraints to monitored volcanic behavior.

References

Andò, B., and Carbone, D., 2001, A methodology for reducing the effect of meteorological parameters on a continuously recording gravity meter: IEEE Transactions on Instrumentation and Measurments, v. 50, no. 5, p. 1248-1254.

Andò, B., and Carbone, D., 2004, A test on a Neuro-Fuzzy algorithm used to reduce continuous gravity records for the effect of meteorological parameters: Physics of the Earth and Planetary Interiors, v. 142, p. 37.

Battaglia, M., Gottsmann, J., Carbone, D., and Fernàndez, J., 2008, 4D volcano gravimetry: Geophysics, v. 73, no. 6, p. WA3-WA18.

Battaglia, M., Segall, P., and Roberts, C., 2003, The mechanics of unrest at Long Valley caldera, California. 2. Constraining the nature of the source using geodetic and micro-gravity data: Journal of Volcanology and Geothermal Research, v. 127, no. 3-4, p. 219-245.

Berrino, G., Rymer, H., Brown, G.C., and Corrado, G., 1992, Gravity-height correlations for unrest at calderas: Journal of Volcanology and Geothermal Research, v. 53, no. 1-4, p. 11-26.

Boy, J.P., Hinderer, J., and Gegout, P., 1998, Global atmospheric loading and gravity: Physics of the Earth and Planetary Interiors, v. 109, no. 3, p. 161-177.

Carbone, D., and Rymer, H., 1999, Calibration shifts in a LaCoste-and-Romberg gravimeter: comparison with a Scintrex CG-3M: Geophysical Prospecting, v. 47, no. 1, p. 73-83.

Eggers, A.A., 1987, Residual gravity changes and eruption magnitudes: Journal of Volcanology and Geothermal Research, v. 33, no. 1-3, p. 201-216

El Wahabi, A., Ducarme, B., Van Ruymbeke, M., and d'Oreye, N., 1997, Continous gravity observations at Mount Etna (Sicily) and correlations between temperature and gravimetric records: Cahiers du Center Europèen de Gèodynamique et de Sèismologie, v. 14, p. 105.

Gottsmann, J., Folch, A., and Rymer, H., 2006, Unrest at Campi Flegrei: A contribution to the magmatic versus hydrothermal debate from inverse and finite modeling: Journal of Geophysical Research, v. 111, no. B07203.

Gottsmann, J., Fournier, N., and Rymer, H., 2004, g_log4PDA: an application for continuous monitoring of gravity using La Coste&Romberg Aliod 100 systems and Palm OS® run hand-held computers: Computers & Geosciences, v. 30, p. 553.

Hautmann, S., Gottsmann, J., Camacho, A.G., Fournier, N., Sacks, I.S., and Sparks, R.S.J., 2010, Mass variations in response to magmatic stress changes at Soufrière Hills Volcano, Montserrat (W.I.): Insights from 4-D gravity data: Earth and Planetary Science Letters, v. 290, no. 1-2, p. 83-89.

Rymer, H., and Brown, G.C., 1986, Gravity fields and the interpretation of volcanic structures: Geological discrimination and temporal evolution: Journal of Volcanology and Geothermal Research, v. 27, no. 3-4, p. 229-254.

Rymer, H., 1989, A Contribution to precision microgravity data analysis using LaCoste and Romberg gravity meters: Geophysical Journal International, v. 97, no. 2, p. 311-322.

Rymer, H., 1994, Microgravity change as a precursor to volcanic activity: Journal of Volcanology and Geothermal Research, v. 61, no. 3-4, p. 311-328.

Sasagawa, G.S., Klopping, F., Niebauer, T.M., Faller, J.E., and Hilt, R.L., 1995, Intracomparison tests of the FG5 absolute gravity meters: Geophysical Research Letters, v. 22, no. 4, p. 461-464.

Swanson, D.A., Duffield, W.A., Jackson, D.B., and Peterson, D.W., 1979, Chronological narrative of the 1969-71 Mauna Ulu eruption of Kīlauea Volcano, Hawaii: Geological Survey Profesional Paper 1056.

Telford, W.M., Geldart, L.P., and Sheriff, R.E., 1990, Applied geophysics (2nd ed.): New York, U.S.A., Cambridge University Press, 770 p.

Williams-Jones, G., Rymer, H., Mauri, G., Gottsmann, J., Poland, M.P., and Carbone, D., 2008, Toward continuous 4D microgravity monitoring of volcanoes: Geophysics, v. 73, no. 6, p. WA19-WA28.

Williams-Jones, G., Rymer, H., and Rothery, D.A., 2003, Gravity changes and passive SO2 degassing at the Masaya caldera complex, Nicaragua: Journal of Volcanology and Geothermal Research, v. 123, no. 1-2, p. 137-160.

Appendix B: Magnetic methods

Introduction

Volcanic areas are often structurally complex due to their dynamic behavior which can include eruptions, earthquakes, and flank collapses. With the majority of a volcano inaccessible beneath the surface, it becomes necessary to rely heavily on geophysical techniques to identify subsurface structures. Magnetic field surveys are one of the simplest geophysical methods that can be utilized to investigate in detail the near surface structures, or deeper regional changes.

The SI unit for magnetic fields is the Tesla (T), which is the same as a Newton per Ampere meter ($N\ A^{-1}\ m^{-1}$). One Tesla would represent a large magnetic field and thus measurements are usually given in nT. The Earth's magnetic field has a magnitude of 20,000 to 70,000 nT, dependant on a location's elevation and magnetic latitude (e.g., Redford, 1980; Telford et al., 1990). Before surveying, it is important to understand the three general components of the Earth's magnetic field: 1) a large and slow varying internal source, 2) small and fast varying external sources and 3) a ground material source.

The slow large varying internal source is described by a dynamo in the Earth's outer core (e.g., Alldredge and Hurwitz, 1964). This can be approximated by a simple dipole field with its north, or positive end, pointing towards the Earth's North Pole. As with a dipole, the magnetic field lines at the Earth's surface change with distance from the poles. The field lines are described in a spherical

coordinate system of magnetic inclination and declination. Near the magnetic equator, the potential field lines spread out, creating a lower magnetic magnitude while being nearly horizontal (inclination of 0°). At the poles, the field lines are tighter, have a higher magnitude and are nearly vertical (inclination of -90° at the South Pole, +90° at the North Pole). The elevation of a measurement above the Earth's surface also affects its expected magnitude as it is further from the dipole; thus, if a survey covers a large area or elevation range, it is important to correct for changes in location and create a common baseline across the whole survey. The International Geomagnetic Reference Field (IGRF) is used to calculate the correction for each measurement to remove the effect of magnetic declination and elevation from the data (Barton, 1997). It is beyond the scope of this Appendix to discuss the source of the Earth's magnetic field, as the details are complex and do not have a direct bearing on magnetic survey techniques used in this thesis (Chapter 3).

The external field is primarily produced by the Sun, as its radiation output varies over different temporal cycles. The longest temporal wavelength change in solar radiation, recognized in magnetic surveying, is 22 years due to sunspot cycles (Babcock, 1960). The magnitudes of shorter wavelength variations are dependent on latitude and can be either seasonal or diurnal. Diurnal changes constitute a change of approximately 30 nT over a 24 hour period (e.g., Telford et al., 1990). The shortest time scale and largest amplitude (possibly 1000s nT) for measurable changes in the Earth's magnetic field are due to magnetic storms that are linked to solar flares and sunspot activity. These magnetic storms are

more common at higher latitudes when the polar auroras are strong. While the Sun is the largest source of external magnetic influence, the Moon also affects Earth's field by interacting with the ionosphere causing changes in the field of about 2 nT over approximately 25 hours.

Ground material or the rock properties can locally have large effects on the magnetic field (e.g., Redford, 1980; Telford et al., 1990). In instances where a large high grade magnetic ore body is present, the field can nearly double in size over a very short area (Green, 1960). The magnetic response of a material is the addition of two properties, remnant magnetism (ferromagnetic component) and magnetic susceptibility (paramagnetic component). Remnant magnetism is a measure of a material's ability to retain a magnetic moment and magnetic susceptibility is the response of a material to an external field. The minerals primarily responsible for remnant magnetism in igneous rocks are iron-titanium oxides (e.g., Green, 1960; Telford et al., 1990). The effect of the ground material response on the measured magnetic field strength may not be simple, especially when surveying at low magnetic inclinations due to topography (Gupta and Fitzpatrick, 1971). The resulting field may be chaotic and without the ability to remove, or at least characterize the effect of topography in areas with large elevation changes, it is impossible to interpret the data.

A further complication to the interpretation of magnetic anomalies is that some processes can destroy or add to the magnetic response of a rock. One example is temperature, the Currie point is the temperature at which a material's remnant magnetism is destroyed. Magnetite, which is common in igneous rocks,

has a Currie temperature of approximately 580 °C and thus, it is expected that any igneous rock within the crust above this temperature will not react appreciatively in the Earth's magnetic field (Zablocki and Tilling, 1976). When a magma or a rock cools below its Currie temperature, any ferromagnetic minerals will lock in remnant magnetism based on the external field at the time of cooling. This remnant magnetism will exist until destroyed by heat or alteration. Alteration of magnetic minerals to non magnetic minerals is another process which can reduce or eliminate the magnetic response of the ground (e.g., Telford et al., 1990; Hildenbrand et al., 1993). In rare instances, the alteration processes can create new minerals that increase the magnetic response of a material. An example is large olivine cumulates, which can break down into magnetite increasing the magnetic response (Toft et al., 1990). Alteration is an important concern in volcanic areas due the presence of hydrothermal fluids within often incoherent material possibly creating a complex pattern in the magnetic field.

Interpretation is further complicated by the nature of magnetic anomalies. Their spatial extents are usually quite small and there are usually a large number of anomalies in any given area due to inhomogeneities in the Earth's crust. Volcanic areas are practically complex with many inhomogenities in both material type and alteration. Therefore, it is common to have anomalies that are several 1000s of nT in size that cover very small areas (Gudmundsson and Milsom, 1997).

Instrumentation

Mineral exploration companies have been using the Earth's magnetic field for prospecting for over 160 years. The first written publication describing magnetic techniques to find iron bearing ores was by Thalén in 1879. The World War II invention of the flux-gate magnetometer to locate submarines, and later the proton precession magnetometer, allowed for accurate spatial mapping of the Earth's magnetic field (Paterson and Reeves, 1985). The instruments have been used in a variety of different ways including resource exploration, archeology, ordinance and weapons detection, and volcanology. The instrument used for surveys at both Kĩlauea and Masaya volcano was a GEM Overhauser magnetometer. This instrument works similarly to a proton precession system where the magnitude of the Earth's magnetic field is measured by measuring the precession of spinning charged particles (Hrvoic, 1989). The magnetometer's sensor contains a liquid rich in hydrogen atoms and free unpaired electrons that is then subjected to radio frequency magnetic field. The excited and spinning charges allow for quick and accurate measurements of the magnetic field.

Magnetic measurements with an Overhauser magnetometer are magnitudes only, as no vector information is obtained by measuring the precession frequency of charged particles. Since field magnitudes are measured, the orientation of the instrument has no effect on the resulting measurement, greatly simplifying survey procedures; to be consistent the sensor was oriented parallel to lines in each survey.

Survey Parameters and Procedures

The parameters used to carry out a magnetic survey depend on depth, size, and strength of the magnetic anomalies targeted for study. To provide the most robust data, the survey should be completed in a grid. This is easily possible when the data is collected by plane or helicopter; however, it is not always realistic for ground-based surveys. The magnetic data collected for this thesis was through ground-based surveys, thus aeromagnetic survey procedures will not be discussed further. Accessibility is especially a concern over volcanic areas, making a network of profiles a reasonable concession. Profiles can provide depth information but cannot provide the spatial extent necessary for 2D and 3D inversions thus a grid is preferable where possible.

At Masaya volcano, magnetic measurements were made on lines 50 m apart with data points every 25 m along lines. Due to steep volcanic terrain and time constraints, many areas could not be surveyed in a grid pattern. This is not a problem as the non-grid areas were mostly outside of the area of interest and were used to obtain a better idea of the background field strength. At Kīlauea volcano, magnetic measurements were made in lines 200 m apart with data points every 25 m along lines. This provides good coverage along a single profile but poor coverage between lines. This caused significant problems with modeling and interpretation of the two anomalies identified in Chapter 3 (Fig. 3-9a). Unfortunately, it was impossible to know what the survey was going to find beforehand, so the survey was designed to cover as much area around

Halema'uma'u as possible, with sufficient station spacing to identify structural anomalies. This data is presented as a gridded dataset to spatially show the distribution of the anomalies.

In order to cover large areas quickly, a handheld GPS was used to provide location of each measurement. The GPS was set to take a position every 5 seconds instead of every point allowing for quick surveying. The location of each measurement was then obtained by extrapolating between GPS locations using the time stamp of both the GPS and the magnetic measurements. A handheld GPS has a horizontal accuracy of 3 to 15 m and 6 to 30 m vertical accuracy dependant on satellite availability and position. Unless the vertical elevation within the survey is larger than 30 m, the IGRF should not be removed when using a handheld GPS. Data collected at Masaya volcano was corrected for the IGRF due to significant elevation changes (>100 m) across the survey area. The topography of the survey area at Kĩlauea varied slowly and not by more than 40 m; hence, the IGRF was not corrected for as it would cause a larger amount of error.

While solar magnetic forcing is small, it is always necessary to determine the magnitude of the diurnal variation to characterize possible error sources. To accomplish this, the magnetometer was deployed in a quiet area away from roads where it would not be disturbed. The diurnal variation measured at both survey sites was less than 30 nT and was not corrected as only one working meter was available; the diurnal variation is also much smaller than the anomalies in either survey area. To be sure that the external field was stable and

there were no magnetic storms occurring while surveying, repeat measurements were made periodically.

As mentioned earlier, the magnetic response of the ground can cause the local magnetic field to appear chaotic due to topography, particularly at low magnetic inclinations (e.g., Gupta and Fitzpatrick, 1971; Telford et al., 1990). The magnetic inclination and declination at Masaya is approximately 40° and 0°, respectively, and Kīlauea is approximately 36° and 9°, respectively. Due to pit craters at both field sites, there is a significant topographic effect within the data sets which cannot be directly corrected for. The magnetic properties of igneous rocks can change quickly, so without enough samples to provide magnetic susceptibility and remnant magnetization measurements, it is impossible to properly characterize the topographic response (Bambrick et al., 1982). Instead, forward models with an assumed magnetic susceptibility for basalt were used to determine what effect topography would have on the data set.

Forward Modeling

Forward magnetic models were used in two different capacities in Chapter 3 using software called MAG3D (MAG3D, 2007). The first was to produce a model of each field site's magnetic response to topography. This was done using digital elevation models and an assumed average magnetic susceptibility of the ground. This is a qualitative approach which can be used to identify which anomalies are created from topography changes and not due to structural changes. This procedure was successful in both data sets; however, if there is any structural change near the topographic anomalies, it is masked and lost. The

second case where magnetic models were used were to try and describe anomaly B in Figure 3-5a. Rigorous modeling could not be done in this case due to the data not being in a true grid; therefore, only very simple dykes were forward modeled.

Conclusion

At each field site, ground based magnetic surveys are used to identify volcanic structures. The field procedures used at both are nearly identical with the exception of line spacing being greater at Kĩlauea. Ground based surveys, where the data are collected in a grid, are not common in volcanic areas due to accessibility and topography effects. It is, however, still possible to obtain data that can be used to identify structures and model some of their characteristics.

References

Alldredge, L.R., and Hurwitz, L., 1964, Radial Dipoles as the sources of the Earth's main magnetic field: Journal of Geophysical Research, v. 69, no. 12, p. 2631-2640.

Babcock, H.W., 1960, The topology of the Sun's magnetic field and the 22 year cycle: Astrophysical Journal, v. 133, p. 572.

Bambrick, J., Letros, S., Strangway, D.W., and Geissman, J., 1982, Apparent magnetic susceptibility (SUSC) mapping in theory and practice, Presented at the 52nd Annual International. Meeting, Society of Exploration Geophysicists, Dallas.

Barton, C.E., 1997, International Geomagnetic Reference Field: The seventh generation: Journal of Geomagnetism and Geoelectricity, v. 49, no. 2-3, p. 123-148.

Green, R., 1960, Remanent magnetization and the interpretation of magnetic anomalies, Blackwell Publishing Ltd, 98 p.

Gudmundsson, M.T., and Milsom, J., 1997, Gravity and magnetic studies of the subglacial Grímsvötn volcano, Iceland: Implications for crustal and thermal structure: Journal of Geophysical Research, v. 102, no. B4, p. 7691-7704.

Gupta, V.K., and Fitzpatrick, M.M., 1971, Evaluation of terrain effects in ground magnetic surveys: Geophysics, v. 36, no. 3, p. 582-589.

Hildenbrand, T.G., Rosenbaum, J.G., and Kauahikaua, J.P., 1993, Aeromagnetic study of the island of Hawaii: Journal of Geophysical Research, v. 98, no. B3, p. 4099-4119.

Hrvoic, I., 1989, Proton Magnetometers for Measurement of the Earth's Magnetic field: Workshop on Magnetic Observatory Instrumentation Espoo, Finland.

MAG3D 2007, A program library for forward modeling and inversion of magnetic data over 3D structures: developed under the consortium research project Joint/Cooperative Inversion of Geophysical andGeological Data: UBC-Geophysical Inversion Facility,Department of Earth and Ocean Sciences, The University of British Columbia, Vancouver., v. version 20070309.

Paterson, N.R., and Reeves, C.V., 1985, Applications of gravity and magnetic surveys: The state-of-the-art in 1985: Geophysics, v. 50, no. 12, p. 2558-2594.

Redford, M.S., 1980, Magnetic method: Geophysics, v. 45, no. 11, p. 1640-1658.

Telford, W.M., Geldart, L.P., and Sheriff, R.E., 1990, Applied geophysics (2nd ed.): New York, U.S.A., Cambridge University Press, 770 p.

Toft, P.B., Arkani-Hamed, J., and Haggerty, S.E., 1990, The effects of serpentinization on density and magnetic susceptibility: a petrophysical model: Physics of the Earth and Planetary Interiors, v. 65, no. 1-2, p. 137-157.

Zablocki, C.J., and Tilling, R.I., 1976, Field measurements of apparent Curie temperatures in a cooling basaltic lava lake, Kĩlauea Iki, Hawaii: Geophysical Research Letters, v. 3, p. 487-490.